Investigation of molecular mechanisms underlying antibacterial potential of Allylarene and Stilbene class of phytochemicals

By

DEEPTI SINGH

Enrolment No. LIFE 01201504014

BHABHA ATOMIC RESEARCH CENTRE

A thesis submitted to the

Board of Studies in Life Sciences

In partial fulfillment of requirements

for the Degree of

DOCTOR OF PHILOSOPHY

of

HOMI BHABHA NATIONAL INSTITUTE

September, 2020

Homi Bhabha National Institute[1]

Recommendations of the Viva Voce Committee

As members of the Viva Voce Committee, we certify that we have read the dissertation prepared by **Deepti Singh** entitled"**Investigation of molecular mechanisms underlying antibacterial potential of Allylarene and Stilbene class of phytochemicals**"and recommend that it may be accepted as fulfilling the thesis requirement for the award of Degree of Doctor of Philosophy.

Chairman-	**Dr. Sunil Kumar Ghosh**	
Guide-	**Dr. Mahesh Subramanian**	15th April 2021
Examiner -	Name & Signature with date (Prof. Ranjana Pathania)	16th April 2021
Member 1-	**Dr. Santosh Kumar Sandur**	
Member 2-	**Dr. Anand Ballal**	17 Apr. 2021
Member 3-	**Dr. Shashidhar**	17th April 2021

Final approval and acceptance of this thesis is contingent upon the candidate's submission of the final copies of the thesis to HBNI.

I/We hereby certify that I/we have read this thesis prepared under my/our direction and recommend that it may be accepted as fulfilling the thesis requirement.

Date: 15th April 2021

Place: Mumbai.

Signature

Dr. Mahesh Subramanian

(Guide)

[1] This page is to be included only for final submission after successful completion of viva voce.

DECLARATION

I, hereby declare that the investigation presented in the thesis has been carried out by me. The work is original and has not been submitted earlier as a whole or in part for a degree / diploma at this or any other Institution / University.

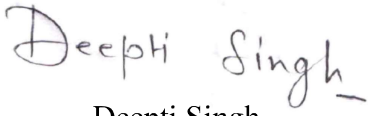

Deepti Singh

List of Publications arising from the thesis

1. **Deepti Singh**, Shwetha Narayanamoorthy, Sunita Gamre, Ananda Guha Majumdar, Manish Goswami, Umesh Gami, Susan Cherian, and Mahesh Subramanian. "Hydroxychavicol, a key ingredient of Piper betle induces bacterial cell death by DNA damage and inhibition of cell division." Free Radical Biology and Medicine 120 (2018):62-71.
2. **Deepti Singh**, Rebecca Mendonsa, Mrunesh Koli, Mahesh Subramanian, and Sandip Kumar Nayak. "Antibacterial activity of resveratrol structural analogues: A mechanistic evaluation of the structure-activity relationship." Toxicology and applied pharmacology 367 (2019): 23-32.
3. **Deepti Singh**, Ananda Guha Majumdar, Sunita Gamre, and Mahesh Subramanian. "Membrane damage precedes DNA damage in hydroxychavicol treated *E. coli* cells and facilitates cooperativity with hydrophobic antibiotics. "Biochimie 180 (2021): 158-168**.**

Chapters in books and lectures notes

Nil

Conferences/symposium

1. **Poster presented** titled "Hydroxychavicol, a key ingredient of *Piper betle* induces bacterial cell death by DNA damage and inhibition of cell division" **Deepti Singh**, Shwetha Narayanamoorthy, Sunita Gamre, Ananda Guha Majumdar, Manish Goswami, Umesh Gami, Susan Cherian, Mahesh Subramanian at "World Congress on Infectious Diseases and Antibiotics 2018" held at Indian Institute of Science, Bengaluru, Karnataka, India between 28th December 2018 to 29th December 2018.

2. **Poster presented** titled "Molecular events leading to bacterial cell death upon treatment with phytochemical Hydroxychavicol" **Deepti Singh** and Mahesh Subramanian at "EMBL Symposium: New Approaches and Concepts in Microbiology" held at Heidelberg, Germany between 10th July 2019 to 13th July 2019.
3. **Delivered talk (oral presentation)** titled "Molecular mechanisms behind the antibacterial activity of an Allylarene Hydroxychavicol: Implications towards overcoming multidrug resistance" **Deepti Singh** and Mahesh Subramanian at "17th Annual Meeting of SFRR-India (SFRR INDIA-2020) & International Conference on Role and Management of Oxidative Stress in Human Disease" held at Mumbai, India between 12th February 2020 to 15th February 2020.

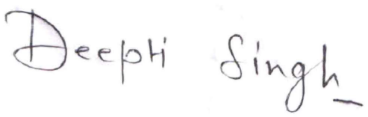

Deepti Singh

DEDICATIONS

This thesis is dedicated to

My loving parents

(Dr. Abhai Raj Singh and Ilaka Devi)

TABLE OF CONTENT

List of Figure

List of tables

Summary

Antibiotic resistance is a global problem and there is an urgent need to augment the arsenal against pathogenic bacteria. Botanical sources remain a vital source of diverse organic molecules that possess antibacterial property as well as augment existing antibacterial molecules. *Piper betle*, a climber, is widely used in south and south-east Asia whose leaves and nuts are consumed regularly. Hydroxychavicol (HC) isolated from *Piper betle* has been reported to possess antibacterial activity. It is currently not clear how the antibacterial activity of HC is manifested. In this investigation, we show HC generates superoxide in *E. coli* cells. Antioxidants protected *E. coli* against HC induced cell death while *gshA* mutant was more sensitive to HC than wild type. DNA damage repair deficient mutants are hypersensitive to HC and HC induces the expression of DNA damage repair genes that repair oxidative DNA damage. HC treated *E. coli* cells are inhibited from growth and undergo DNA condensation. *In vitro* HC binds to DNA and cleaves it in presence of copper. Our data strongly indicates HC mediates bacterial cell death by ROS generation and DNA damage. Further HC is active against a number of gram negative bacteria isolated from patients with a wide range of clinical symptoms and varied antibiotic resistance profiles. HC also resulted in membrane compromise revealing its pleiotropic effects on cellular targets. The kinetics and exact sequence of events leading to inhibition of growth and cell death in *E. coli* after HC treatment was elucidated. HC treated cells were found to experience oxidative stress as early as 10 min, while evidence of membrane damage was apparent at 30 min. DNA damage repair genes were found to be activated at 60 min. Our study reveals for the first time that HC could sensitize bacteria to clinically used antibiotics due to its outer membrane damaging property.

Stilbenes structurally possess 1,2-diphenylethylene nucleus and can be divided into monomers and oligomers. Resveratrol is the most acclaimed stilbene demonstrated to possess

a myriad of beneficial properties. However, resveratrol is present in low quantities in natural resources and also has low bioavailability. A general consensus about the substitutions that improve the activity remains elusive in stilbene class of molecules especially in regard to antibacterial activity. Lack of this knowledge remains a major hurdle in developing stilbene based antibacterial molecules. A panel of gram positive and gram negative bacteria were employed for screening the comparative efficacy of the stilbenes. Employing the notorious nosocomial agent *S. aureus*, we show how changes in structure of stilbene alter not only the antibacterial activity but also the underlying mechanisms. We showed dimerization, halogenation and hydroxy group in conjunction with methoxy group resulted in the best antibacterial molecules. Our work with different stilbenes identified Dimer Stilbene (DS) as a potent inhibitor of *S. aureus*. A screen revealed DS to exhibit positive co-operativity with antibiotics that target protein synthesis. The co-operativity screening between DS and other antibiotic showed that DS exhibits positive co-operativity with antibiotics that target protein synthesis. DS exhibited synergy with the aminoglycoside kanamycin and additive effect with tetracycline. The efficacy of DS against clinical MSSA and MRSA were similar. Laboratory generated kanamycin resistant strain and clinical strains were sensitized to kanamycin by co-treatment with DS. DS cured *S. aureus* infection in mice (skin infection model) as a standalone drug as well as in conjunction with kanamycin. Synergy with kanamycin was also observed in other stilbenes apart from DS. Stilbenes could be exploited towards combating *S. aureus* infections either as standalone drugs or in combination with existing antibiotics. Thus the work presented here identified interesting antibacterial molecules from natural resources and elucidated the mechanism of action of them, toxicity and efficacy in animal models.

Summary

Antibiotic resistance is a global problem and there is an urgent need to augment the arsenal against pathogenic bacteria. Botanical sources remain a vital source of diverse organic molecules that possess antibacterial property as well as augment existing antibacterial molecules. *Piper betle*, a climber, is widely used in south and south-east Asia whose leaves and nuts are consumed regularly. Hydroxychavicol (HC) isolated from *Piper betle* has been reported to possess antibacterial activity. It is currently not clear how the antibacterial activity of HC is manifested. In this investigation, we show HC generates superoxide in *E. coli* cells. Antioxidants protected *E. coli* against HC induced cell death while *gshA* mutant was more sensitive to HC than wild type. DNA damage repair deficient mutants are hypersensitive to HC and HC induces the expression of DNA damage repair genes that repair oxidative DNA damage. HC treated *E. coli* cells are inhibited from growth and undergo DNA condensation. *In vitro* HC binds to DNA and cleaves it in presence of copper. Our data strongly indicates HC mediates bacterial cell death by ROS generation and DNA damage. Further HC is active against a number of gram negative bacteria isolated from patients with a wide range of clinical symptoms and varied antibiotic resistance profiles. HC also resulted in membrane compromise revealing its pleiotropic effects on cellular targets. The kinetics and exact sequence of events leading to inhibition of growth and cell death in *E. coli* after HC treatment was elucidated. HC treated cells were found to experience oxidative stress as early as 10 min, while evidence of membrane damage was apparent at 30 min. DNA damage repair genes were found to be activated at 60 min. Our study reveals for the first time that HC could sensitize bacteria to clinically used antibiotics due to its outer membrane damaging property.

Stilbenes structurally possess 1,2-diphenylethylene nucleus and can be divided into monomers and oligomers. Resveratrol is the most acclaimed stilbene demonstrated to possess

a myriad of beneficial properties. However, resveratrol is present in low quantities in natural resources and also has low bioavailability. A general consensus about the substitutions that improve the activity remains elusive in stilbene class of molecules especially in regard to antibacterial activity. Lack of this knowledge remains a major hurdle in developing stilbene based antibacterial molecules. A panel of gram positive and gram negative bacteria were employed for screening the comparative efficacy of the stilbenes. Employing the notorious nosocomial agent *S. aureus*, we show how changes in structure of stilbene alter not only the antibacterial activity but also the underlying mechanisms. We showed dimerization, halogenation and hydroxy group in conjunction with methoxy group resulted in the best antibacterial molecules. Our work with different stilbenes identified Dimer Stilbene (DS) as a potent inhibitor of *S. aureus*. A screen revealed DS to exhibit positive co-operativity with antibiotics that target protein synthesis. The co-operativity screening between DS and other antibiotic showed that DS exhibits positive co-operativity with antibiotics that target protein synthesis. DS exhibited synergy with the aminoglycoside kanamycin and additive effect with tetracycline. The efficacy of DS against clinical MSSA and MRSA were similar. Laboratory generated kanamycin resistant strain and clinical strains were sensitized to kanamycin by co-treatment with DS. DS cured *S. aureus* infection in mice (skin infection model) as a standalone drug as well as in conjunction with kanamycin. Synergy with kanamycin was also observed in other stilbenes apart from DS. Stilbenes could be exploited towards combating *S. aureus* infections either as standalone drugs or in combination with existing antibiotics. Thus the work presented here identified interesting antibacterial molecules from natural resources and elucidated the mechanism of action of them, toxicity and efficacy in animal models.

CHAPTER 1. INTRODUCTION

1.1. Infectious diseases are a major concern for human health.

As per the World Health Organization's 2019 report, life expectancy at birth in low-income countries (62.7 years) is 18.1 years lower than in high-income countries (80.8 years) compared with a global difference of 4.4 years between men and women. Major conditions contributing most to the reduced life expectancy in low-income countries are, for both sexes, as follows: lower respiratory infections (life expectancy reduced by 2.09 years), diarrhoeal diseases (1.97 years), stroke (1.45 years), HIV/AIDS (1.45 years), TB (1.35 years), ischaemic heart disease (1.35 years), malaria (0.96 years), road injury (0.75 years), birth asphyxia and birth trauma (0.63 years), and protein-energy malnutrition (0.62 years). The top two contributing factors are bacterial infections that are further convoluted by drug resistance. More than half of under-5 child deaths are due to diseases that are preventable and treatable through simple, affordable interventions. The leading causes of death in young children over 28 days of age remain pneumonia, diarrhoea, birth defects, and malaria (in endemic regions) in that order. Rates of death from all conditions are higher in low-income countries, but children in low-income countries are more than 100 times more likely to die from infectious diseases than those in high-income countries. It is clear than infectious diseases are a major killer, especially in low income countries. Major contributor to neonatal (0-28 days) death is acute respiratory diseases and diarrhoeal diseases. In case of postneonatal (1-59 months) death, the major contributors are prematurity, birth asphyxia/trauma and sepsis/other infections of newborn [1]. Antibiotic resistance is a huge challenge faced by humanity that is threatening to push health care towards the pre-antibiotic era. As per the data by canter for disease control USA at least 2.8 million people get an antibiotic-resistant infection, and more than 35,000 people die because of antibiotic resistant bacteria [2]. CDC of USA has classified

bacterial infections into urgent threats, serious threats, concerning threats and watch list. The classification is based on clinical impact, economic impact, incidence, 10-year projection of incidence, transmissibility, availability of effective antibiotics, and barriers to prevention. The urgent threat category consists of carbapenem resistant Acinetobacter*, Candida auris, Clostridioides difficile,* carbapenem resistant Enterobacteriaceae and, drug resistant *Neisseria gonorrhoeae*. The serious threat list consists of the following drug resistant bacteria namely Campylobacter, Candida, non-typhoidal Salmonella, *Salmonella typhi, Shigella, Streptococcus pneumoniae,* Tuberculosis, ESBL producing Enterobacteriaceae*,* Vancomycin resistant *Enterococci*, multidrug resistant *Pseudomonas aeruginosa* and methicillin resistant *Staphylococcus aureus*. The list of bacteria classified as concerning threats is erythromycin resistant group A Streptococcus and clindamycin resistant group B Streptococcus. The watch list consists of azole resistant *Aspergillus fumigatus*, drug resistant *Mycoplasma genitalium* and drug resistant *Bordetella pertussis* [2]. Realizing the importance of the toll of infectious diseases on the society of a developing country like India, the government embarked upon the issue of antimicrobial resistance programme called "National Program on Containment of Antimicrobial Resistance". This programme was launched under the 12^{th} five-year plan (2012-17). The activities included under this programme are surveillance for containment of AMR in various geographical regions, development and implementation of national infection control guidelines, training and capacity building of professionals in relevant sectors, promotion for rationale prescribing/use of antibiotics, and development of National Repository of Bacterial strains/cultures. After the multi country survey by WHO on Southeast Asia regarding antimicrobial resistance in 2015, the Ministry of Health and Family Welfare (MoHFW), Government of India, developed National Action Plan in the year 2017 to combat AMR. MoHFW identified antimicrobial resistance as a strategic priority and containment of antimicrobial resistance was attempted by the flagship programme called Pharmacovigilance

Programme in 2017 [3]. Realizing the complex nature of the antimicrobial resistance and the gravity of the problem of ever increasing number of resistant bacteria governments of India and UK joined hands for collaborative research to find comprehensive and creative solutions. In November 2016 a 13 million pounds UK-India research programme was unveiled to work on antimicrobial resistance [4].

1.2. Treatment challenges and failure of antibiotics in recent times

The antibiotic treatment was hailed as a boon to humans due to its ability to cure infections and reduce mortality by several-fold compared to pre-antibiotic era [5]. However, the antibiotic treatment came a full circle starting with the cure of bacteraemia patients in 1942 to the loss of a patient in 2008 to vancomycin resistant *Enterococcus faecium* in spite of the best medical efforts [6]. In a recent report from the Organisation for Economic Cooperation and Development (OECD), drug-resistant bacteria contribute to 20% of total bacterial infections in Europe, North America and Australia. If not for remedial measures the drug resistant infections (to the second and third line of antibiotics) are set to rise to 70% in 2030 [7]. The rate of drug resistance among eight bacteria falling into high priority class has increased from 14% in 2005 to 17% in 2015 in OCED countries. This includes *E. coli* resistant to third generation cephalosporins and methicillin resistant *Staphylococcus aureus* [7]. It has been estimated that around 2.4 million people in OECD countries would die from 2015 to 2050 because of multi-resistant bacterial infections, as per the current trends [7]. Figures showed that the rate of resistance among eight high priority antibiotic resistant bacteria—including *E. coli* resistant to third generation cephalosporins and methicillin resistant *Staphylococcus aureus* (MRSA)—had increased from 14% in 2005 to 17% in 2015 in OECD countries [7]. Analysis of the trends and drivers of antibiotic consumption from 2000 to 2015 in 76 countries revealed between 2000 and 2015, antibiotic consumption, expressed in defined daily doses (DDD), increased 65% (21.1–34.8 billion DDDs), and the antibiotic consumption

rate increased 39% (11.3–15.7 DDDs per 1000 inhabitants per day). The increase was driven by low and middle-income countries (LMICs) [8]. The objective was to find out if consumption of certain antibiotics is due to resistance development in bacteria towards first line antibiotics. Although no concrete conclusion could be provided in this direction, a direct correlation between GDP and antibiotic consumption was observed [8] especially in developing countries. This catches humanity in a vicious loop as increased and inappropriate use leads towards the selection of drug resistant population. Spread of resistant bacteria across geographical boundaries has also been observed. Metallo β-lactamase was reported first in 1991 in *Serratia marcescens* in Japan [9]. Later metallo β-lactamase containing strains were found to be endemic in Greece Taiwan and Japan [10]. Death rate associated with metallo β-lactamase containing bacteria was found to be between 18% to 67% [11]. In 2008 New Delhi Metallo β-lactamase containing strain was reported in Sweden from an Indian patient. Since 2010, NDM-1 producers have been identified on all continents except Central and South America [12]. Between 2004 and 2007 in India, *E. coli* isolated from the community exhibited resistance to ampicillin (75%), nalidixic acid (73%) and co-trimoxazole (59%) in a study that encompassed close to 1800 strains [13]. In case of aminoglycosides represented by gentamicin 30% strains were found to be resistant [14]. The already precarious situation of resistance to third-generation cephalosporins (70% to 83%) and fluoroquinolones (78% to 85%) nosedived further [15]. Though a silver lining where resistance to third generation cephalosporins decreased from 90% to 80% in *Klebsiella pneumoniae*, the resistance towards fluoroquinolones increased from 57% to 73% [15]. In a study in a tertiary care setting in New Delhi carbapenem resistance among *K. pneumoniae* increased from 2% in 2002 to 52% in 2009 [16]. In Salmonella isolates, resistance to fluoroquinolones was found to increase from 8% in 2008 to 28% in 2014 while resistance to ampicillin and cotrimoxazole was found to decrease in an Indian study [15]. This is a typical

example of antibiotic rotation policy that could bring back certain antibiotics if discontinued for a certain period of time. Gram negative bacteria create a huge problem in post-surgery recovery. An increase of 1.6% in surgical site infections was reported from Mumbai caused by gram negative bacilli [17]. Resistance to colistin on the rise due to use of it against multidrug resistant *Acinetobacter baumannii* [17]. Resistance to methicillin in *S. aureus* has been found to vary between 32% to 80% among clinical isolates [18]. Alarmingly methicillin resistance was found to increase from 29% in 2009 to 47% in 2014 [15]. In a study in India that encompassed six cities/10 hospitals regarding surgical site infections revealed surgical site infections rates were higher than those reported by the CDC National Healthcare Safety Network (CDC-NHSN) but similar to International Nosocomial Infection Control Consortium (INICC). This study observed 1189 surgical site infections, associated with 28340 surgical procedures between January 2005 to December 2011, and provided important insights into the epidemiology of surgical site infections in India [19].

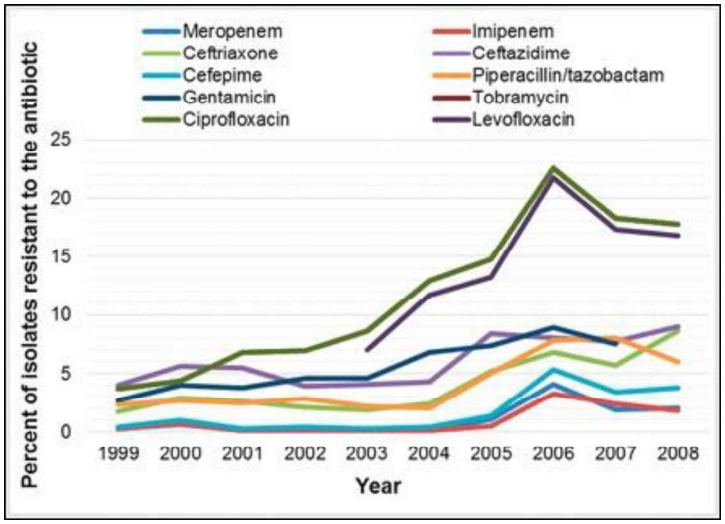

Figure 1.1. Percentage of Enterobacteriaceae strains from a US surveillance study that shows increasing resistance to 10 antibiotics over a 10-year period. Adopted from Rhomberg, 2009 [20].

An ICMR sponsored study published in 2019 [21] exemplifies the growing threat of drug resistance in bacteria.

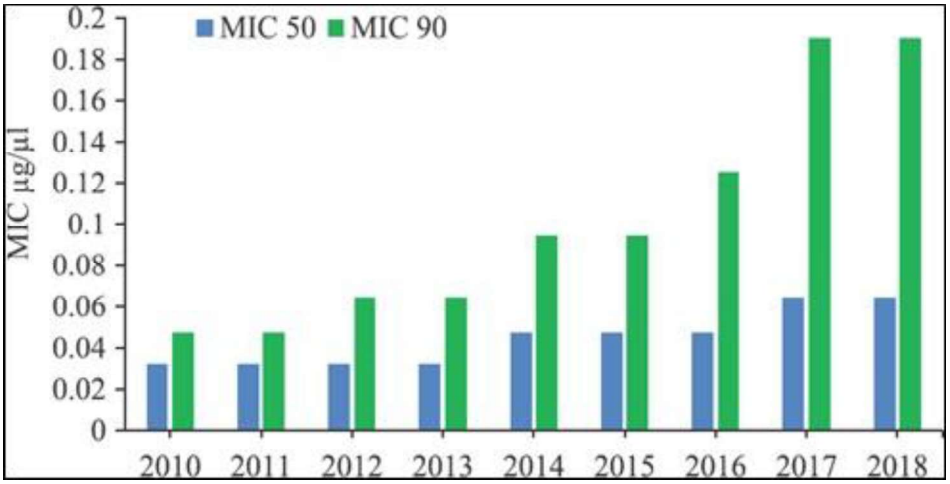

Figure 1.2. Creeping minimum inhibitory concentrations (MIC) for ceftriaxone in Salmonella Typhi and Salmonella Paratyphi A isolated from four nodal centers in ICMR-AMRSN from 2013 to 2018 (N=877). Adapted from Walia, 2019[21]

1.3. Antibiotic resistance mechanisms in bacteria

Antibiotics affect bacterial cells in a multitude of ways and bring cell death or inhibition of growth. Commonly used antibiotics target cell wall synthesis (β-lactams), protein synthesis (aminoglycosides, tetracyclines, chloramphenicols, macrolides), transcription (rifamycins), DNA synthesis (quinolones) and folate synthesis (sulphonamides). Since the discovery of penicillin in 1928 and its popular use several others were discovered and a huge volume of scientific research helped us unravel the mechanism of action of several antibiotics. However, the application of these antibiotics in clinics also slowly selected bacteria that were resistant to several of these antibiotics.

In 1940, even before the widespread use of penicillin in clinics, a bacterial penicillinase was identified by two members of the penicillin discovery team.

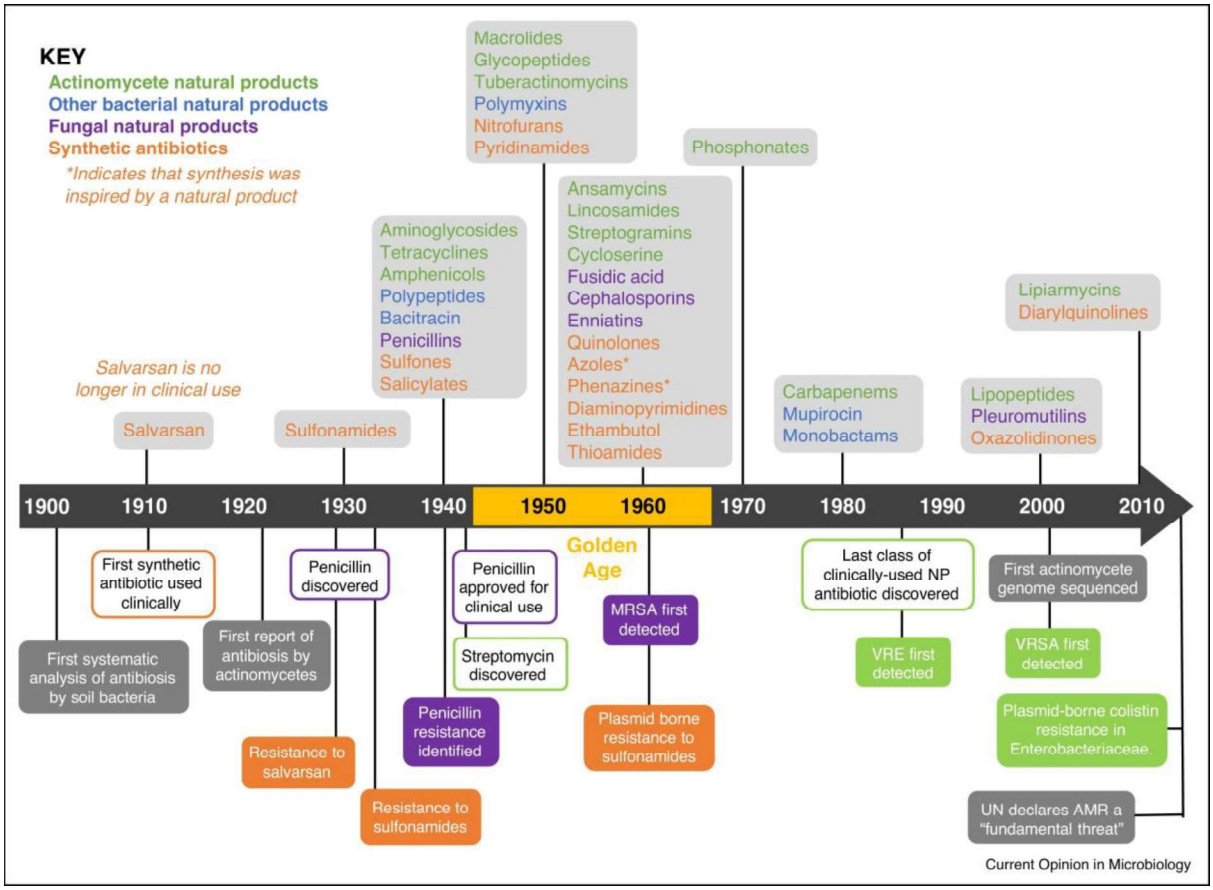

Figure 1.3. Emergence of resistance to different antibiotics [22]. Colour represent the source of antibiotics: green = actinomycetes, blue = other bacteria, purple = fungi and orange = synthetic

When streptomycin was used for the treatment of tuberculosis, resistant bacteria appeared during the course of the treatment itself. In mid 1950s the antibiotic resistance factors were found to be carried on parts of DNA that could be disseminated through an entire population of bacteria [22].

The antibiotic resistance is found to be either intrinsic or acquired [23]. *Mycobacterium tuberculosis* is intrinsically resistant to β-lactams as it carries a β-lactamase in its genome [24]. In addition to intrinsic resistance, bacteria can develop or acquire resistance to antibiotics by one of ***the three fundamental mechanisms***. First, minimize the effective concentrations of the antibiotic in the bacterial cells due to poor penetration or efflux; second,

alteration of the antibiotic target by genetic mutation or post-translational modification; and third, alteration of the antibiotic by chemical modification or hydrolysis [23].

Antibiotic entry into the cell is mainly through porins present in the outer membrane [23]. Mutations and reduced expression of porin genes result in a decrease in the entry of antibiotics and thus its effective concentration and efficacy. In nature, bacteria are bestowed with different efflux pumps that actively transport foreign molecules out of the cell. Many such efflux pumps form part of the strategy that bacteria employ to escape the effect of antibiotics. Mutations in the genes that encode pumps or their overexpression can give a survival advantage to bacteria against antibiotics. Antibiotics can be modified once they enter the cell. An array of enzymes has been identified in bacteria that act on different antibiotics. Within a single class of antibiotic variants of enzymes have been identified that act on different molecules belonging to a particular class. For e.g. β-lactamases that could act on different kinds of β-lactam antibiotics are known today. These enzymes have been known to be present in different bacteria like *E. coli*, *K. pneumoniae*, *P. aeruginosa* etc. Transfer of different chemical groups like phosphate, acyl, nucleotidyl has also been known that result in the decreased efficacy of the antibiotic. Particularly in case of aminoglycosides, it has been known that enzymes like acyl transferases, nucleotidyl transferases, and phosphotransferase impart resistance towards this class of antibiotics. Another mechanism of resistance exhibited by bacteria to escape the antibiotic that has entered the cell is to alter the target. Mutations that modify the target in a way that reduces the binding of the antibiotic without compromising its normal cellular function get selected and lead to emergence of a resistance population. Rifampicin-resistant *M. tuberculosis* contains mutations in the *rpoB* gene encoding the β-subunit of RNA polymerase [24]. Methylation of 23S ribosomal RNA (rRNA) by Erm methyltransferase leads to resistance towards macrolides. Synthesis of alternate pathways/products that are insensitive to antibiotics has also been observed, e.g. in

case of methicillin resistance, synthesis of PBP2a (methicillin insensitive) allows cells to continue cell wall synthesis. MfpA protein in *M. tuberculosis* allows synthesis of a pentapeptide that mimics B DNA structurally and binds to DNA gyrase protecting them from quinolones, thus contributing to resistance [23]. Further transcriptional regulation of a host of activities at gene level resulting in expression of proteins that help the bacteria overcome the effect of antibiotics has been identified [25]. For e.g. in Mycobacteria, the transcription factor WhiB7 is induced after stress induced by antibiotics. This results in expression of several antibiotic resistance-associated genes like *tap* (a multidrug transporter) and *ermMT* (ribosomal methyltransferase) [26].

Apart from antibiotic resistance another phenomenon that leads to low clearance of bacterial infections is persistence. Antibiotics kill bacteria by a rapid phase in which most bacteria are killed and another phase in which a low number of bacteria persist and are not killed. After clearance of antibiotic, these persister bacteria contribute to reoccurrence of infection. The persisters are genetically identical and they escape antibiotic by getting into an altered metabolic state. *M. tuberculosis* is one of the main human pathogens in which persistence has been observed.

Although resistance in bacteria to antibiotics has been studied and understood extensively, newer phenomena like persistence and tolerance do contribute significantly to antibiotic failure. Traditionally resistance is defined as an ability of a bacterium to grow in the constant presence of antibiotics whose concentration is not too high. In contrast, tolerance has been identified recently that allows the bacterium to survive exposure of high concentration of antibiotic for a limited time period, which usually is the case in clinic based on the pharmacological properties of the antibiotic. Tolerance by lag is the term that identifies the antibiotic driven phenotype in a bacterium and the target genes associated with it [27].

1.4. Impact of antibacterial resistance on health management

Recent studies have shown that infections caused by antibiotic-resistant bacteria result in higher mortality rates, longer duration of hospital stays, and higher health care costs compared to those that result from infections with their antibiotic-susceptible counterparts [28, 29]. Bacteria are responsible for approximately 90% of all HAIs [30]. Over 50% of healthcare-associated infections (HAIs) are caused by resistant strains [31]. Intensive care unit (ICU) patients are the most affected by HAI [30]. With 5% and 7.1% incidence rates in the US and the EU, respectively HAI is a major contributor to healthcare in the developed World [32]. In developing countries, HAI incidence is estimated to be 15.5% due to less stringent sterile medical practices [32]. Immunocompromised patients are more prone to HAI and exhibit higher mortality rates. On a comparative scale, infections by drug resistant bacteria possess a higher risk of fatality compared to drug sensitive ones [32]. The reason for this has been noted as prolonged bacterial load and lack of appropriate therapy rather than enhanced virulence [33]. The economic cost of AMR is narrowly defined as the incremental cost of treating patients with resistant infections as compared with sensitive ones, and the indirect productivity losses due to excess mortality attributable to resistant infections [31]. The total economic cost of resistant bacteria includes the direct and indirect costs. While the direct cost is the cost incurred during the treatment of a drug resistant pathogen compared to the sensitive counterpart, the indirect economic losses are due to productivity loss and premature death that affects the society.

The total economic cost of bacterial drug resistance the five pathogens (1. *Staphylococcus aureus* resistant to Oxacillin, 2. *Escherichia coli* resistant to 3rd generation cephalosporin, 3. *Klebsiella pneumoniae* resistant to 3rd generation cephalosporin, 4. *Acinetobacter baumannii* resistant to carbapenems, 5. *Pseudomonas aeruginosa* resistant to carbapenems) was $0.5 billion and $2.8 billion in Thailand (a developing country) and the United States (developed

country), respectively [31]. For e.g. the direct and indirect annual cost of drug resistance in bacteria in Thailand due to MRSA was estimated at $29 million and $151 million, respectively [31].

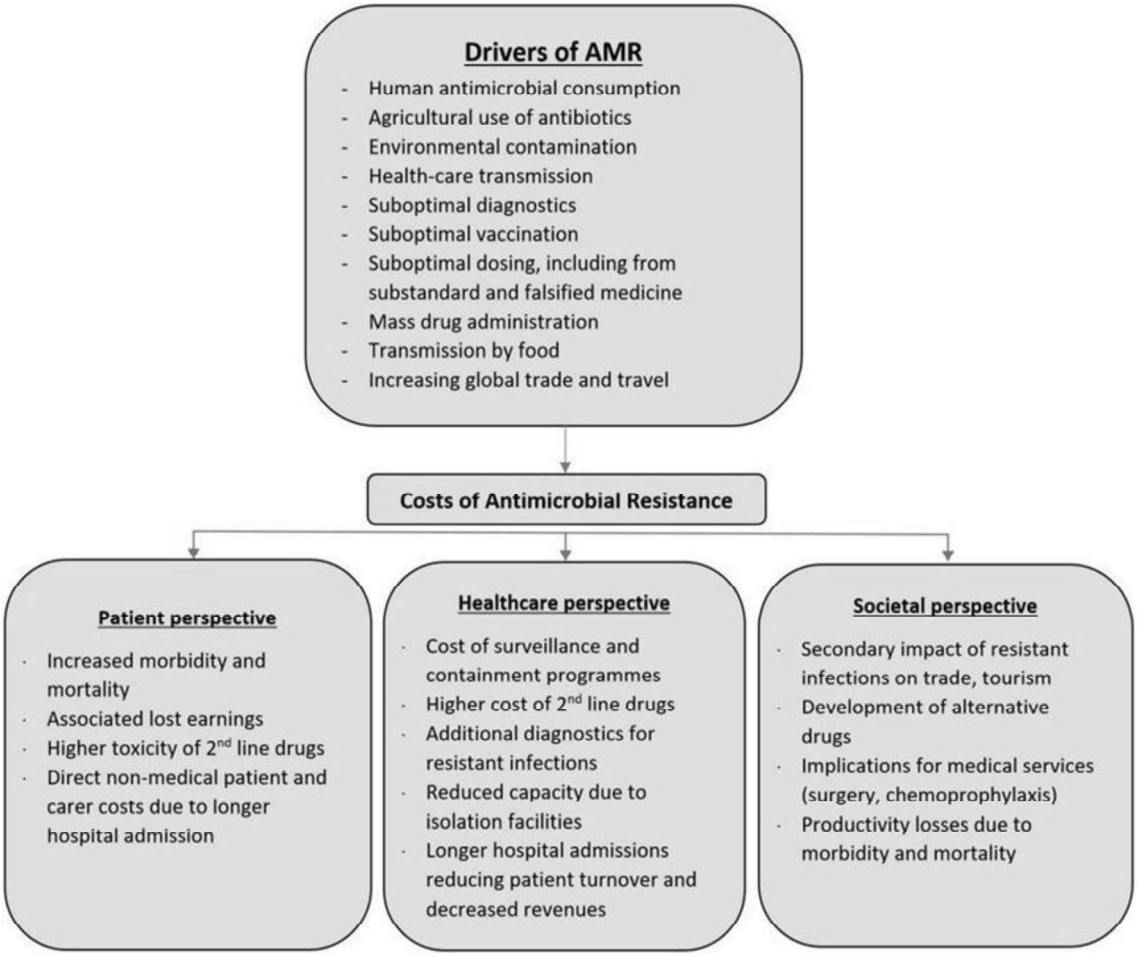

Figure 1.4. Enumerating the economic cost of antimicrobial resistance per antibiotic consumed to inform the evaluation of interventions affecting their use. Figure adapted from Shrestha [31].

A US study [28], revealed that HAI with drug resistant bacteria has a quantifiable and significant additional cost. Resistance was associated with a 29.3% higher total hospital cost and a 23.8% increased LOS compared to the cost and LOS for HAIs caused by susceptible counterparts. The different bacteria included in the study are Acinetobacter spp., *E. coli*, Enterobacter spp., Klebsiella spp., and Pseudomonas spp. The database used for this analysis

was created from a query of a larger database of all patients diagnosed with HAI in South Carolina medical hospital, Charleston between 1998 and 2008. He studies a cohort comprised of a sample of 662 patients from the age of newborn to 93 years admitted to an ICU or general hospital ward [28]. The impact of drug resistant bacteria on human health is so significant and beyond any doubt that it affects many walks of our life. When Louis Rice was unhappy with the pledge of the National Institute of Health for antibiotic resistant bacteria, he wrote a commentary in 2009 coining the term in 2009, ESKAPE [34]. The term an acronym for the most notorious drug resistant bacteria *Enterococcus faecium, Staphylococcus aureus, Klebsiella pneumoniae, Acinetobacter baumannii, Pseudomonas aeruginosa*, and *Enterobacter* species was to get the attention of policymakers towards the impending doom [34].

1.5. Novel approaches to antibacterial drug discovery and repurposing

The golden era of antibiotics has reaped of the benefits of early entry and plucked the proverbial low hanging fruits. More efforts and novel approaches are required to hunt newer molecules that could help humanity against pathogenic bacteria. Some novel approaches have become possible due to advent of newer technologies and advancement in science.

Nonculturable bacteria have become a target in our search for newer antibiotics. Bacteria produce antibiotics to eliminate competitors. Conventional antibiotics such as streptomycin have been derived from bacteria that grow on artificial solid or liquid media. It is believed a vast majority of species of bacteria do not grow on artificial media [35]. One approach to tap the potential of nonculturable bacteria is the use of a metagenomic approach. Large fragments of non-culturable bacterial genomes can be cloned and expressed using recombinant DNA technology that could yield us a clue towards a previously unknown molecule that targets bacteria [36]. Another successful approach to identify antibiotics from nonculturable bacteria is the invention of iChip which takes the growth conditions to the natural habitat of the

antibiotic producer rather than bringing it to the laboratory. The iChip was invented by Kim Lewis and Slava Epstein at Northeastern University in Boston, MA, USA in 2010 [37]. Using this technique teixobactin was discovered by the same authors in 2015 [38].

1.5.1. Trojan horse

Iron is essential for all forms of life. It also plays a critical role in the life of pathogenic bacteria by contributing to virulence. Bacteria possess several methods for iron assimilation. The most common method is the production of siderophores, low molecular weight iron (III) chelators, that chelate, and transport iron into the cell from extracellular environment [39, 40]. Due to the obligate iron requirement by the pathogens, a window of opportunity is created that could be exploited to kill the same if this iron uptake channel may be used to deliver agents that would kill the pathogen. Three approaches currently being pursued in this area include: 1) iron starvation via competitive chelation [41] 2) inhibition of siderophore biosynthesis [42] 3) siderophore-mediated drug delivery [40]. In an overly competitive environment bacteria have learned to hijack siderophore-iron complexes produced by other species [43]. As evolution would have it certain microorganisms devised methods to exploit this iron hijack for delivery of toxic molecules to siderophores. Naturally occurring siderophore drug conjugates are referred to as sideromycins. Some of the sideromycins known so far are danomycins, salmycins, albomycins, ferrimycins, and microcins [40]. Many research groups have been inspired by this and embarked on a quest to rationally design siderophore-drug conjugates and use them as Trojan horse [40].

1.5.2. Hybrid strategy

After the countless attempts to discover new synthetic scaffolds capable of overcoming drug resistance hybrid strategy was thought of. Molecular hybrids were developed by combining two agents into one heteromeric entity with the hope of deriving better activity than either

alone. Covalent linkers were designed to be either cleavable or non-cleavable. The hypothesis of antibiotic hybrids integrates the desire to overcome resistance by two agents into one with a single pharmacokinetic profile, an offshoot of combination therapy. Such hybrid molecules have been synthesized and evaluated employing β-lactam [44], aminoglycosides [45], and quinolones [46]. Certain other approaches pursued by different research groups towards finding a solution to drug resistant bacteria are phage therapy, antibody conjugates, and microbiome [47]. Phages have played a game of hide and seek about their pathogen treatment potential for decades, yet there is no treatment option that is visible on the horizon. This may be interpreted as this technology has a low chance of success. However, some groups pursue this seriously and with a hope for a breakthrough [47]. It is a well accepted fact now that the treatment outcome of an individual depends on the human gut microbiome. Any treatment can result in a disturbance the same e.g. antibiotic treatment, anticancer treatment etc. Since rate of restoration of this can have a bearing on the efficacy, many strategies have been tried to restore the gut microbiome e.g. with a fecal transplant, isolation of bacteria from healthy subject, and restoration of microbiome using them, organ specific microbiome restoration in lungs, etc [47]. Antibodies against bacteria or the toxins produced by them have also been attempted as a therapeutic module as an alternative to antibiotics [47]. In general phage therapy, gut microbiome and antibody therapy need a lot more research and development before they could become regular therapies that could replace antibiotics.

Over the past decade, it has become well accepted that the human gut microbiome has a major impact on the health and stability of the host. Broad-spectrum traditional antibiotics can eliminate large portions of the commensal bacteria, which can allow opportunistic pathogenic bacteria to establish in some circumstances.

1.6. Plants as a resource of antibacterial drugs

Medicinal properties of plants have been exploited by humans since very early times. The diversity of organic molecules that are bioactive in plants is very large compared to man-made chemical libraries. Many communities World over rely on plant products to find a cure for different ailments [48]. Plants remain a source of a wide variety of molecules like vitamins, carotenoids, flavonoids, isothiocyanates, sulfides, thiols, phenols, and alkaloids. These molecules contribute towards the management and cure of different ailments like diabetes, hepatitis, arthritis, cardiovascular, cerebrovascular diseases, and cancer [49]. A historical perspective of how plants have contributed towards management and cure of different ailments has been very well compiled already [50]. Plant-associated bacteria as agents for the management of soil and plant health are very well studied and documented [51]. However, information on bacteria infected plants as a source of antibacterial compounds is limited but not unexplored [52]. There is a vast difference in the repertoire of compounds that are constitutively produced and produced during infections in plants [53]. It is believed that of 250,000 species of higher plants worldwide, about 14%–28% have been investigated for a cure in a scientific manner [54]. This has left sufficient scope and opportunity to explore medicinal plants as an unexploited resource to find novel effective therapeutic compounds [55]. The low molecular weight molecules produced in response to microbial infections called phytoalexins are a source of antibacterial molecules. They involve a wide array of structures based on the type of plant and pathogen [53, 56]. Constitutively produced antibacterial molecules present in plants are called phytoanticipins [57] (since they are probably produced in anticipation to a bacterial attack). Plants have been estimated to produce over 1,00,000 low molecular mass natural products [57]. The pathways by which these molecules are produced have been worked out elaborately [57]. The antibacterial compounds produced by plants can be classified based on chemical structures into 11

different groups [58]. These include monoterpenes, sesquiterpenes, diterpenes, triterpenes, phenylpropanoids and stilbenoids, simple phenols and tropolones, flavonoids, alkaloids, polyketides and polyenes, sulfur products, and acyl phloroglucinols [58]. Apart from antibacterial compounds plants also produce resistance modifying agents that potentiate the activity of an antibiotic against a resistant strain e.g. piperine has been reported as the inhibitor of bacterial NorA efflux pump that sensitizes bacteria to ciprofloxacin [59]. Plants have also been reported to produce molecule that reverses the methicillin resistance by selectively inhibiting penicillin binding protein 2' as in the case of epicatechin gallate [60]). Totarol, a diterpene potentiate methicillin activity against MRSA by interfering with penicillin binding protein 2' expression [61]. Plant derived molecules like isopimarane diterpenes, reserpine, 5'-methoxyhydnocarpin, flavonolignan silybin, methoxylated flavones, and isoflavones have been shown to inhibit a variety of multidrug resistant pumps in *S. aureus* [58]. These reports go on show not only the chemical diversity of different plant derived molecules but also the diversity of their functions that could be exploited towards combating drug resistant bacteria. Unlike antibiotics that are isolated from soil bacteria plant derived molecules tend to have additional benefits in a complex multi-cellular human being. The beneficial effects of phytochemicals are attributed to their antimicrobial and antioxidant properties. In addition, the inclusion of phytochemicals in the diets alters and stabilizes the intestinal microbiota and reduces microbial toxic metabolites in the gut, owing to their direct antimicrobial properties on various pathogenic bacteria, which results in relief from intestinal challenge and immune stress, thus improving performance. Another important beneficial effect of dietary inclusion of phytochemicals is a reduction in oxidative stress and an increase in antioxidant activity in various tissues, and thus, improved health. Phytochemicals also exert their action through immunomodulatory effects such as increased proliferation of immune cells, modulation of cytokines, and increased antibody titer. Hence a host of benefits

could be achieved by a phytochemical rich preparation that covers different aspects of nutrition and health with minimal undesirable effects. The mechanism of action of phytochemicals is not clearly understood in most cases but may depend upon the composition of the active ingredients in the product being used. Some of the successful plant derived molecules that have been employed as antimicrobial agents is listed in Table 1.1.

Table 1.1. List of plant derived antibacterial compounds. The table adapted from Khameneh, 2019 [62].

Common name	**Scientific name**	**Compound**	**Target**	**Dosage form**
Barberry	*Berberis vulgaris*	Berberine	Bacteria, protozoa	Soft gel 1000 mg
Black pepper	*Piper nigrum*	Piperine	Fungi, Lactobacillus, Micrococcus, *E. coli*, *E. faecalis*	
Burdock	*Arctium lappa*		Bacteria, fungi, viruses	Capsule 475 mg
Caraway	*Carum carvi*		Bacteria, fungi, viruses	Capsule 1000 mg
Cascara sagrada	*Rhamnus purshiana*	Tannins	Bacteria, fungi, viruses	Capsule 425, 450 mg
Chamomile	*Matricaria chamomilla*	Anthemic acid	*M. tuberculosis, S. typhimurium, S. aureus*	
Clove	*Syzygium aromaticum*	Eugenol	General	Capsule 500 mg
Cranberry	Vaccinium spp.	Fructose	Bacteria	Capsule 500 mg
Eucalyptus	*Eucalyptus globulus*	Tannin	Bacteria, viruses	Inhaler and tablet
Garlic	*Allium sativum*	Allicin, ajoene	General	Tablet
Goldenseal,	*Hydrastis canadensis*	Berberine, hydrastine	Bacteria, *Giardia duodenale*, Trypanosomes	Solution, 500 mg per dosage
Green tea	*Camellia sinensis*	Catechin	General	
Licorice	*Glycyrrhiza glabra*	Glabrol	*S. aureus*, *M. tuberculosis*	Capsule 450 mg

Oak	*Quercus rubra, Allium cepa*	Tannins, Quercetin		Capsule 500 mg, 650 mg
Oregon grape	*Mahonia aquifolia*	Berberine	Plasmodium, Trypansomes, general	Capsule 500 mg
Senna St. John's wort	*Hypericum perforatum*	Hypericin, others	General	Table 450 mg
Thyme	*Thymus vulgaris*	Caffeic acid, Thymol, Tannins	Viruses, bacteria, fungi	Capsule 450 mg
Turmeric	*Curcuma longa*	Curcumin, Turmeric oil	Bacteria, protozoa	

Development of plant based antibacterial molecules has also witnessed improvement over the original discovery by making small structural changes. The antibacterial activity of Berberine was originally discovered followed by studies that revealed it to inhibit FtsZ [63]. This resulted in rational design of berberine based FTsZ inhibitors with broad spectrum antibacterial activity [64]. Similarly, derivatives of the antibacterial compounds carvacrol [65], cinnamaldehydes [66], emodin [67] and pinosylvin acid [54] were synthesized and evaluated for antibacterial activity with an objective to identify the groups contributing towards antibacterial activity and achieve better activity than the parent. Thus, plants form an important repository of antibacterial molecules that has serious relevance due to their consumption in the form of food and/or nutraceutical. Validation of some of the medicinal effects towards curing bacterial infections by certain plants should lead us towards antibacterial molecules, resistance modifiers, and resistance reversing phytochemicals. An effective antibacterial should have high selective toxicity, with potent activity at achievable concentrations against target bacteria and minimal effects on the host, chemical and physical stability after formulation to comply with the pharmaceutical specification, good bioavailability when administered by the chosen route, an appropriate pharmacokinetic profile and ideally, not readily give rise to resistant variants [68].

1.7. Conundrum of ROS and bacterial cell death

Antibacterial drugs either are bacteriostatic or bactericidal. Common antibiotics largely target inhibition of DNA replication and repair, inhibition of protein synthesis, and inhibition of cell-wall [69]. Although most of the molecular targets of the antibiotics have been worked out elaborately knowledge of specific sequence of events that translate the initial injury to cell death is lacking in many cases [70]. A hallmark research by Jim Collin's group proposed in 2007 [70]) that hydroxyl radicals are formed due to internal iron in the cells by Fenton reaction. This hydroxyl radical formation preceded by depletion of cellular NADH is common to bactericidal drugs and forms a route towards cell death. Further this did not happen in case of bacteriostatic drugs. However, this theory was contested in 2013 by two separate groups. Experiments proving that different antibiotics were equally effective in absence of oxygen ruled out direct involvement of ROS. Further direct measurement of hydrogen peroxide revealed post antibiotic treatment, hydrogen peroxide did not increase significantly to cause hydrogen peroxide stress. Free iron content also was found not to increase after treatment with different antibiotics [71]. Another independent study also found killing by antibiotics does not correlate to ROS production and it is difficult to propose ROS as a reason for cell death induced by different antibiotics [72]. It still remains a mystery, how cell death occurs after treatment with antibiotics, though the molecular target that undergoes damage is identified in several cases. It is also an open question if a common mechanism of cell death exists after treatment with different classes of antibiotics or each has its own set of molecular events that executes cell death in bacteria. In addition a report in 2015 revealed ROS contributed to antibiotic mediated killing in certain bacterial species. It also proposed enhancing ROS production or interfering with the protection against ROS may form a novel strategy to improve efficacy of antibiotics [73]. Despite the controversy surrounding the involvement of ROS in a common cellular death pathway after treatment with antibiotics, a

host of other reports have observed involvement of ROS in bacterial cell death. For e.g. Catechin a flavonol present in several plants was found to mediate the antibacterial effect by generating ROS [74]. Chloro-benzoquinones have been shown to cause oxidative damage through iron mediated ROS production in *E. coli* [75]. Epigallocatechin gallate, another flavonol was found to generate ROS and act in synergy with superoxide producing molecule paraquat [76]. A host of natural products possessing antibacterial activity have been reported to produce ROS and their antibacterial activity has been attributed to this property [77]. It has also been noted that binding of azole antibiotics to *Staphylococcus aureus* flavohemoglobin increases intracellular oxidative stress due to higher production of superoxide by flavohemoglobin [78]. Even inorganic moieties like silver ions [79] and engineered ZnO and TiO2 nanoparticles [80] have been shown to mediate antibacterial activity due to ROS generation and oxidative stress. These results indicate an intricate role of ROS in cell death upon treatment with different antibacterial molecules. To further add to the existing contradictions, a report showed sub-lethal vancomycin treatment may induce protective ROS in hVRSA, whereas reduction in ROS level in hVRSA strains (h=heterogenous) may increase their vancomycin susceptibility. Moreover, a low dose of ROS in VSSA (vancomycin susceptible *S. aureus*) strains may promote their survival after vancomycin exposure. These findings reveal that modest ROS generation may be protective for vancomycin resistance in hVRSA [81]. Diffusible ROS was found not to play a role in the antibacterial action of phytoalexin resveratrol [82] stating different natural products may not follow a common mechanism despite having structural similarity. From these reports, one can safely conclude ROS does play a very important role in killing bacteria after treatment with different antibacterial drugs. However, it is not clear as of now if ROS pathway is a common mechanism that perceives insults to different targets in the cell and executes death. It is also not known if the cells that are protected by the external addition of antioxidants after

exposure to genotoxic antibacterial agents do survive with certain mutations or their genome completely repaired.

1.8. Factors unique to phytochemical drugs

Though traditionally used for health benefits scientific documentation of the action of phytochemicals is largely lacking. It is necessary to understand the mechanisms behind the action of phytochemicals at the cellular level as well as animal level. This will enable the rational use of them employing appropriate concentrations, devise strategies to combine them with existing therapies and understand the pleiotropic effects. Phytochemicals unlike antibiotics have been known to affect different targets inside the cell that contribute to cell death.

Many phytochemicals exhibit nonmonotonic dose/concentration-response termed biphasic dose-response [83]. The phytochemicals Resveratrol, Genistein, Quercetin, Biochanin A, Kaempferol, and Sulforaphane have been recorded to exhibit biphasic behavior towards different biological endpoints [83]. The reason behind such behavior is not known in most cases and it will be most intriguing to know the different molecular targets, the intensity of the response, and subsequently how the fate of the cell is decided.

Another perennial question that remains in phytochemical research is whether it is prudent to use of crude extracts or isolated pure compounds. Traditional medicines have always been extracts and not pure compounds. The Indian traditional medicinal system always uses crude extracts only an does not prefer the use of pure compound. On contrary, the western medicine always uses the principal component responsible for the biological activity and not a mixture of several molecules. This contradictory school of thoughts have always been at logger's heads. However, there is no denial towards the fact that both have made immense contributions to saving human lives from different ailments. The extracts are believed to work in a synergistic fashion contributed by the different components present [84] which

cannot be matched by a single component alone. In case of *Hypericum hircinum*, the methanolic extract possessed antimicrobial activity while none of the individual components possessed any antimicrobial activity [85]. In case of artemisinin, the antiplasmodial activity of the extract is better than the pure compound because the extract helps better absorption of artemisinin [86]. The same has been observed in case of *Cinchona* alkaloids as well [86]. Mechanistic understanding of the antibacterial activity of the phytochemicals is necessary as only this would lead to their proper utilization as standalone drugs or as helper molecules. For e.g. Clavulanic acid a natural product that by itself did not possess any antibacterial activity was found to be an excellent augment for β-lactam amoxicillin due to its ability to inhibit β-lactamases [87]. Similarly, the Berberis medicinal plants produce Berberine that is antibacterial but suffers due to efflux. Later it was found Berberis plants also produce a multidrug pump inhibitor 5′-methoxyhydnocarpin that by itself is not antibacterial [88]. Catechins, polyphenols derived from tea leaves, have been shown to have antibacterial properties, through direct killing of bacteria as well as through inhibition of bacterial toxin activity [89]. Similarly, resveratrol was shown to affect gram negative bacterium *E. coli* by membrane damage and site specific ROS damage [82]. Berberine, a natural alkaloid was shown to damage intracellular proteins, affected synthesis of DNA, and fragmented the membrane [90]. Another phytochemical epigallocatechin gallate affected the proteins involved in the septum formation, DNA segregation, and cell division [91]. Thus, though we have a plethora of phytochemicals that act as antibacterial agents, we have not understood the mechanism of action of many of these completely. This could be a serious impediment towards realizing their potential and developing them as successful drugs.

The objective of the current investigation

- To evaluate and develop plant derived molecules as potential antibacterial agents
- To understand the mechanism of action.
- To evaluate if they could be augment activity of exiting antibiotics.
- To test potential molecules in animal model.

CHAPTER 2. MATERIALS AND METHODS

2.1 Materials

2.1.1. Plasticware and Glassware

Microcentrifuge tubes (1.5 mL and 2 mL), 50 mL conical tubes, and tips boxes were procured from Tarsons, India or Axygen, USA. PCR tubes (0.2 mL) and pipettes tips were obtained from Axygen, USA. The 96-well plates and cryovials were obtained from Laxbro, India, and Axygen, USA. All glassware and glass Petri dishes were from Corning USA or Borosil, India. All plasticware and glassware were sterilized by autoclaving at 15 psi/121 ℃ for 15 min.

2.1.2. Chemicals, Media, Buffers and Reagents

Table 2.1.1. List of chemicals used in present study.

Name of the chemicals	**Source**
6× gel loading dye	New England Biolabs Inc.
Agar	Becton Dickinson, USA
Agarose	Sigma-Aldrich Corporation, USA
ATP Determination Kit (A22066)	Thermo Fisher Scientific, USA
BHI Broth	HiMedia, India
Bipyridyl	Sigma-Aldrich Corporation, USA
Bradford Reagent	BioRad, USA
Calcein	Thermo Fisher Scientific, USA
Carboxyfluorescein succinimidyl ester (CFSE)	Thermo Fisher Scientific, USA
Chloramphenicol	Sigma-Aldrich Corporation, USA
Cyclophosphamide monohydrate	HiMedia, India
DCFDA	Sigma-Aldrich Corporation, USA
DHE	Sigma-Aldrich Corporation, USA
Dimethyl Sulfoxide (DMSO)	Santa Cruz Biotechnology, USA
DMEM	HiMedia, India
Doxorubicin	Sigma-Aldrich Corporation, USA
EDTA	Merck, Germany
Ellman's Reagent	Thermo Fisher Scientific, USA
Erythromycin	Sigma-Aldrich Corporation, USA
Ethidium bromide (EtBr)	SISCO Research Laboratories Pvt. Ltd. (SRL) – India
Ezy MIC™ Strip	HiMedia, India
Fetal Bovine Serum	Thermo Fisher Scientific, NY, USA

GIBCO® trypsin solutions	Thermo Fisher Scientific, USA
Glutathione	Sigma-Aldrich Corporation, USA
GSH Assay kit CS0260	Sigma-Aldrich Corporation, USA
Heat and Run DNase- gDNA	Arctic Zymes, Norway
HEPES dry powder	Sigma-Aldrich Corporation, USA
Hoechst 3342	Sigma-Aldrich Corporation, USA
Kanamycin	Sigma-Aldrich Corporation, USA
Lysozyme	Sigma-Aldrich Corporation, USA
MTT	Sigma-Aldrich Corporation, USA
Mucin from porcine stomach	Sigma-Aldrich Corporation, USA
Mueller Hinton (MH) broth	HiMedia, India
NaCl	Sigma Aldrich, MO, USA
Neocuproine	HiMedia, India
N-Lauroylsarcosine	Sigma-Aldrich Corporation, USA
Novobiocin	Sigma-Aldrich Corporation,
NucleoSpin RNA II	(Macherey-Nagel, Germany) Kit
Penicillin	Sigma-Aldrich Corporation, USA
$CsCl_2$ purified Plasmid DNA	Bangalore Genei, India
Propidium iodide	Sigma-Aldrich Corporation, USA
Protein carbonylation kit	Cayman Chemical, Ann Arbour, MI, USA
qScript cDNA synthesis kit	Quanta Biosciences, USA
Rifampicin	HiMedia, India
RNAse A	Sigma-Aldrich Corporation, USA
Streptomycin	Sigma-Aldrich Corporation, USA
Syber green II dye	Thermo Fisher Scientific, USA
SYTO-PI kit (L7012)	Thermo Fisher Scientific, USA
TBARS assay kit	Cayman Chemical, Ann Arbour, MI, USA
Tetracycline	Sigma-Aldrich Corporation, USA
Thiazolyl Blue Tetrazolium Bromide	Sigma-Aldrich Corporation, USA
Thiourea	Sigma-Aldrich Corporation, USA
Triton X-100	Sigma-Aldrich Corporation, USA
Trypan blue	Thermo Fisher Scientific, USA
Tryptone	Becton Dickinson, USA
Vancomycin	HiMedia, India
Yeast Extract	Becton Dickinson, USA

2.1.1.1. LB Medium

LB medium is known as Lysogeny Broth or Luria Broth or Luria Bertani medium.

Table 2.1.2 Composition of LB medium (1000 mL)

Ingredients	**Weight (g)**
Tryptone	10

Yeast extract	5
NaCl	10

For LB agar preparation, 2% Bacto agar was added in 1000 mL LB medium and autoclaved at 15 psi/121 ℃ for 15 min**.** Autoclaved LB agar was cooled down to 55 ℃ and then poured into sterile Petri plates for solidification. Solidified LB agar dishes were inverted and placed in the incubator for 16-18 h at 37 ℃. At the end of incubation, plates were sealed with parafilm and stored in plastic bags at 4 ℃ for 10 to 15 days.

2.1.1.2. MH Medium

To prepare MH medium, 21 g was dissolved in 1000 mL of distilled water.

Table 2.1.3. Composition of MH medium (1000 mL)

Ingredients	**Weight (g)**
Beef infusion	300
Casein acid hydrolysate	17.5
Starch	1.5

For MH agar, 2 % Bacto agar added to medium and autoclaved under standard conditions as described above.

2.1.1.3. BHI Medium

To prepare BHI medium, 37 g was dissolved in 1000 mL distilled water and autoclaved at 15 psi/121 ℃ for 15 min**.**

Table 2.1.4 Composition of BHI medium (1000 mL)

Ingredients	**Weight (g)**
HM infusion powder	12.5
BHI powder	5
Proteose peptone	10
Dextrose (Glucose)	2

NaCl	5
Na_2HPO_4	2.5

Final pH was adjusted 7.4±0.2 at 25 ℃.

For BHI agar, 1.5% Bacto agar was used to solidify the medium and autoclaved at 15 psi/121 ℃ for 15 min**.**

2.1.1.4. NB Medium

To prepare NB medium, 25 g was dissolved in 1000 mL distilled water and sterilized by autoclaving at 15 psi/121 ℃ for 15 min.

Table 2.1.5. Composition of NB medium (1000 mL)

Ingredients	**Weight (g)**
Peptone	10
Beef extract	10
NaCl	5

Final pH was adjusted 7.3±0.1

2.1.1.5. DMEM Medium

DMEM medium was used to grow the animal cell lines. DMEM medium was supplemented with 10% FBS, 2 mM glutamine and 100 unit/mL penicillin and 100 μg/ml streptomycin**.**

2.1.1.6. PBS buffer

Table 2.1.6. Composition of PBS (1000 mL)

Ingredients	**Weight (g)**
Sodium chloride	8
NaH_2PO_4	0.24
Na_2HPO_4	1.44
KCl	0.2

All contents were dissolved in 1000 mL ion free water and mixed with a magnetic stirrer. The buffer was autoclaved at 15 psi/121 ℃ for 15 min.

2.1.1.7. Saline

Saline was prepared by dissolving 0.83 g sodium chloride in 100 mL ion free water. Saline was sterilized by autoclaving at 15 psi/121 ℃ for 15 min.

2.1.1.8. TAE buffer

Table 2.1.7. TAE buffer composition for 1000 mL

Ingredients	**Weight (g)**
Tris	4.8
Glacial acetic acid	1.14
0.5 M EDTA	2

All contents were dissolved in 1000 mL ion free water and mixed with a magnetic stirrer and autoclaved at 15 psi/121 ℃ for 15 min.

2.1.1.9. HEPES buffer

To prepare 100 ml of 0.1 M of HEPES buffer, 2.38 g HEPES added in 80 mL of ion free water and adjusted to pH 7.4 with 5 N NaOH solution. The buffer solution was autoclaved at 15 psi/121 ℃ for 15 min.

2.1.1.10. Glycerol stock

Glycerol was used as a cryoprotectant. The stock solution of glycerol (80%) was prepared in distilled water and autoclaved at 15 psi/121 ℃ for 15 min.

2.1.1.11. SDS-polyacrylamide gel

Table 2.1.8. Composition of 5% stacking and 12% resolving gel

Ingredients	**5% Stacking gel (mL)**	**12% Resolving gel (mL)**
Water	3.4	5.8

30% acrylamide	0.83	8
Tris-Cl	0.63 (pH 6.8, 1 M)	5.8 (pH 8.8, 1.5 M)
10% SDS	0.05	0.2
10% Ammonium persulfate	0.05	0.2
TEMED	0.005	0.01
Total volume	5	20

2.1.1.12. Lysozyme

To prepare 10 mg/mL lysozyme, 10 mg lysozyme was dissolved in 1 mL of PBS.

2.1.1.13. To prepare SDS PAGE running buffer

Table 2.1.9. SDS PAGE running buffer composition for 1000 mL

Ingredients	**Weight (g)**
Tris base	3
Glycine	14.4
SDS	10

2.1.1.14. Tris-Cl, pH 8.8

To prepare 500 mL volume of 1.5 M Tris-Cl, 90.75 g Tris base was dissolved in 400 mL distilled water and concentrated HCl was used to adjust pH 8.8. The solution was autoclaved at 15 psi/121 ℃ for 15 min and stored at ambient temperature.

2.1.1.15. Tris-Cl, pH 6.8

To prepare 500 mL volume of 0.5 M Tris-Cl, 40.38 g Tris base was dissolved in 400 mL of distilled water and pH 6.8 adjusted with concentrated HCl. The solution was autoclaved at 15 psi/ 121 ℃ for 15 min and stored at ambient temperature.

2.1.1.16. SDS solution

To prepare 10% SDS stock, 10 g SDS was dissolved in 100 mL of distilled water and stored at ambient temperature.

2.1.1.17. APS

To prepare 10% APS stock, 1 g APS was dissolved in 10 mL autoclaved distilled water and stored at 4 ℃ for 2-3 weeks.

2.1.1.18. SDS-PAGE gel staining and destaining solution

To prepare staining solution of SDS-PAGE gel, 0.5% CBB 250 dye was dissolved in 500 mL methanol, 100 mL glacial acetic acid in 400 mL distilled water. Solution was filtered by the filter paper for removal of insoluble elements.

To prepare destaining solution of SDS PAGE, 100 mL methanol mixed with 100 mL glacial acetic acid, 20% glycerol in 780 mL of distilled water.

2.1.1.19. Cracking buffer

Table 2.1.10. 2× cracking buffer composition for 10 mL

Ingredients	**Volume (mL)**
10% (w/v) SDS	4
Glycerol	2
1 M Tris-Cl (pH 6.8)	1.2
Distilled water	2.8

Bromophenol blue (0.02%, w/v) was added and stored 2× cracking buffer at room temperature.

2.1.1.20. Magnesium chloride solution ($MgCl_2$)

To prepare 1 M $MgCl_2$, 9.52 g of $MgCl_2$ was dissolved in 100 mL ion free water and autoclaved at 15 psi/ 121 ℃ for 15 min.

2.1.1.21. Agarose gel

To prepare 1% agarose gel, 1 g agarose was added in 100 mL TAE buffer, and heated at high temperature to dissolve agarose. EtBr (10 µL from 20 mg/mL stock solution) was added, mixed and poured in the casting tray with a comb in place. After solidification, the comb was removed and the agarose gel was used for electrophoresis of DNA.

2.1.1.22. Ethidium bromide solution

The 20 mg/mL EtBr stock was prepared by dissolving 200 mg EtBr in 10 mL of autoclaved ion free water. The stock was aliquoted in different tubes, wrapped with aluminium foil and stored at 4 ℃.

2.1.1.23. DNA loading dye

To prepare 6× DNA loading dye, 25 mg bromophenol blue, 25 mg xylene cyanol and 3.3 mL glycerol were dissolved in 6.7 mL autoclaved distilled water. The dye was aliquoted in different tubes and stored at -20 ℃.

2.1.1.24. Fluorescent dyes

DCFDA, DHE, Calcein, Hoechst, CFSE, RH123 and PI dyes were employed in the current investigation. The stock solutions were prepared as given below.

Table 2.1.11. List of fluorescent dye solutions

Sr. No.	**Fluorescent Dye**	**Stock solution**
1	CFSE	20 mM in DMSO
2	DCFDA	20 mM in DMSO
3	DHE	20 mM in DMSO
4	Calcein	2 mM in DMSO
5	Hoechst 33342	5 mg/mL in DMSO
6	PI	20 mM in DMSO
7	SYTO 9	3.34 mM in DMSO

8	RH123	1 mg/mL in DMSO

All dyes were light sensitive. The stock solutions were wrapped in aluminium foil and stored at -20 ℃.

2.1.1.25. Reagents for DTNB assay

The composition of reaction buffer was 0.1 M sodium phosphate, pH 8.0, containing 1 mM EDTA. Ellman's Reagent (DTNB 4 mg/mL) was prepared by dissolving 4 mg reagent in 1 mL of reaction buffer.

2.1.1.26. Reaction buffer composition for ATP estimation

To prepare 10 mL of reaction buffer, 0.5 mL reaction buffer (part of the kit) from 20× stock solution, 0.1 mL DTT from 0.1 M stock solution, 0.5 mL D-luciferin from 10 mM stock solution and 2.5 µL firefly luciferase from 5 mg/mL stock was added in 8.9 mL of distilled water.

2.1.1.27. Reagent for lipid peroxidation estimation

To prepare reagent used for developing the chromogen, 530 mg TBA was dissolved in 50 mL of acetic acid solution (20%) and mixed with 50 mL of sodium hydroxide (1×) in a 150 mL glass beaker. That solution was stable at ambient temperature for 24 h.

2.1.1.28. Reagents for protein carbonylation estimation

To prepare DNPH (2,4-dinitrophenylhydrazine) solution, a vail content (provided by kit) was dissolved in 10 mL of 2.5 M HCl, dissolved DNPH aliquoted and stored at 4 ℃ for one week.

2.1.3. List of antibiotics

Table 2.1.12. List of antibiotics used in the current investigation

Sr. No.	**Antibiotic**	**Stock solution**
1	Kanamycin	100 mg/mL in ion free water

2	Chloramphenicol	10 mg/mL in 100% ethanol
3	Tetracycline	10 mg/mL in 70% ethanol
4	Rifampicin	10 mg/mL in 100% methanol
5	Erythromycin	10 mg/mL in 100% ethanol
6	Novobiocin	100 mg/mL in ion free water
7	Vancomycin	100 mg/mL in ion free water

2.1.4. List of bacterial strains

Table 2.1.13. List of microbial strains used in the current investigation were procured from IMTECH, Chandigarh, India.

Sr. No	Name of the culture	MTCC number
1.	*Pseudomonas aeruginosa*	2488
2.	*Salmonella enterica subsp arizonae*	660
3.	*Proteus vulgaris*	426
4.	*Klebsiella pneumoniae*	10309
5.	*Escherichia coli* BW25113	-
6.	*Staphylococcus chromogenes*	6153
7.	*Staphylococcus epidermidis*	3615
8.	*Staphylococcus aureus*	737
9.	*Streptococcus mutans*	497

Table 2.1.14. List of mutant strains used in the current investigation were procured from keio collection.

Sr. no.	Name of the strain	Referred in the text as	Genotype
1.	*E. coli* K12 BW25113	BW25113/ wild type	F^-, Δ(araD-araB)567, ΔlacZ4787(::rrnB-3), λ^-, rph-1, Δ(rhaD-rhaB)568, hsdR514
2.	JW1625	Nth	F^-, Δ(araD-araB)567, ΔlacZ4787(::rrnB-3), λ^-, Δnth 738::kan, rph-1, Δ(rhaD-rhaB)568, hsdR514
3.	JW0704	Nei	F^-, Δ(araD-araB)567, ΔlacZ4787(::rrnB-3), λ^-, Δnei 738::kan, rph-1, Δ(rhaD-rhaB)568, hsdR514
4.	JW3610	mutM	F^-, Δ(araD-araB)567, ΔlacZ4787(::rrnB-3), λ^-, ΔmutM 738::kan, rph-1, Δ(rhaD-

			rhaB)568, hsdR514
5.	JW3677	recF	F⁻, Δ(araD-araB)567, ΔlacZ4787(::rrnB-3), λ⁻, ΔrecF 735::kan, rph-1, Δ(rhaD-rhaB)568, hsdR514
6.	JW2788	recB	F⁻, Δ(araD-araB)567, ΔlacZ4787(::rrnB-3), λ⁻, ΔrecB745::kan, rph-1, Δ(rhaD-rhaB)568, hsdR514
7.	JW0205	dnaQ	F⁻, Δ(araD-araB)567, ΔlacZ4787(::rrnB-3), λ⁻, ΔdnaQ745::kan, rph-1, Δ(rhaD-rhaB)568, hsdR514
8.	JW2669	recA	F⁻, Δ(araD-araB)567, ΔlacZ4787(::rrnB-3), λ⁻, ΔrecA774::kan, rph-1, Δ(rhaD-rhaB)568, hsdR514
9.	JW4019	uvrA	F⁻, Δ(araD-araB)567, ΔlacZ4787(::rrnB-3), λ⁻, ΔuvrA753::kan, rph-1, Δ(rhaD-rhaB)568, hsdR514
10.	JW1173	umuC	F⁻, Δ(araD-araB)567, ΔlacZ4787(::rrnB-3), λ⁻, ΔumuC753::kan, rph-1, Δ(rhaD-rhaB)568, hsdR514
11.	JW2663	gshA	F⁻, Δ(araD-araB)567, ΔlacZ4787(::rrnB-3), λ⁻, ΔgshA753::kan, rph-1, Δ(rhaD-rhaB)568, hsdR514
12.	JW5503	tolC	F⁻, Δ(araD-araB)567, ΔlacZ4787(::rrnB-3), λ⁻, ΔtolC753::kan, rph-1, Δ(rhaD-rhaB)568, hsdR514
13.	JW0114	acnB	F⁻, Δ(araD-araB)567, ΔlacZ4787(::rrnB-3), λ⁻, ΔacnB753::kan, rph-1, Δ(rhaD-rhaB)568, hsdR514
14.	JW1122	Icd	F⁻, Δ(araD-araB)567, ΔlacZ4787(::rrnB-3), λ⁻, Δicd753::kan, rph-1, Δ(rhaD-rhaB)568, hsdR514
15.	JW0723	cydB	F⁻, Δ(araD-araB)567, ΔlacZ4787(::rrnB-3), λ⁻, ΔcydB753::kan, rph-1, Δ(rhaD-rhaB)568, hsdR514
16.	JW3205	Mdh	F⁻, Δ(araD-araB)567, ΔlacZ4787(::rrnB-3), λ⁻, Δmdh753::kan, rph-1, Δ(rhaD-rhaB)568, hsdR514
17.	JW0716	sucB	F⁻, Δ(araD-araB)567, ΔlacZ4787(::rrnB-3), λ⁻, ΔsucB753::kan, rph-1, Δ(rhaD-rhaB)568, hsdR514
18.	JW2514	iscS	F⁻, Δ(araD-araB)567, ΔlacZ4787(::rrnB-3), λ⁻, ΔiscS753::kan, rph-1, Δ(rhaD-rhaB)568, hsdR514

2.1.5. Clinical Isolates

After BARC Hospital ethical committee approval, clinical isolates of gram negative bacteria and gram positive bacteria were obtained from BARC Anushakti Nagar hospital. *S. aureus* (ATCC 25923) was obtained from Radiopharmaceutical Division (RPhD). Permission to use the bacterial strains isolated from the patients during the diagnostic procedures, for experiments in our investigation was obtained from the BARC Hospital ethics approval committee.

Table 2.1.15. List of clinical isolates used in the current investigation.

Sr. No	Name of the Clinical isolates	Number of isolates
1.	*Pseudomonas aeruginosa*	1
2.	*Proteus mirabilis*	3
3.	*Klebsiella pneumoniae*	9
4.	*Escherichia coli*	14
5.	*Methicillin-sensitive Staphylococcus aureus*	4
6.	*Methicillin-resistant Staphylococcus aureus*	2

2.1.6. Procurement of cell lines

L929 (mouse fibroblast cell line) and INT 407 (human cervical cell line) were procured from National Centre for Cell Sciences, Pune, India.

2.1.7. Procurement of animals

Swiss mice were used in this study. They were procured from BARC animal house facility. The animals used in each experiment were either males or females, but not mixed. The body weight of the animals procured was in the range of 20-25 g.

2.2. Methods

2.2.1. Methods related to isolation, storage of compounds and bacteria

2.2.1.1. Long term storage of bacterial cultures/mammalian cells

The long term storage of bacterial cultures was achieved by preparing glycerol stocks and storing them at -70 ºC. Sterile glycerol solution (80%) was prepared by autoclaving (15 psi/121ºC, 15 min). A single colony was inoculated in the growth medium and grown to mid log phase (Absorbance 600 nm = 0.5). The sterile glycerol solution and the mid log phase growth of culture was mixed in a 1:4 ratio in a sterile screw capped vial in a BSL-2 cabinet.

The mammalian cells were grown in a complete DMEM medium to 80% confluence in T-75 flasks and harvested by 0.05% trypsin treatment (5 mL) for 5-7 min. The cells were washed with sterile PBS twice before trypsin addition. The trypsin was inactivated by addition of medium with FBS (10 mL). The cells were collected by centrifugation (1000 ×g/5 min). The cells were counted in a haemocytometer after treatment with 0.4% trypan blue to check for viability. The cell density was adjusted to 1×10^6 cells/mL in a complete DMEM medium supplemented with 5% DMSO on ice. The vials were stored in freezer box at -70 ºC to allow temperature to decrease at the rate of 1 ºC/min. After overnight incubation, the vials were transferred to liquid nitrogen storage containers for long term storage.

2.2.1.2 Short term maintenance of bacterial cultures/mammalian cells

The cultures were revived from -70 ºC storage by streaking them on sterile agar solidified growth medium in Petri plates. The cultures were grown by incubating the plates at 37 ºC for 24 h. The plates were stored at 4 ºC and used for not more than 1 week.

For short term maintenance and use in experiments, the mammalian cells were revived from liquid nitrogen storage. The contents of the vials were thawed, diluted with 10 mL DMEM medium (supplemented with 10% FBS) in an animal cell culture lab inside a biosafety

cabinet. The diluted contents were centrifuged (1000 × g/5 min) and the cell pellet resuspended gently in the same medium. The contents were transferred to a T-25 flask with vented lid and incubated at 37 ºC in 5% CO_2 atmosphere for 24 h. The cells were maintained or propagated in the growth medium with 10% FBS by serial passage. The cells used in experiments were passaged less than 10 times.

2.2.1.3. Isolation of HC from *Piper betle* leaves

HC was isolated from *Piper betle* leaves by solvent extraction and characterized by NMR spectroscopy [92]. The leaves were dried at ambient temperature for 4-5 days, crushed into a coarse powder in a mixer. Dried, powdered leaves (500 g) were immersed in methanol (1.5 L) overnight at ambient temperature. The extract was condensed and treated with charcoal (50 g). The filtrate after charcoal treatment was passed through silica gel column (100–200 mesh size; solvent petroleum ether: ethyl acetate 0–15%) to purify HC by column chromatography. The structure and purity of HC was confirmed by NMR. The yield of HC was 1 g from 100 g of dried Piper betel leaves. This part of the work was performed by a collaborator.

2.2.1.4. Synthesis and characterization of dimer stilbene (DS)

4-Methoxybenzaldehyde (**1**) was treated with low valent titanium reagent (LVT) (generated by refluxing Zn with $TiCl_4$ in THF for 3-4 hrs) to get trans-stilbene **2** which on demethylation using BBr_3 at ambient temperature in 12 h yielded its dimer **3** [93].

Scheme 1

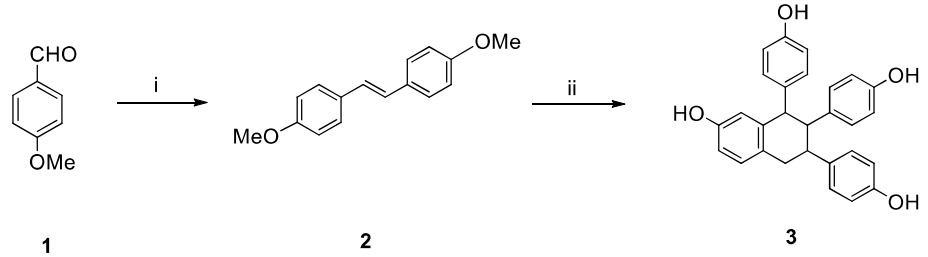

1 **2** **3**

i) Zn dust, $TiCl_4$, Dry THF, reflux, 6 hrs; ii) BBr_3, Dry DCM, 25^{o}C, 12 hrs.

a. Synthesis of 4,4'-dimethoxy stilbene (**2**)

To a mixture of Zn dust (1.44 g, 22.03 mmol) in dry THF (50 mL) at 0 ºC $TiCl_4$ (4.18 g, 22.03 mmol) was added dropwise and the mixture was refluxed with constant stirring for 3-4 h. The mixture was then cooled to 0 ºC and p-methoxybenzaldehde (**1**) (1.00 g, 7.34 mmol) was added dropwise with constant stirring and the mixture was refluxed for 3 h. After completion of reaction, it was quenched with ethyl acetate and water, the organic layer was separated, washed with water and brine and purified by column chromatography to get 4,4'-dimethoxy stilbene (**2**) (0.80 g) as a white solid (Yield 90.70 %).

b. Synthesis of DS (**3**)

To a mixture of 4,4'-dimethoxy stilbene (**2**) (1.00 g, 4.16 mmol) in dry DCM (50 mL) BBr3 (3.13 g, 12.48 mmol) was added dropwise at -30 ºC with constant stirring. The mixture was then brought to ambient temperature and stirred for 12 h. After completion of reaction it was quenched with water and extracted with ethyl acetate. The organic layer was separated, washed with water and brine and purified by column chromatography to get DS (**3**) (0.78 g) as a white solid (Yield 88.38 %). This part of the work was performed by a collaborator.

2.2.1.5. Preparation of stock solution of test compounds

The stock solution of the respective test compounds was prepared by dissolving the compounds in DMSO. Appropriate dilutions were prepared as per the experimental need. The final concentration of DMSO was 1% (v/v) or less. All the experiments had vehicle control. The stock of the compound was aliquoted and stored at -20 ºC for not more than a month. Whenever a stock was thawed it was used within a week and stored at 4 ºC during this period.

2.2.2. Methods related to evaluation of growth and viability of bacteria

2.2.2.1. Assessment of bacterial sensitivity

a) Micro dilution method and b) Plating

The sensitivity of different microorganisms was evaluated according to CLSI guidelines (Kassim, Omuse et al. 2016) by preparing MH medium with different concentrations of test compounds in 1% DMSO. The microtiter plate based assay was performed with an initial cell number of 5×10^5 cells per well in a volume of 0.2 mL. After incubation for 18 h, the absorbance was measured at 600 nm. Minimum Inhibitory Concentration (MIC) was determined by absence of visible growth at the minimum concentration of the test compound. Minimum Bactericidal Concentration (MBC) was determined by spotting 10 µL from the treatments that did not show visible growth on agar solidified growth medium in Petri plate. After 24 h of incubation, the minimum concentration of the test compound that revealed a complete absence of growth was taken as the MBC.

2.2.2.2. Study of growth curve of bacteria

Growth curve of each bacterium (*E. coli* or *S. aureus*) treated with different concentrations of test compounds was performed in a microtiter plate by quantifying absorbance at 600 nm at regular intervals in a microplate reader equipped with temperature controlled (37 °C) compartment. MH medium was prepared with different concentrations of test compound in 1% DMSO. The initial cell number was 5×10^5 cells per well in a volume of 0.2 mL. At the end of the incubation period, the readings were plotted in the form of a graph.

2.2.2.3. Assessment of time dependent killing of bacteria by test compounds

Time kill curve assay was performed for assessing time dependent killing of bacteria by test compounds. Mid log culture of bacteria (*E. coli* or *S. aureus*) was obtained as mentioned above. The cells were diluted (1:100) in 5 mL LB or NB medium in a 50-mL plastic tube and treated with vehicle or different concentrations of compound (HC or DS). The tubes were incubated in a shaker incubator 37 °C/120 rpm. After specific time points, 0.5 mL of culture was withdrawn from sample tubes and diluted in saline. The diluted samples were plated on MH agar plate to determine viability.

2.2.2.4. Assay of viability by SYTO-PI staining

Mid log phase culture (0.5 mL) of *E. coli* was washed, resuspended in 0.5 mL 1% glucose-PBS and treated with vehicle (1% DMSO) or different concentrations of HC for different time periods. At the end of the incubation, cells were centrifuged, washed once with 0.5 mL PBS and resuspended in 0.5 mL PBS. The samples were stained with PI (30 μM) and SYTO (5 μM) for 10 min in dark and the green to red fluorescence ratio was measured employing a fluorescence microplate reader (Tecan Infinite M200, Switzerland). The excitation/emission maxima for these dyes are about 480 nm/500 nm for SYTO 9 stain and 490 nm/635 nm for PI.

2.2.2.5. Study of the post exposure effect of antibacterial test compounds

Mid log culture of *S. aureus* was 1: 100 times diluted in 5 mL of 1% glucose-saline to attain a cell density of ~$3x10^6$ cfu/mL. Samples were treated with vehicle or different concentrations of DS for 1 h at 37 ºC. After 1 h of treatment, samples were 1:100 times diluted in nutrient medium. Further, 0.2 mL from diluted samples were distributed into well of 96 well plate in triplicate. The remaining volume was used to evaluate the viability of cells by an agar plating method. The post-exposure effect on the growth of bacteria was monitored by the growth curve and monitoring the viability [94].

2.2.2.6. Study of resistance generation to the test compounds

Resistance generation in *S. aureus* was evaluated by comparing the MIC of parent cells to that of the cells exposed to DS. Initially wild type cells were exposed to different concentrations of DS and MIC was determined as described above. The cells that survived the highest concentration of DS were plated and single colonies were isolated. This was considered as cells of 1st passage. In the next experiment MIC of wild type cells and cells of 1st passage was determined. This was done sequentially till 10 passages. Resistance

generation was monitored by determining any change in MIC of the population that underwent passage [95].

2.2.2.7. Determination of proliferation of bacteria by CFSE dilution method

Mid log culture (0.5 mL) of *E. coli* was labelled for 30 min with 20 µM CFSE. After labelling, the cells were washed thrice with PBS. Labelled cells (20 µL) were inoculated in 0.5 mL LB medium with or without HC (500, 750 µg/mL) and incubated in a shaker incubator at 37 ºC/120 rpm. After different time points, aliquots (0.1 mL) were withdrawn from each sample to determine CFSE fluorescence in the cells by a fluorescence microplate reader (Tecan Infinite M200, Switzerland). The excitation/emission wavelengths for CFSE fluorescence was 491 nm/520 nm.

2.2.2.8. Effect of different factors on the antibacterial activity of test compounds

The experiment was carried out as per the protocol given in section 2.2.2.1. Additionally, protection offered by GSH (5 mM) or Thiourea (150 mM) or Bipyridyl (500 µM) was investigated by preincubating the cells with the respective agents for 30 min before addition of HC. After incubation for 16-18 h different dilutions were spotted to quantify the viable bacteria.

To study the effect of magnesium and EDTA on HC induced cytotoxicity, different concentrations of magnesium chloride (5-20 mM) and EDTA (0.5-10 mM) were employed. *E. coli* cells were preincubated with either magnesium chloride or EDTA for 10 min and HC (250 to 400 µg/mL) was added to the samples. The samples were incubated at 37 ºC for 16-18 h after which the extent of growth of *E. coli* was quantified by absorbance at 600 nm. The viability of the cells in samples with no visible growth was determined by spotting an aliquot (10 µL) on LB agar plate. The plate was incubated at 37 ºC for 24 h and observed visually and the image was captured.

2.2.2.9. Determination of cell death by DNA condensation (Hoechst staining)

Cell death in the form of DNA condensation was visualized in *E. coli* cells after treatment with different concentrations of HC (500 and 750 µg/mL) for 2 h. Mid log phase cells (0.5 mL) were washed and resuspended in 0.5 mL 1% glucose-saline and treated with different concentrations of HC for 2 h. After the incubation period, the samples were treated with 5 µg/mL Hoechst 33342 dye for 10 min and incubated in dark at ambient temperature. The cells were analysed by Partec CyFlow Space flow cytometer (Partec, Germany) employing the UV laser for excitation. The samples were analysed by Cyflow software associated with the instrument.

2.2.2.10. Effect of pretreatment of HC on antibiotic sensitivity

Mid log culture of *E. coli* (1 mL) was treated with HC (500, 750 µg/mL) for 1 h at 37 ºC in 1% glucose-saline. Post incubation, cells were washed and resuspended in fresh 1% glucose-saline. HC treated cells were inoculated in MH medium (0.2 mL in 96 well plate) in the presence or absence of different concentrations of antibiotics. The plate was incubated at 37 °C for 18 h and analysed at 600 nm to quantify the extent of growth. Cell viability was evaluated by spotting 10 µL from each well on MH agar plate, followed by incubation at 37 ºC for 24 h. The extent of growth was visually observed and image of the plate was acquired.

2.2.2.11. Screening for co-operativity between DS and antibiotics

Epsilometer test is a classical method to evaluate MIC of antibacterial agents. It is a plastic strip at which an increased concentration of an antibiotic is impregnated and disk diffusion pattern is used to determine MIC value of antibiotics. The co-operativity effect between DS and different antibiotics was screened by E- test [96]. Mid log phase culture of *S. aureus* was (1:100) diluted in 1% glucose-saline and treated with vehicle or non-lethal concentration of DS (5 µg/mL) for 1 h in 1 mL volume. After 1 h, cells were washed once with saline and poured to form a lawn on the MH agar plate and dried inside a BSL-2. Antibiotic strips containing a gradient concentration of each antibiotic were carefully placed in the center of

the agar plate with sterile forceps. Antibiotic cooperativity was determined by comparing the intersection of the strip and the growth inhibition ellipse in vehicle treated and compound treated bacteria after incubation for 24 h at 37 ºC in a bacterial growth incubator.

2.2.2.12. Evaluation of cooperativity between stilbenes and antibiotics by Checkerboard assay.

The checkerboard assay was used to evaluate the cooperativity between stilbenes and selected antibiotics. The overnight culture of *S. aureus* was diluted in MH medium to 5×10^5 or 10^6 cfu/mL (1 mL) and treated with different concentrations of each stilbene, antibiotic, or a combination of stilbene and antibiotic. In a 96 well microtiter plate, each well contained the desired concentration of stilbene, antibiotic or a combination of both in a 0.2 mL volume. This was incubated for 16-20 h at 37 °C in an incubator. After incubation, the extent of growth was determined by the absorbance at 600 nm in a microplate reader (Synergy H1, BioTek, VT, USA). The fractional inhibitory concentration index (FICI) was calculated according to the following formula.

$$FICI = \frac{(MIC\ of\ drug\ A\ combination)}{(MIC\ of\ drug\ A\ alone)} + \frac{(MIC\ of\ drug\ B\ combination)}{(MIC\ of\ drug\ B\ alone)}$$

The interpretation of results was as follows:

FICI ≤0.5 synergy; FICI > 0.5 but ≤ 0.75 partial synergy; FICI >0.75 but ≤ 1 additive; FICI >1.0 but ≤ 2.0 indifferent and FIC ≥ 4 antagonistic [97]. Synergy was defined as four folds decrease of MIC of both agents in combination, two folds decrease was additive, while in case of partial synergy combination of two compounds result in a four-fold decrease in MIC of one agent and two fold decrease of other agent. In case of indifference, no change in MIC of both compounds in combination was observed. Antagonistic results in four folds increase in MIC of both test compounds in combination [98].

2.2.3. Methods related to estimation of biochemical parameters

2.2.3.1. Protein estimation

Total protein content in bacterial cell lysate was estimated by the Bradford dye (BioRad) kit protocol. Different dilution of lysate was prepared in 1 mL volume of saline, 160 µL of each diluent was thoroughly mixed with 40 µL Bradford dye reagent in 96 well plate. Plate was incubated for 10-15 min at ambient temperature. After incubation 96 well plate was read at 595 nm. The amount of protein was estimated by comparing the absorbance of the test sample with a standard of BSA protein.

2.2.3.2. SDS PAGE gel

To cast the SDS polyacrylamide gel, two glass plates were assembled in the gel casting apparatus, tightened with provided patch clamp and gap sealed with 1% agarose. Initially, 20 mL resolving gel (12%) was prepared and poured gel between the casting plate. It was overlayered with distilled water and allowed to polymerise the 12% stacking gel. After polymerisation, overlay water was removed and rinsed with distilled water by micropipette tip. After that 5 mL stacking gel was prepared and poured over the resolving gel, a teflon comb inserted in the gel and allowed to polymerised for 30 min. After complete polymerisation, comb was removed and wells were rinsed with water. Apparatus was disassembled, removed assemble gel and placed in a gel running chamber. Gel running apparatus filled with 1× SDS PAGE running buffer.

Samples were heat denatured by incubating with 50 µL of 1× Cracking buffer at 95 ℃ for 30 min. Centrifuged at 11000 × g for 10 min, supernate was collected in a tube and loaded in the SDS-PAGE gel. The SDS-PAGE gel was run at 100 V for 1 h till dye reached to resolving gel boundary after that voltage increased to 200 V until dye touched to the bottom of the gel. After complete running, power turn off, apparatus disassembled. Gel was carefully removed from the glass plate and dipped in a staining solution. Gel stained with 200 mL CBB dye for

4 h. After 4 h, staining dye was aspirated and gel again cover with destain solution (50% w/v methanol and 10% v/v glacial acetic acid in ion free water) for visualization.

2.2.3.3. Estimation of oxidative stress

Mid log culture (0.5 mL) of *E. coli* was washed and resuspended in 1% glucose-saline (0.5 mL) and treated with vehicle or HC (500 or 750 µg/mL) for different time periods. At the end of the incubation period, cells were washed and resuspended in PBS. The cells were stained with DCFDA (20 µM for microscopy; 100 µM for microplate reader detection) or DHE (10 µM for microscopy; 20 µM for microplate reader detection) for 20 min in dark at ambient temperature. At the end of the incubation period the cells were observed under a fluorescence microscope with blue (DCFDA) or green (DHE) excitation filters. The samples were also analysed by a fluorescence microplate reader (Tecan Infinite M200, Switzerland) for the purpose of quantification. The fluorescence values were expressed as specific fluorescence intensity which is fluorescence normalized over absorbance at 600 nm. The excitation/emission wavelength for DCFDA fluorescence was 488 nm/530 nm and that of DHE was 518 nm/610 nm.

In case of *S. aureus*, the experiment was performed essentially as described above. The cells were treated with different stilbenes (100 µg/mL) for 1 h. The oxidative stress was detected by employing HPF (10 µM) or DHE (20 µM). The oxidative stress was quantified by employing a microplate reader (Tecan Infinite M200, Switzerland). The excitation/emission wavelengths for HPF fluorescence was 488 nm/530 nm.

2.2.3.4. Estimation of non protein thiol content

Mid log culture (0.5 mL) of *E. coli* was washed and resuspended in 1% glucose-saline (0.5 mL) and treated with vehicle or HC (750 µg/mL) for 1 h. The cells were lysed by sonication (Branson ultrasonic probe sonicator, USA: 1 cycle consist of total 1 min time, 1 s on, 1 s off, and 25 % amplitude) and intracellular non-protein thiols were estimated by DTNB method.

Samples (0.25 mL) were added to tubes containing 50 µL DTNB (4 mg/mL) and 2.5 mL reaction buffer (0.1 M sodium phosphate, pH 8.0, containing 1 mM EDTA). After incubation for 15 min, the samples are read at 412 nm in a spectrophotometer (Jasco V570, Japan).

2.2.3.5. Estimation of lipid peroxidation

Lipid peroxidation of *E. coli* cell membrane was investigated by TBARS assay. Mid log phase of *E. coli* culture (10 mL) was treated with vehicle or HC 750 µg/mL in 10 mL PBS and incubated for 2 h at 37 ℃ in 50 mL capacity tube. At the end of incubation, cells were centrifuged at 11000 × g for 10 min at 4 ℃. Supernate was discarded and pellet washed, resuspended in 1 mL PBS (1.5 mL microcentrifuge tube). Pellet was lysed by sonication (Branson ultrasonic probe sonicator, USA: 1 cycle consist of total 1 min time, 1 s on, 1 s off, and 25 % amplitude). Lysed cells were centrifuged at 11000 × g for 10 min at 4 ℃. Lysate was collected in a new 1.5 mL microcentrifuge tube and debris discarded. Lysate was used for estimation for lipid peroxidation employing TBARS assay kit Cayman 10009055. Different dilutions of MDA were prepared in water in glass tubes. 0.1 mL of lysate or standard was taken in a 5 mL glass tube and mixed with 0.1 mL SDS by gentle swirling. Colour reagent (4 mL) was added and the samples were placed in a boiling water bath for 1 h. After 1 h incubation, tubes were immediately placed on ice for 10 min, centrifuged at 1600 × g at 4 ℃. After the samples attained ambient temperature 0.15 mL of sample was used to read fluorescence at excitation/emission 530 nm/550 nm respectively in a multi well plate reader.

2.2.3.6. Estimation of protein carbonylation

Mid log phase culture of *E. coli* (10 mL) was treated with vehicle or HC 750 µg/mL in 10 mL PBS for 2 h at 37 ℃ (50-mL tube). After 2 h of incubation cells were centrifuged at 11000 × g for 10 min at 4℃. Supernate was discarded and pellet was resuspended in 1 mL PBS. Lysate was prepared by sonication of pellet (Branson ultrasonic probe sonicator, USA: 1

cycle consist of total 1 min time, 1 s on, 1 s off, and 25 % amplitude). Lysed cells were centrifuged at 11000 × g for 10 min at 4 ℃ and lysate was collected in fresh 1.5 mL tube and debris discarded. Carbonylated protein content was estimated in the lysate using a kit (CYMAN, 1005020). Lysate (0.2 mL) was transferred in two different tubes and processed as sample and control. DNPH solution (0.8 mL) was added in the sample tube and 0.8 mL HCl (2.5 M) added in the control tube. Both were incubated in dark at room temperature for 1 h and vortexed at every 15 min. Further, 1 ml TCA (20% stock solution) was added, vortexed and incubated on ice for 5 min. Both control and sample tubes were centrifuged at 10000 × g for 10 min at 4 ℃. Supernate was discarded and pellet resuspended in 1 mL of (1:1) ethanol/ethyl acetate mixture. The tubes were centrifuged at 10000 × g for 10 min at 4 ℃. This step was repeated twice to wash the pellet. Pellet was dissolved in 0.5 mL guanidinium and vortexed, centrifuged at 10000 × g at 4 ℃ for 10 min. Supernate was collected from both control and test sample and 0.22 mL was used to read absorbance at 360 nm in a multi well plate reader.

2.2.3.7. Estimation of Potassium

Mid log culture of *E. coli* (1 mL) was washed, resuspended in saline (1 mL) and treated with different concentrations of HC for 1 h. After treatment, the supernate and cells were separated by centrifugation (11000 × g, 10 min). The supernate collected (0.9 mL) was diluted in ion free water to 5 mL. The quantity of potassium in supernate was determined by atomic absorption spectrophotometry (manufacturer and make).

2.2.3.8. Estimation of ATP

Mid log culture *E. coli* (1 mL) was washed, resuspended in saline (1 mL) and treated with different concentrations of HC for 1 h. After treatment, the supernate and cells were separated by centrifugation (11000 × g, 10 min). After collection of supernate by centrifugation, the intracellular content of the cells was collected in saline by sonication (Branson ultrasonic

probe sonicator, USA total time: 1 minute comprising 2 s on/5 s off cycles at 25% amplitude) followed by centrifugation (11000 × g, 10 min). Either supernate or lysate (20 µL) was mixed with 0.1 mL of reaction buffer in a 96 black well plate and the resulting chemiluminescence was read in a microplate reader immediately (Synergy H1, BioTek, VT, USA). Reaction buffer alone was used for background luminescence correction. The samples were normalized based on the protein content.

2.2.3.9. Estimation of membrane polarization

Mid log *E. coli* culture (0.5 mL) was washed and resuspended in same volume of 1% glucose-saline and treated with HC for 1 h. After 1 h cells were washed, resuspended in 1% glucose-saline (0.5 mL) and stained with 1 µg/mL Rhodamine 123 for 10 min in the dark (Warnes, Caves et al. 2012). Excess stain was removed by centrifugation and the fluorescence was quantified in a microplate reader with excitation/emission as 488 nm/530 nm. The absorbance of each sample at 600 nm was also recorded to ensure the same density of cells across samples.

2.2.3.10. Co-detection of oxidative stress and membrane damage by microscopy

Mid log culture *E. coli* (1.5 mL) was washed resuspended in 1% *glucose*-saline (1.5 mL). The cells were stained for 5 min with 20 µM DCFDA. Cells were washed and distributed in 0.2 mL volumes and treated with HC 500 µg/mL for different time periods. At the end of incubation, the cells were washed, resuspended in 1% glucose-saline and stained with 30 µM PI in the dark for 10 min. Finally, the cells were washed again and resuspended in a smaller volume (25 µL saline). A 2 µL aliquot was mounted on an agarose coated slide and observed under a fluorescence microscope (LSM 780, Carl Zeiss, Germany) for DCFDA and PI fluorescence.

2.2.3.11. Determination of toxicity in mammalian cells and calculation of therapeutic index.

To evaluate the cytotoxic effect of stilbenes **1**, **2**, **3**, **7**, **8** and **11**, L929 (mouse fibroblast cell line) and INT 407 (human cervical cell line) were employed. In a 96 well plate 5000 cells were allowed to attach overnight in 0.2 mL DMEM medium supplemented with 10% FBS before treatment with stilbenes. The extent of growth inhibition after incubation period (24 h) was calculated from vehicle treated samples, taken as 100% growth by MTT method. At the end of the incubation period 0.5 µg/mL MTT was added and incubated for 4 h. At the end of 4 h, formazone was solubilized in 0.1 mL DMSO. The plated were read at absorbance 570 nm in a microplate reader (Synergy H1, BioTek, VT, USA) to quantify the viable cells. The therapeutic index was calculated as the ratio of the IC_{50} observed against INT407 (human) and the MIC (against *S. aureus*).

2.2.3.12. Isolation of RNA and preparation of cDNA

RNA was extracted from mid log phase culture (5 mL) of *E. coli* treated with HC (500, 750 µg/mL) for different time periods. After treatment, cells were centrifuged at 11000 × g at 4 ºC and pellet collected in a microcentrifuge tube. The supernate was discarded and the pellet was homogenized in 0.2 mL TE buffer (10 mM Tris-HCl, 1 mM EDTA; pH 8) containing 1 mg/mL lysozyme. The samples were vortexed vigorously and incubated at 37 ºC for 10 min. Further 1.8 mL RA1 buffer and 18 µL β-mercaptoethanol were added and vortexed to achieve complete lysis. Nucleospin® filter midi column was placed on the collection tube. The samples were passed through the column by centrifugation for 10 min at 4500 × g. The column was discarded and the eluent was mixed with 1.8 mL of ethanol (70%). The samples were vortexed for 3-5 s. The samples were added in Unclosing® RNA midi column and allowed to bind RNA to the column. Columns were centrifuged at 4500 × g for 10 min, flow through was discarded and the columns were placed in a new tube. Membrane desalting buffer (2.2 mL) was added into each column and centrifuged for 10 min at 4500 × g. DNase reaction buffer was prepared in a sterilized tube (25 µL of rDNase added in 0.235 mL

reaction buffer of rDNase) and the mixture was directly added to the center of the column. Columns were incubated at ambient temperature for 15 min, after which 2.6 mL of wash buffer RAW2 was added. Columns were centrifuged for 3 min and the flow through was discarded. Columns were washed two times with 2.6 mL volume of buffer RA3, centrifuged for 5 min at 4500 × g. The columns were placed in a new tube and 0.25 mL RNase-free water was added, incubated for 5 min at ambient temperature. Columns were centrifuged for 5 min at 4500 × g for elution of RNA.

The purity of RNA was evaluated by NanoDrop. The concentration and purity of RNA were determined by the ratio of absorbance of RNA samples at absorbance 260 nm/280 nm and 260 nm/230 nm. For RNA, absorbance 260 nm/280 nm ratio greater than 1.8 or~2.0 while absorbance 260 nm/280 nm ratio ≥ 2.0 was considered acceptable.

(b) Removal of DNase contamination: The RNA was treated with DNase (ArcticZymes, Norway) to remove DNA contamination. RNA (8 µL~1.5 µg) was mixed with 10× reaction buffer (1 µL), HL-dsDNase (1 µL) and incubated for 10 min at 37 ℃ for genomic DNA digestion. Samples were incubated at 58 ℃ for 5 min for inactivation of enzyme HL-dsDNase.

(c) cDNA synthesis: DNase treated RNA was used for synthesis of complementary DNA (cDNA) employing qScript cDNA synthesis kit (Quanta Biosciences, USA) using 1.0 µg of RNA. RNA was mixed with 5× Reaction buffer (1 µL) and qScript RT enzyme (1 µL) in 20 µL reaction volume. cDNA was synthesized using the following program samples: 22 ℃ for 5 min, 42 ℃ for 30 min, and 85 ℃ for 2 min.

2.2.3.14. Determination of relative gene expression by real-time quantitative PCR (qPCR).

The qPCR was performed with 10 ng cDNA using the KAPA SYBR Fast qPCR kit (Kapa Biosystems, USA) and 0.1 pM of each primer in a 20 µL reaction. The qPCR run and analysis were performed on LightCycler 480 (Roche, USA). The thermo-cycling conditions

included, one cycle of denaturation at 95 °C for 4 min, followed by 45 cycles of denaturing at 95 °C for 2 s and annealing/extension at 60 °C for 40 s. The Ct values were normalized against the *cysG* gene encoding siroheme synthase [99] and the relative gene expression was determined using the ΔΔCt method [100]. The genes evaluated in the study are listed with their primer details in the table 2.2.1.

Table 2.2.1. List of Primers used to analyse expression of the DNA damage response genes after treatment with HC in E. coli.

Sr. No.	Gene Name	NCBI Gene ID	5' Primer	3' Primer
1.	*Nth*	947122	TTGAACTGGGCGTTGAAG	CGTGTCGACAGCAATAGTC
2.	*nei*	945320	CCAACGACTTAACGCTCTAC	ATGCGTGGTCAGTTGTTC
3.	*uvrA*	948559	CGGGACGTTTCAGCTTTA	GCCTCTTCGATGGTCATATC
4.	*umuC*	946359	GTTCTCGATTTGGCGGATAC	ACGAGCGGGAACAGATAA
5.	*recA*	947170	CGGAAATCGAAGGCGAAA	ACGAACAGAGGCGTAGAA
6.	*dinB*	944922	CGCCTCCGACATGAATAA	GCATCACCAGATCACACTT
7.	*recN*	947105	CGATCCCAACCGACTATTTG	GTGCCTGCTGATGATGTT
8.	*sulA*	947335	TGGGCTACCCTTAACGAA	GCTTACCGGACGCATAATAA
9.	*cysG*	947880	GCAGATGCAGGCATGTTA	CATCGACCACGTTACAGAAG

2.2.4. Methods related to study of physical attributes of the cells and biomolecules

2.2.4.1. Detection of surface perturbations by SEM

Mid log culture of bacteria was treated with different concentrations of HC for 3 h in LB medium (1 mL). Cells were observed under a scanning electron microscope (Carl Zeiss,

Germany) for surface perturbations induced by HC after coating with gold in an ion coater (KIC-1A, Coxem, Korea)

Mid log phase culture of *E. coli* was treated with HC (250, 500 and 750 µg/mL) for 3 h (in 1 mL LB medium) and mid log phase culture of *S. aureus* was treated with different stilbenes (100 µg/mL each) for 6 h (in 1 mL MH medium). Cells were centrifuged and washed with saline and fixed overnight in 2.5% glutaraldehyde in 0.2 mL saline at 4 °C. Fixed cells were washed thrice in deionized water (1 mL) and dehydrated in a series of graded ethanol (1 mL, 20-90%). Dehydrated cells were finally suspended in 100% ethanol (20 µL). A 2 µL aliquot was on glass coverslip placed on aluminium stub (by adhesive tape) and sputtered coated with gold at 7 mA for 120 s. The cells were observed under a focused ion beam scanning electron microscope (Gemini, Carl Zeiss, Jena, Germany) for surface perturbations and the images were acquired with the camera attached to the instrument.

2.2.4.2. Detection of filamentation by crystal violet staining

Mid log phase culture of *E. coli* was treated with different concentrations of HC (125, 250, 500, 750 µg/mL) and vehicle in LB medium after which the representative population from each sample was mounted on clean glass slides, stained with crystal violet (0.5% w/v) for 3 min and observed under a microscope (LSM 780, Carl Zeiss, Germany). For every sample at least ten fields were observed for every time point. The samples were visually analysed for the presence of filamented cells.

2.2.4.3. Detection of physical changes by live cell imaging

Microscopic slides preparation: Slides were wiped with isopropyl alcohol, coated with 1% agarose (prepared in distilled water) and dried at ambient temperature. Molten 1% agarose (0.5 mL) was allowed to flow on the surface of a clean glass slide held at an angle and the excess was allowed to drain. After drying the slide in air under a BSL-2 for 15 min a second layer was formed similarly and air dried for 30 min. The slides were stored in airtight self

sealing plastic bag at 4 ºC till use. On the day of experiment the slides were brought to ambient temperature and the sample cells contained in molten 1% agar containing growth medium (20 µL) was placed centrally on the slide and a coverslip was placed over the same. After 10 min the slides were observed under the microscope.

Mid log phase culture of *E. coli* (20 µL) was mixed with 0.2 mL molten LB agar (1%) containing 500 µg/mL HC. The mixture was mounted on a glass slide with a base coat of 1% agarose. A glass slides thus prepared was mounted on a microscope (LSM 780 Carl Zeiss, Germany) stage within a temperature controlled chamber (37 ºC) and observed continuously employing a 63× objective.

2.2.4.4. Detection of *in vitro* DNA Damage and the effect of different factors

Cesium chloride purified plasmid DNA (150 ng, 2 µL) was incubated in 10 mM HEPES with HC (500 µg/mL) and copper acetate (50 µM) or FeAmSO4 (50 µM) in a total reaction volume of 20 µL. After incubation for 1 h, the contents were mixed with 6× loading dye, loaded on a 1% agarose gel and the different forms of resultant DNA were separated by electrophoresis. The buffer used for electrophoresis was TAE buffer. The DNA bands were visualized by ethidium bromide staining (50 µg/mL) and documented with Kodak Gellogic 200 documentation system [101]. The effect of different factors like EDTA (50 µM), Thiourea (150 mM), Neocuproine (50–150 µM) were evaluated. The extent of damage was observed visually due to the conversion of CC form of DNA to other forms. To assess the DNA cleavage induced by different stilbenes, the experiment was carried out essentially in the same manner with stilbenes (50 µg/mL each) instead of HC.

2.2.4.5. Detection of DNA damage by comet assay

Mid log phase culture of *E. coli* (0.5 mL) in 1% glucose-saline was treated with HC (500 µg/mL) for 1 h. After 1 h the cells were washed with saline and the pellet obtained by centrifugation (11000 × g/10 min) was stored at -20 °C overnight. The pellets were thawed

with 0.5 mL saline. Each sample was diluted 1:100 in 0.5% agarose in saline and mounted on a clean glass slide with a base coat of 1% agarose and a second layer of 0.5% agarose. A final layer of 0.5% agarose containing 5 µg/mL RNase A, 1 mg/mL lysozyme, and 0.25% sodium N lauroylsarcosine was laid above the layer containing the sample. Once the layer was set at 4 °C for 10 min the slides were incubated at 37 °C for 30 min. The slides were further incubated for 1 h in lysis buffer at RT (2.5 M NaCl, 100 mM EDTA, 10 mM Tris pH 10, 1% sodium lauroylsarcosine, and 1% Triton X-100) followed by a 2 h incubation in enzyme digestion buffer (2.5 M NaCl, 10 mM EDTA, 10 mM Tris pH 7.4, and 0.5–0.6 mg/mL of proteinase K) at 37 °C. Slides were equilibrated for 20 min in electrophoresis tank buffer (300 mM sodium acetate and 100 mM Tris, pH 9). Slides were electrophoresed in the same buffer for 50 min at 12 V. Following electrophoresis, slides were sequentially immersed in 1 M ammonium acetate prepared in ethanol for 20 min, absolute ethanol for 30 min, and 70% ethanol for 10 min. The slides were air dried at RT. Prior to staining, slides were pre-treated with 90 µL of a freshly prepared solution containing 5% DMSO in 10 mM NaH_2PO4. The slides were stained with 40 µL of 1:1000 dilute SYBR II dye for 10 min. The samples slides were observed under a fluorescent microscope (Zeiss LSM 780, Carl Zeiss, Germany) using a 63× objective. The data was plotted as the proportion of comets to normal cells in each sample [102]. At least 100 cells were counted for every slide analysed under the microscope.

2.2.4.6. Qualitative determination of DNA binding

The ability of HC to bind plasmid DNA was determined spectrophotometrically (Jasco V570, Japan). To a fixed concentration of HC (66 µM) in HEPES buffer (pH 7.4, 1 mL) plasmid DNA pBR322 was added incrementally (175 ng in 1 µL). The change in spectra of HC was followed by the spectral scan after each addition. The extent of binding was expressed as a percent change in hypo/hyperchromicity. Doxorubicin (50 µM) was used as a known DNA binding molecule.

In case of stilbenes, the DNA binding ability of different stilbenes was evaluated by addition of a fixed concentration of plasmid DNA (1050 ng/6 µL) to 50 µM of each compound in 10 mM HEPES buffer pH 7.4 (1 mL). Initially, the spectrum of each stilbene was recorded, following which DNA was added, mixed and after 5 min the spectrum was recorded again. The extent of binding was revealed by the degree of change in the spectrum of the free compound. The quantum of change was expressed as a percent change in the absorbance at λmax [103] as per the equation:

$$\%\ Hypo\ or\ hyperchromicity = \frac{(Ef - Eb)}{Ef} \times 100$$

Where Ef, Eb correspond to the extinction coefficients of the free and bound forms of the complex.

2.2.4.7. Estimation of rate of cell lysis (SDS assay)

Mid log phase culture of *E. coli* was treated with HC for 1 h in 1 mL LB medium. The cells were washed and resuspended in fresh LB (1 mL). Aliquots (0.2 mL) were pipetted into flat bottom 96 well plates in triplicate. SDS (20 µL from 1% w/v stock) was added to each well resulting in a final concentration of 0.1%. The absorbance at 600 nm was monitored continuously for 15 min in a microplate reader (Omega, BMG Biotek, Germany) with reading intervals at 30 s.

2.2.5. Methods related to animal experiments

2.2.5.1. Permissions, procurement and housing of mice

In vivo experiment was done on Swiss mice after approval from BARC Animal Ethics Committee. The project approval number is BAEC/07/17 (approved in April 2017). All Swiss mice were maintained in the BARC animal care facility. Six to eight-week old mice (weight 22-25 g) were used in the work. Mice were kept in an adequately ventilated cage, with food and water ad libitum. Five mice per cage were maintained during the course of the

experiment. After the animals were procured from the animal house the mice were acclimatized for 1 week before the experiment.

2.2.5.2. Evaluation of toxicity of HC in mice

The *in vivo* toxicity of the test compound was evaluated in Swiss mice. Mice were divided into different groups, each group consisting of five mice. Single bolus dose of HC was given by intraperitoneal (i.p.) or oral route in a volume of 0.1 mL in case of i.p and 0.2 mL in case of oral route. The behavior, food/water intake, weight and survival were monitored for 30 days.

HC was prepared in 5% DMSO saline for i.p. administration and 5% DMSO in edible vegetable oil for oral administration. The different doses of HC administered intraperitoneally were 10, 25, 50, 75, 125, 250 mg/kg body weight and in case of oral administration was 50, 100, 150, 200, 250, 500, 750 mg/kg body weight.

2.2.5.3. Evaluation of efficacy of HC in peritonitis model

Peritonitis infection in mice was induced by administration of 0.2 mL of mid log culture of *E. coli* (10^8 cfu) that was suspended in saline containing 4% gastric mucin. After 1 h and 5 h of infection, mice received different concentrations of HC by i.p. (10, 25, 50 mg/kg body weight) or orally (250 mg/kg body weight). The day of infection was treated as day 1. On the second and third day, two doses of HC were administered by either i.p. or oral routes. The animals were sacrificed 24 h after infection and the number of bacteria in different organs (liver, kidney, spleen) was enumerated. The organs were dissected out and weighed. The organs were homogenized in sterile saline manually inside BSL-2, centrifuged (1000 × g/5 min). The homogenate was diluted and plated on LB agar plates. In another experiment, the survival of the infected mice was monitored that were treated with HC. Each group contained 5 mice and were caged together.

2.2.5.4. Evaluation of efficacy of DS and kanamycin in thigh infection model

S. aureus (ATCC 25923) was used for thigh infection experiments. *S. aureus* was grown on BHI agar plate (1.5% agar) and incubated overnight at 37 ℃. A single colony was inoculated into 5 mL BHI medium and grown in a shaker incubator at 37 ℃ for 16-18 h. Mid log culture of *S. aureus* was obtained by fresh inoculation (1%) in 5 mL medium and grown under shaking conditions at 37 ºC/120 rpm for 3 h. Cells (~5 × 10^6 cfu/mL) were washed in fresh medium and resuspended in 0.1 mL BHI medium.

Six-week-old Swiss mice weighing 23 to 27 g, were rendered neutropenic by intraperitoneal administration of two doses of cyclophosphamide (0.2 mL in saline) administered intraperitoneally 4 days and 1 day (150 mg/kg and 100 mg/kg body weight respectively) before infection [104]. On the day of infection, mice were divided into different groups (3 mice in each). *S. aureus* in BHI medium (0.1 mL) was administered in the right thigh muscles of all groups of mice except one which was injected only BHI medium by i.m (intramuscular) injection. After 2 h, different doses of DS (6.25, 12.5, 25 and 50 mg/kg body weight), kanamycin (3.125, 6.25, 12.5 mg/kg body weight) or a combination of both (DS 12.5 mg/kg and kanamycin 3.125 mg/kg body weight) was given by subcutaneous injection (0.1 mL). DS was prepared in 50% DMSO-saline, kanamycin in saline and sterilized by filtration. After the day of infection, the mice received two treatments per day till the end of the experiment (5 days). The number of mice surviving in each group was recorded along with gait and grimace analysis of each mouse in the experiment.

In a different experiment, the number of bacteria in the thigh of infected animals was recorded. The animals were infected with *S. aureus* as given above, treated with DS, kanamycin or combination of both after 1 h and 3 h. After 24 h of infection, the mice were sacrificed and the muscle tissue was excised. The muscle tissue was weighed and homogenized manually in sterile saline (0.5 mL). The homogenate was centrifuged (1000 × g/5 min) to clear the tissue debris. The clear homogenate containing the bacteria was

enumerated by dilution and plating on BHI agar plates. The plates were incubated at 37 ºC for 24 h before counting the number of bacteria.

2.2.6. Methods related to analysis of data

2.2.6.1. Replicates, reproducibility and statistical methods

Experiments were conducted in triplicates and repeated thrice. The data presented are mean ± Standard deviation (SD) of the three independent experiments. Significant differences between the treatments were evaluated using SD and one-way analysis of the variance (ANOVA) using SPSS 2.0. The data between the two specific different treatments were compared statistically using Student's t-test. The differences were considered significant at $P<0.05$.

CHAPTER 3. RESULTS AND DISCUSSION

3.1. Mechanisms behind the antibacterial activity of HC and its implications towards adjuvant therapy

3.1.1. Investigation of antibacterial mechanism of HC

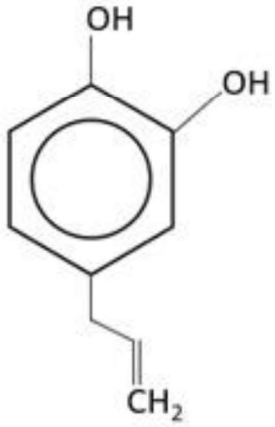

Figure 3.1.1. The chemical structure of HC.

HC inhibited the growth of different bacteria with MIC value ranging from 250-500 µg/mL. The MBC values of HC were in the range of 500-1000 µg/mL (Table 3.1.1).

Table 3.1.1. List of laboratory strains used to evaluate the efficacy of HC. MIC and MBC of HC was determined as per CLSI guidelines.

Sr. No	**Name of the culture**	**MTCC number**	**MIC** (µg/mL)	**MBC** (µg/mL)
1	*Pseudomonas aeruginosa*	2488	750	>1000
2	*Salmonella enterica subsp arizonae*	660	500	1000
3	*Proteus vulgaris*	426	750	1000
4	*Klebsiella pneumoniae*	10309	500	1000
5	*Escherichia coli* BW25113	-	250	500
6	*Staphylococcus aureus*	737	250	500
7	*Staphylococcus chromogenes*	6153	500	500
8	*Staphylococcus epidermidis*	3615	500	500
9	*Streptococcus mutans*	497	1000	>1000

To understand the molecular events leading to cell death induced by HC, we employed *E. coli* as a model organism. HC inhibited *E. coli* K12 BW25113 in a concentration dependent manner as shown in Figure 3.1.2. No growth was observed beyond 750 µg/mL.

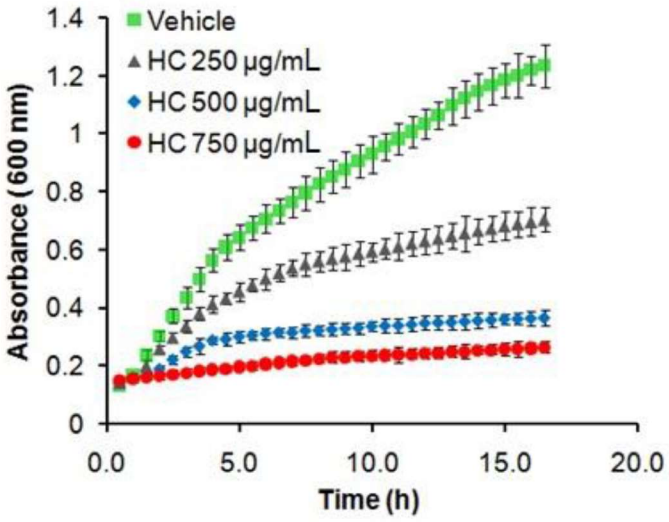

Figure 3.1.2. HC inhibited growth of E. coli in a concentration dependent manner. E. coli was inoculated in LB with vehicle or HC and absorbance was continuously monitored at 37 °C in a plate reader equipped with temperature control. The experiment was done in triplicate and repeated twice. Data presented is mean ± SD.

HC treatment resulted in inhibition of cell division in the time window of 1-4 h as revealed by the Figure 3.1.3A. Viability reduced drastically at 16 h (<99.99%). When analysed by an alternate method, SYTO-PI dual staining, PI positive cells were abundant by 3 h (Figure 3.1.3B). The green/red ratio dropped significantly from 1.408 ± 0.074 at 0 h to 0.366 ± 0.073 at 3 h. This was in agreement with the data obtained by plating.

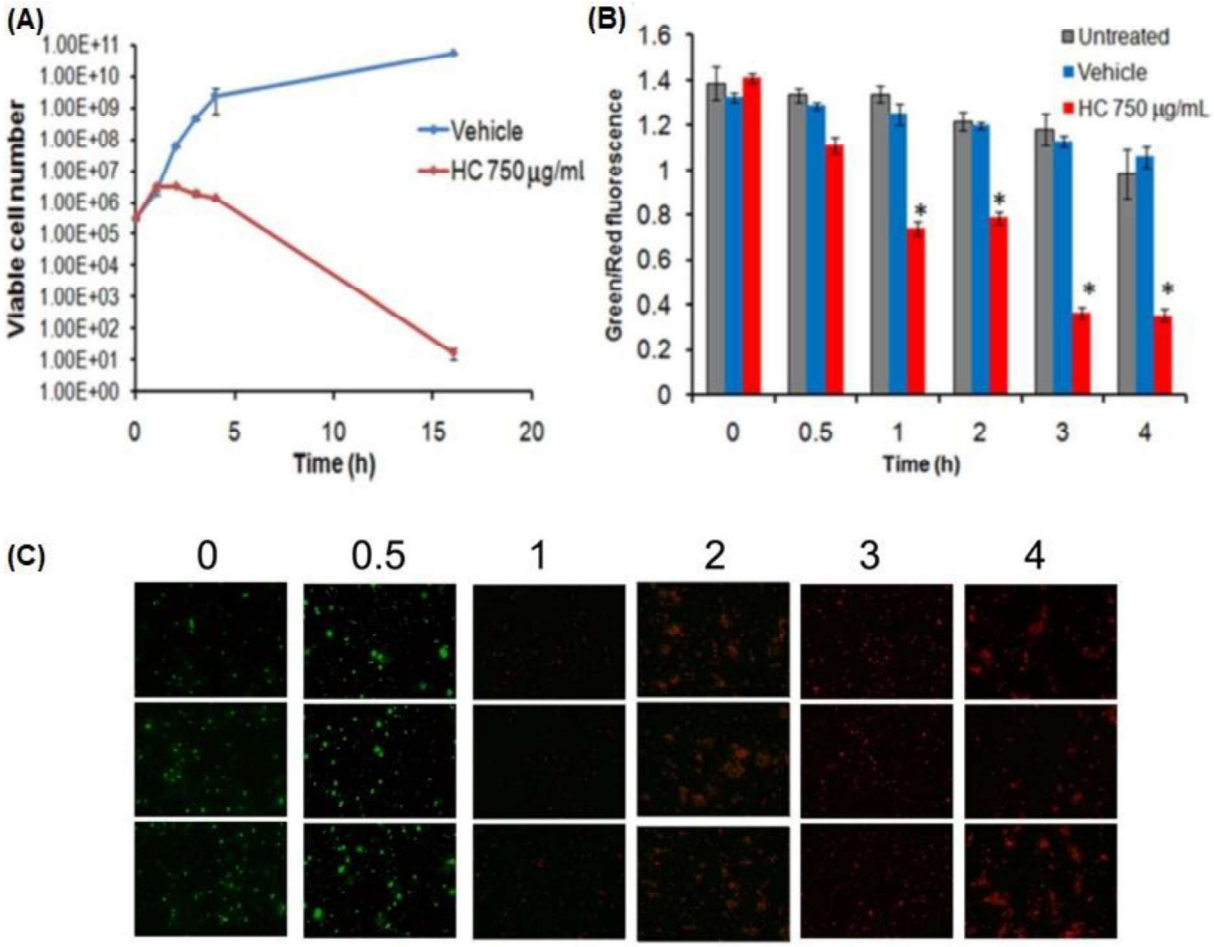

*Figure 3.1.3. Time dependent killing of E. coli by HC. (A) Time dependent killing was monitored by exposing mid log phase cells to HC and enumerating the viable cell number by dilution and plating. The experiment was done in triplicate and repeated twice. Data presented is mean ± SD. (**B**) Time dependent death of E. coli measured by SYTO-PI dual staining. Dead cells uptake PI and result in reduction of Green/Red ratio. HC treated cells were treated with SYTO-PI and the Green/Red fluorescence ratio quantified employing a mutliwell fluorescence plate reader. Data presented is mean ± SD. *Significant difference at $p \leq 0.05$ compared to untreated sample. (**C**) Time dependent death of E. coli was also observed by fluorescence microscopy employing SYTO-PI dual staining.*

3.1.2. Role of oxidative stress in the antibacterial activity of HC

Phenolic molecules are known to participate in metal dependent reactions and produce ROS and consequently oxidative stress inside the cells [105]. Investigation of oxidative stress induced by HC in *E. coli* was carried out employing DCFDA and DHE dyes. Both

concentration dependent and time dependent assays were carried out. Significant increase in ROS generation was observed upon HC treatment at 2 h (1.58 ± 0.12 fold) detectable by DCFDA (Figure 3.1.4B). This further increased to 1.79 fold at 3 h and 3.53 fold at 4 h compared to 0 h. The quantity of ROS generated was directly proportional to the concentration of HC (Figure 3.1.4C and microscopic observation as in Figure 3.1.4A).

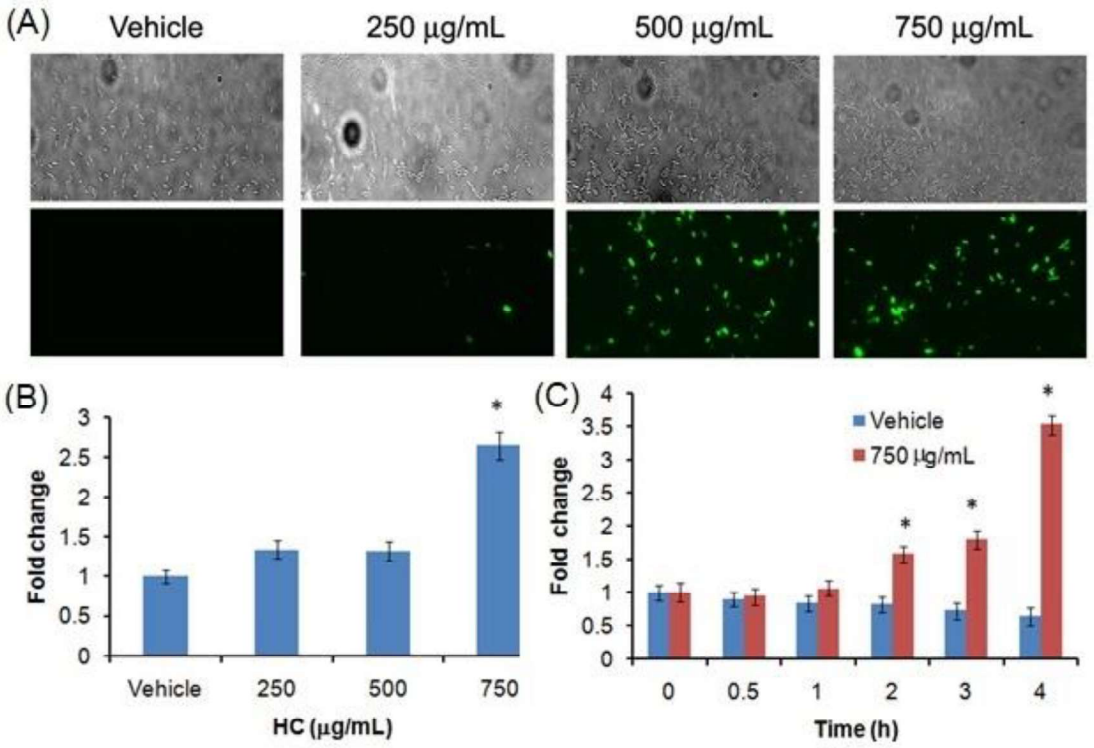

*Figure 3.1.4. ROS generation in E. coli cells after HC treatment. (A) and (B) Concentration dependent detection of ROS by DCFDA after exposure to HC for 2 h. Mid log phase cells exposed to HC were treated with DCFDA in dark and quantified in a fluorescence plate reader. (C) Time dependent detection of ROS by DCFDA after HC treatment (750 µg/mL). The experiment was done in hexaplicate and repeated twice. Data presented is mean ± SD. *Significant difference at $p \leq 0.05$ compared to respective control.*

DCFDA detects several oxidizing species and is not specific for an ROS [106] we employed DHE that is specific to superoxide radical [107]. Catechol containing molecules are known to generate superoxide by single electron reduction of molecular oxygen. This results in a semiquinone which further donates a single electron to molecular oxygen or hydrogen

peroxide to yield superoxide or hydroxyl radical respectively and a quinone [105]. HC treatment lead to significant increase in superoxide detected with DHE. After 1 h of HC treatment 2.15 fold increase in ROS was detected. This further increased and peaked at 2 h (6.25 fold; Figure 3.1.5C). HC treatment resulted in superoxide generation in a concentration dependent manner (microscopic observation as in Figure 3.1.5A; Fig. 3.1.5B). HC did not react directly with either DCFDA or DHE resulting in fluorescence which was confirmed by spectrofluorimetry.

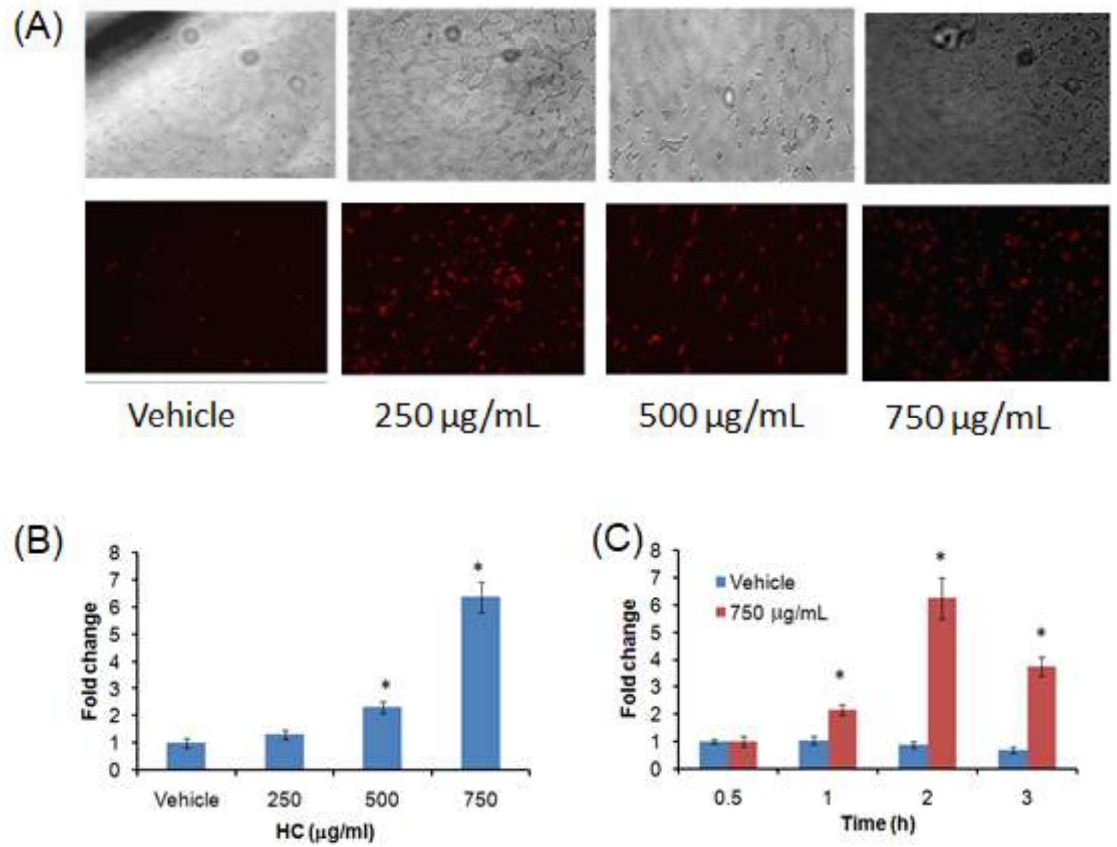

Figure 3.1.5. ROS generation in E. coli cells after HC treatment. A) and (B) Concentration dependent detection of ROS by DHE after exposure to HC for 2 h. (C): Time dependent detection of ROS by DHE methods after HC treatment (750 µg/mL). Mid log phase cells exposed to HC were treated with DHE in dark and quantified in a fluorescence plate reader. The experiment was done in hexaplicate and repeated twice. Data presented is mean ± SD. ∗Significant difference at $p \leq 0.05$ compared to respective control.

To investigate the role of ROS in inhibition of *E. coli* by HC, we employed antioxidants thiourea and GSH. Thiourea and GSH protected *E. coli* from HC induced lethality (Figure 3.1.6A) as revealed by the higher number of colonies compared to HC treated sample, also reduced lower ROS was detected after treatment with HC (Figure 3.1.6B) in the presence of Thiourea and GSH. Compared to vehicle treated cells thiourea or GSH treated cells exhibited 0.8 fold (~20% decrease) DCFDA fluorescence while HC treatment exhibited 1.84 fold fluorescence (~80% increase). Pretreatment with thiourea or GSH resulted in 1.56 fold and 1.29 fold fluorescence in HC treated cells. Neither thiourea nor GSH restored the fluorescence to the value present in the vehicle sample.

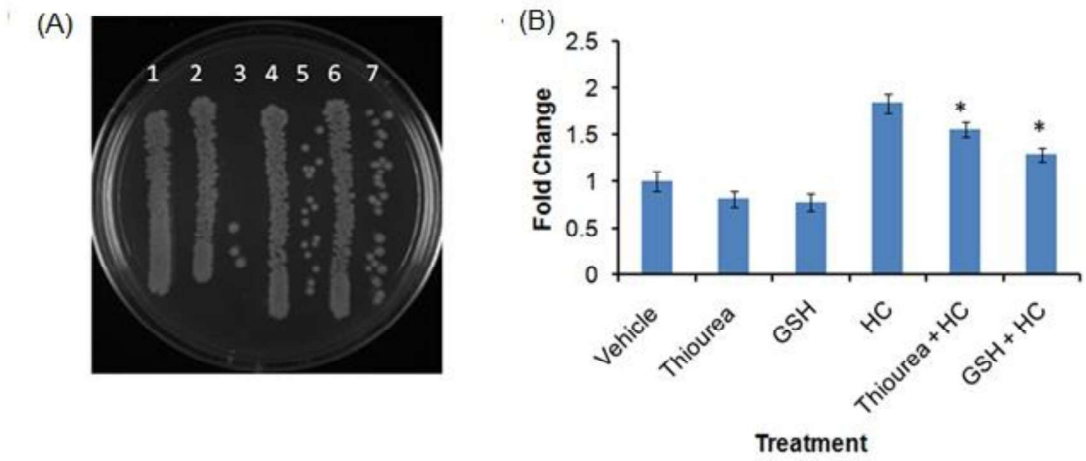

*Figure 3.1.6. Antioxidants protect E. coli against HC induced lethality. Mid log cells were pre-treated with GSH (5 mM) or thiourea (150 mM) for 30 min before addition of HC (750 µg/mL). After 16 h incubation, 10 µL of different dilutions from each sample was spotted and growth observed visually next day. 1. Untreated; 2. Vehicle; 3. HC; 4. GSH; 5. GSH + HC; 6. Thiourea and 7. Thiourea + HC. (B) Pretreatment with GSH (5 mM) and Thiourea (150 mM) reduced the ROS generated by HC treatment. Mid log phase cells were pre-treated with GSH or thiourea, exposed to HC (750 µg/mL) for 2 h. The cells were treated with DCFDA in dark and quantified in a fluorescence plate reader. The experiment was done in hexaplicate and repeated twice. Data presented is mean ± SD. *Significant difference at $p \leq 0.05$.*

Intracellular thiols depleted significantly (0.32 fold compared to vehicle treated cells) upon treatment with HC (Figure 3.1.7).

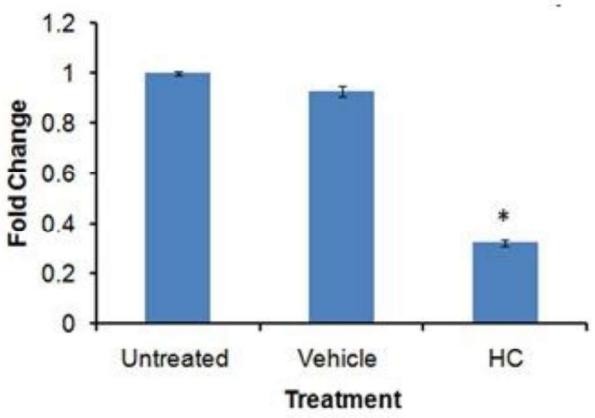

*Figure 3.1.7. HC treatment depletes reduced glutathione in E. coli. Mid log phase cells were treated with vehicle or HC (750 µg/mL) for 1 h in saline and the cells were lysed. The GSH content in lysates was estimated by Ellmans's reagent. The values are mean ± SD. *Significant difference at p ≤ 0.05.*

To further investigate this observation, we employed a mutant deficient in synthesis of intracellular GSH (*gshA*). The mutant (*gshA*) was more sensitive to HC than wild type (Figure 3.1.8A). At 250 and 500 µg/mL HC, wild type cells exhibited 55.34 ± 6.32% and 69.10 ± 6.51 % inhibition respectively while *gshA* mutant exhibited 71.78 ± 5.23% and 90.76 ± 5.44% inhibition. (Figure 3.1.8A). External supplementation of GSH to *gshA* mutant cells resulted in protection against HC induced cell killing (Figure 3.1.8B) suggesting a key role for GSH against HC mediated cytotoxicity.

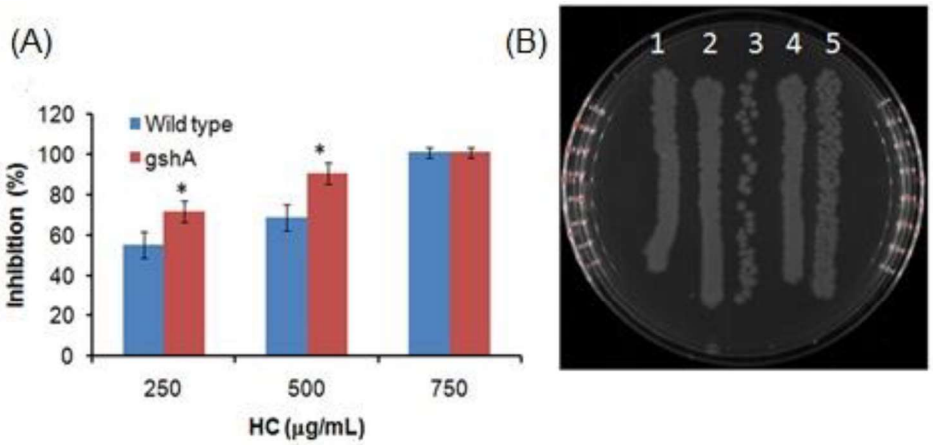

Figure 3.1.8. gshA mutant is more sensitive to HC than wild type(A) Mid log phase cells of wild type and GSH mutant were exposed to different concentrations of HC. After 16 h the extent of inhibition was calculated by taking growth in respective vehicle treated samples as 100 % growth. ⁎Significant difference at $p \leq 0.05$ (B) gshA is rescued by external supplementation of GSH. Mid log gshA cells were pretreated with GSH (5 mM; 30 min) before addition of HC (750 µg/mL). After 16 h incubation 10 µL from each sample was spotted and growth observed visually next day. 1. Untreated; 2. Vehicle; 3. HC; 4. GSH and 5. GSH + HC.

Compared to wild type, *gshA* mutant cells exhibited ~1.7 fold higher fluorescence. However, upon HC treatment the wild type cells exhibited ~1.3 fold (500 µg/mL) and 2.6 (750 µg/mL) fold increase in DCFDA fluorescence (Figure 3.1.9A) compared to vehicle treated cells. In case of *gshA* mutant, HC treatment led to ~1.4 fold (500 µg/mL) and 2.1 (750 µg/mL) fold increase (Figure 3.1.9B) compared to vehicle treated *gshA* cells. The response of wild type and *gshA* mutant to HC treatment is not significantly different when ROS was quantified. However, upon treatment with hydrogen peroxide *gshA* mutant exhibited significantly higher fluorescence than wild type (Figure. 3.1.9A and B).

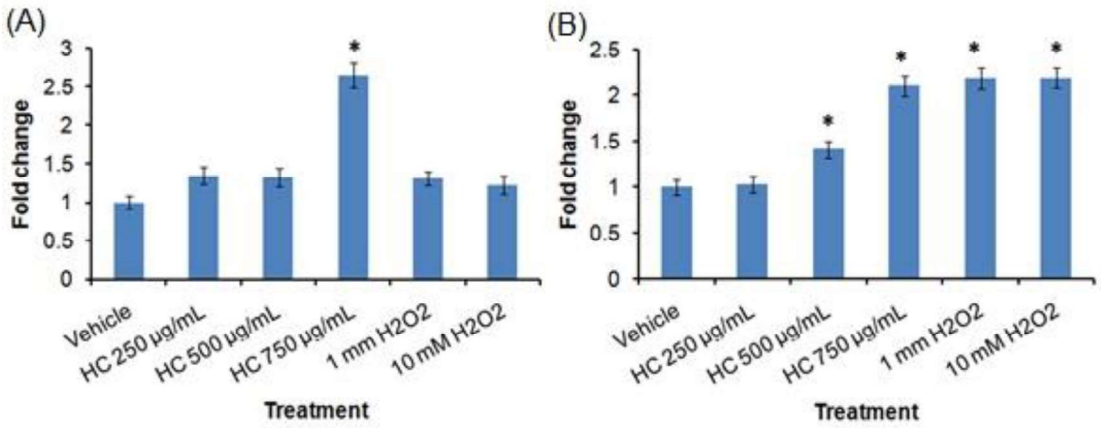

Figure 3.1.9. Mid log phase cells of wild type (A) and gshA (B) were exposed to different concentrations of HC for 2 h. The cells were treated with DCFDA in dark and quantified in a fluorescence plate reader. The experiment was done in hexaplicate and repeated twice. Data presented is mean ± SD. ∗Significant difference at $p \leq 0.05$.

To evaluate if ROS generation by HC involves known metabolic intermediates that could participate in Fenton chemistry, we tested knock out strains of some of the TCA genes like *icdA*, *sucB*, *mdh* and *acnB*. At MIC no difference was observed in the sensitivity of wild type and these mutants. However, at a sub inhibitory concentration (100 µg/mL) reduced sensitivity (higher survival) of these mutants (except in case of *acnB*) was observed (Figure 3.1.10). The mutants exhibited resistance to the tune of 0.3 to 0.5 fold. When probed for ROS generation these mutants exhibited reduced ROS levels compared to wild type after HC treatment (Figure 3.1.10) that correlated to their resistance towards HC.

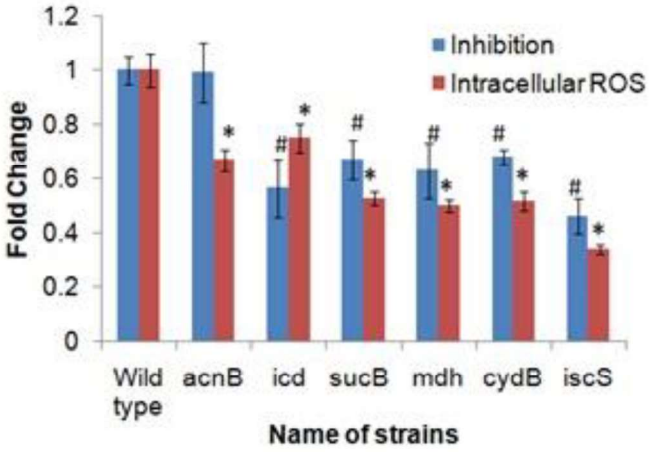

*Figure 3.1.10. Mutants devoid of iron sulfur proteins are less sensitive to HC and exhibit reduced intracellular ROS. Mid log phase cells of different mutants were exposed to HC (100 µg/mL for 16 h for survival measurements; 750 µg/mL for 1 h for ROS quantification). ROS measurement was by DCFDA method for all strains except cydB for which DHE (superoxide anion specific) was used. The extent of difference was expressed as fold change normalized over the response of wild type strain. The experiment was done in triplicate and repeated twice. Data presented is mean ± SD. Significant difference at $p \leq 0.05$ (#) was observed for inhibition data of all mutants (w.r.t wild type) except in case of acnB. *Significant difference at $p \leq 0.05$ was observed for ROS generation data of all mutants (w.r.t wild type).*

Further Bipyridyl, a chelator of Fe^{2+} at 500 µM protected wild type *E. coli* against HC induced toxicity (Figure 3.1.11) revealing a role of Fenton chemistry in HC mediated cell killing.

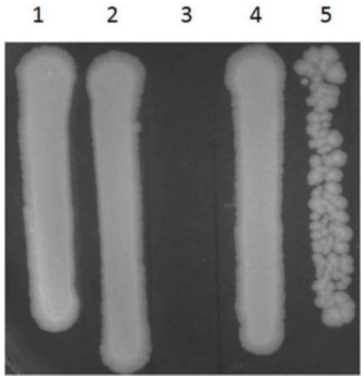

Figure 3.1.11. Bipyridyl, a chelator of iron protects E. coli against HC induced death. Mid log cells were pre-treated with Bipyridyl (500 µM) for 30 min before addition of HC (750

µg/mL). After 16 h incubation, 10 µL of different dilutions from each sample was spotted and growth observed visually next day. 1. Untreated; 2. Vehicle; 3. HC; 4. Bipyridyl; 5. Bipyridyl+ HC.

We also investigated lipid peroxidation in vehicle and HC 750 µg/mL treated cells. Lipid peroxidation was evaluated by TBARS assay. No significant change in lipid peroxidation was observed in HC (750 µg/ml) treated cells compared to vehicle treated cells (Figure 3.1.12).

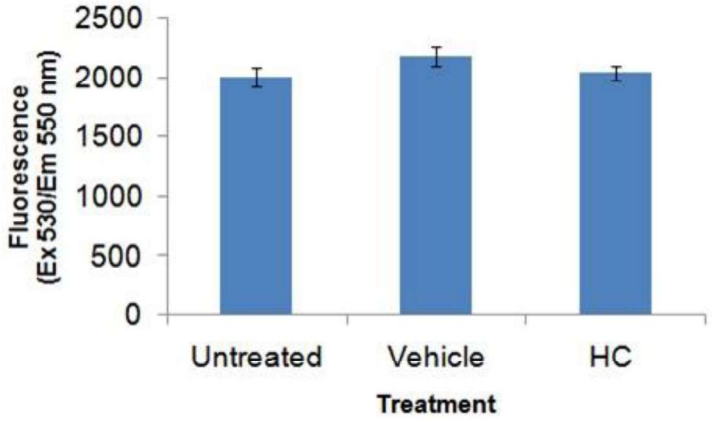

Figure 3.1.12. Detection of lipid peroxidation in HC treated E. coli. Mid log culture (10 mL) was treated with vehicle or HC 750 µg/mL for 2 h in PBS. The cells were lysed by sonication and estimate MDA equivalents by TBARS assay. Data presented is mean±SD

We also investigated the changes in protein carbonylation in HC treated cells compared to vehicle treated cells. No significant change in protein carbonylation was observed in HC treated cells as shown in Figure 3.1.13.

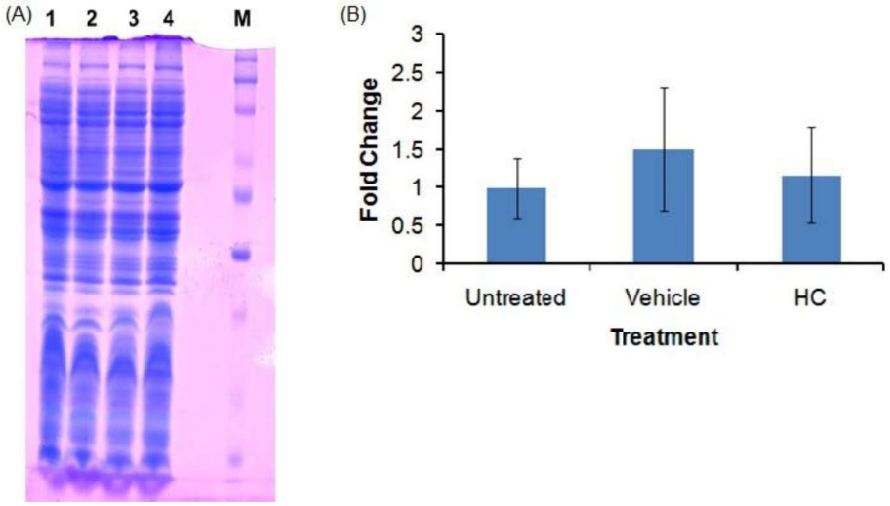

Figure 3.1.13. Detection of changes in total protein and protein carbonylation. (A) Mid log culture (2 mL for each sample) was treated with vehicle or HC at 37 °C for 2 h. The cells were washed and digested in 50 µL of 1× cracking buffer 30 minutes at 95 °C. The proteins were resolved on a 12% PAGE and stained with coomassie brilliant blue for visualization. 1- Untreated, 2-Vehicle, 3- HC 500 µg/mL, 4- HC 500 µg/mL, M- Prestained molecular weight marker (Bioline, USA). (B) Mid log culture (10 mL) was resuspended in 10 mL PBS and treated with vehicle or HC (750 µg/mL) at 37 °C for 2 h. The cells were lysed by sonication and the carbonylated proteins were estimated. Data presented is mean±SD.

3.1.3. Role of DNA damage in the antibacterial activity of HC

DNA damage is an important consequence of ROS generation. DNA damage repair response by the cells plays an important role in repair of DNA and survival of the cells with damaged DNA. DNA damage repair deficient mutants provide valuable insight into the type of damage of a genotoxic insult. We evaluated the sensitivity of different DNA damage repair deficient mutants to HC and compared it to that of wild type. As shown in Figure 3.1.14, DNA damage repair deficient mutants were more sensitive to HC than wild type. The fold change in sensitivity ranged from 1.3 to 2 in case of different mutants.

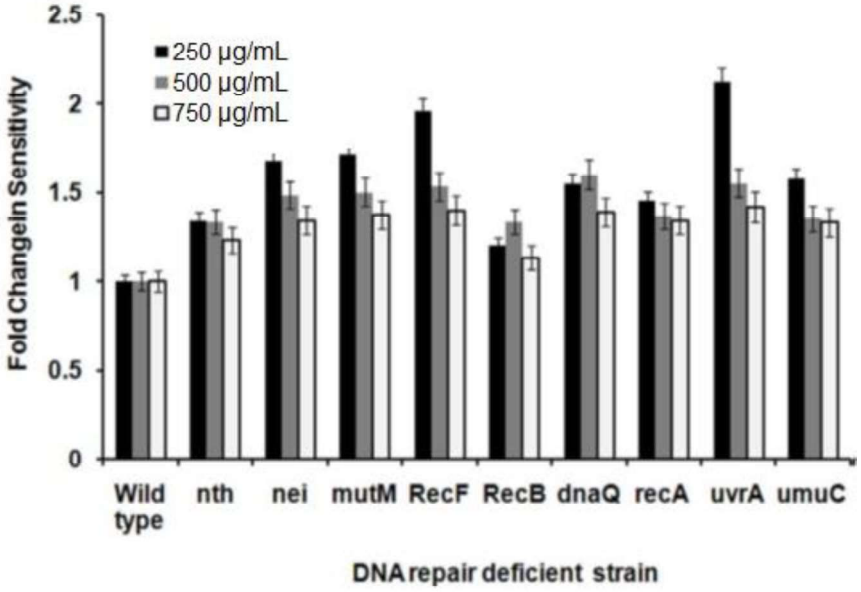

Figure 3.1.14. DNA repair deficient mutants are more sensitive to HC. Mid log phase cells of different DNA damage repair deficient mutants were exposed to increasing concentrations of HC. After 16 h the extent of growth was quantified and compared to the respective vehicle treated cells (100% growth). The extent of inhibition of growth was calculated from the vehicle treated sample. The experiment was done in triplicate and repeated twice. Data presented is mean ± SD. Significant difference at $p \leq 0.05$ observed in all samples compared to wild type except in case of recB treated with 750 µg/mL HC.

Quantitative real time PCR analysis of the genes induced by HC treatment (3 h) revealed significant up regulation of genes involved in DNA damage repair response (Figure 3.1.15). Maximum induction was observed in case of *mutM* (94.24 ± 37.64) followed by *recN* (23.92 ± 9.58). Significant up regulation was also seen in case of *nth* (8.43 ± 0.12) and *nei* (13.94 ± 1.32). The genes *nth*, *nei* and *mutM* are specifically responsible for repairing oxidative damage to DNA resultant from oxidative stress in the cytosol [108].

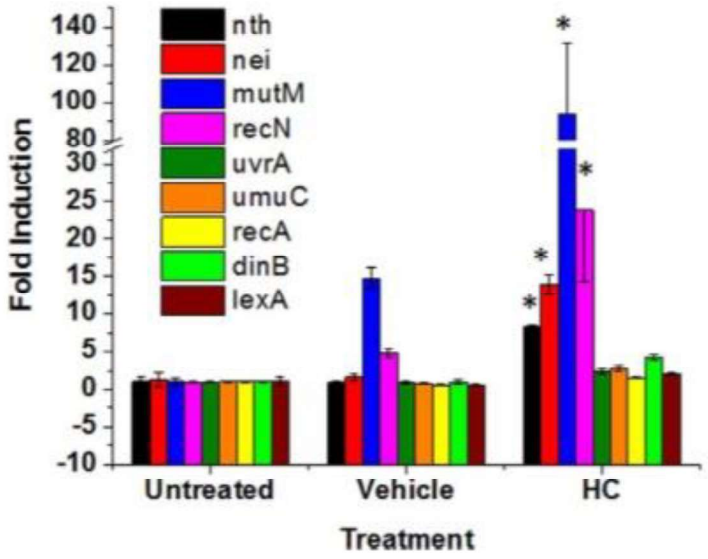

Figure 3.1.15. Quantification of gene expression by real time PCR after HC treatment. Mid log phase cells of wild type E. coli was treated with vehicle or HC (750 µg/mL) for 3 h. RNA was extracted and reverse transcribed. Using equal quantity of cDNA, real time PCR was employed to quantify the expression of different genes involved in DNA damage repair. The experiment was done in triplicate. Data presented is mean ± SD. ∗Significant difference at p ≤0.05.

To verify if superoxide and subsequently other ROS generated by HC results in damage to DNA we evaluated DNA binding and DNA cleavage properties of HC *in vitro*. Spectrophotometric titration of HC and plasmid DNA revealed HC weakly bound to DNA in comparison to classical intercalator doxorubicin (Figure 3.1.16).

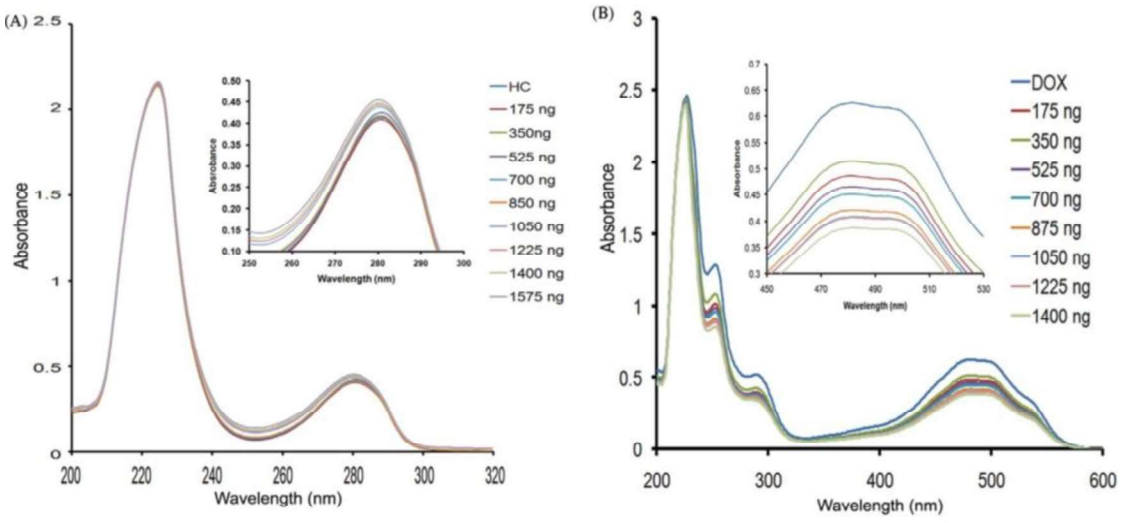

Figure 3.1.16. DNA binding of HC evaluated by spectrophotometry. (A) To a fixed concentration of HC (66 µM), plasmid DNA was added incrementally (175 ng/addition in 1 µL volume). The change in spectra was recorded after every addition. (B) Doxorubicin was employed as a known DNA binding molecule for comparison under identical experimental conditions.

Addition of incremental amount of DNA to HC resulted in a minor change in the spectrum, while strong hyperchromicity was observed in case of doxorubicin (~37% change at 1400 ng of DNA). In the *in vitro* DNA cleavage experiments employing plasmid DNA (pBR322), HC alone did not cleave DNA. HC cleaved DNA in presence of cupric ions and not ferric ions (Figure 3.1.18A). Thiourea, EDTA and neocuproine inhibited the DNA cleavage process (Figure 3.1.18B and C) medicated by HC in the presence of copper.

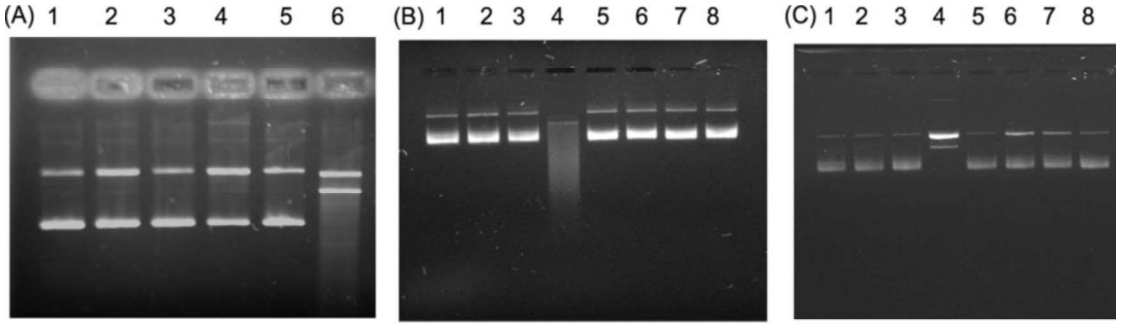

Figure 3.1.17. HC damages plasmid DNA in presence of copper involving a redox reaction. (A) DNA cleavage activity of HC (500 µg/mL) in presence of cupric ions. Lanes1-6

represent: 1. DNA alone (150 ng); 2. DNA + HC lane; 3. DNA + Cu (50 µM); 4. DNA + Fe (50 µM); 5. DNA + HC + Fe and 6. DNA + HC + Cu. (B) DNA cleavage induced by HC (500 µg/mL) is inhibited by EDTA (50 µM) and Thiourea (150 mM). Lanes 1-8 represent: 1. DNA alone; 2. DNA + HC; 3. DNA + Cu; 4. DNA + HC + Cu; 5. DNA + Thiourea; 6. DNA + HC +Cu + Thiourea; 7. DNA + EDTA and 8. DNA + HC +Cu + EDTA. (C) DNA cleavage induced by HC (500 µg/mL) involves reduction of copper. Lanes 1-8 represent: 1. DNA alone; 2. DNA + HC; 3. DNA +Cu; 4. DNA + HC + Cu; 5. DNA + Neocuproine (150 µM); 6. DNA + HC + Cu + Neocuproine (50 µM); 7. DNA + HC + Cu + Neocuproine (100 µM) and 8. DNA + HC + Cu + Neocuproine (150 µM).

3.1.4. Effect of HC on phenotype, cell division and apoptosis like death

In the current investigation, an understanding of the molecular basis of the different phenotypes induced by HC was envisaged. Upon treatment of *E. coli* cells with different concentrations of HC, changes in the cellular morphology were observed. As shown in Figure 3.1.18, filamentation was observed in HC treated samples. The filamentation induced by 125 µg/mL was overcome by the cells within 2 h (Figure 3.1.18), while at 250 µg/mL the filamentation persisted beyond 3 h (Figure 3.1.18). Incidentally, at the highest concentration tested (750 µg/mL) filamented cells were few.

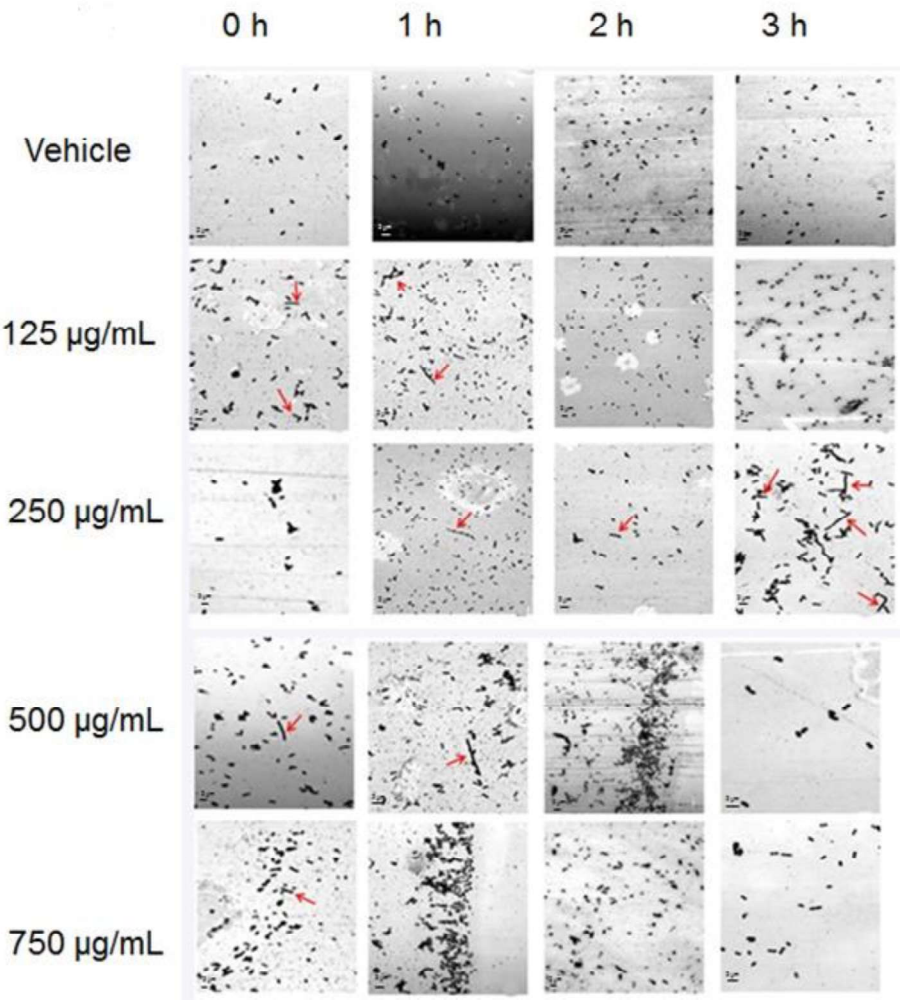

Figure 3.1.18. Phenotypic changes induced by HC on E. coli. Mid log cells were treated with different concentrations of HC for the indicated time. Samples were smeared on glass slides, stained with crystal violet and observed under the microscope.

Similar result was obtained when HC treated samples were observed by scanning electron microscopy (SEM). Filamentation was observed upon HC treatment at 250 µg/mL and 500 µg/mL by SEM (Figure 3.1.19A). At 750 µg/mL, many broken cells were observed corroborating the absence of filamented cells. Quantification of the mean cell lengths and proportion of different phenotypes after treatment with HC is presented in Figure 3.1.19A and B.

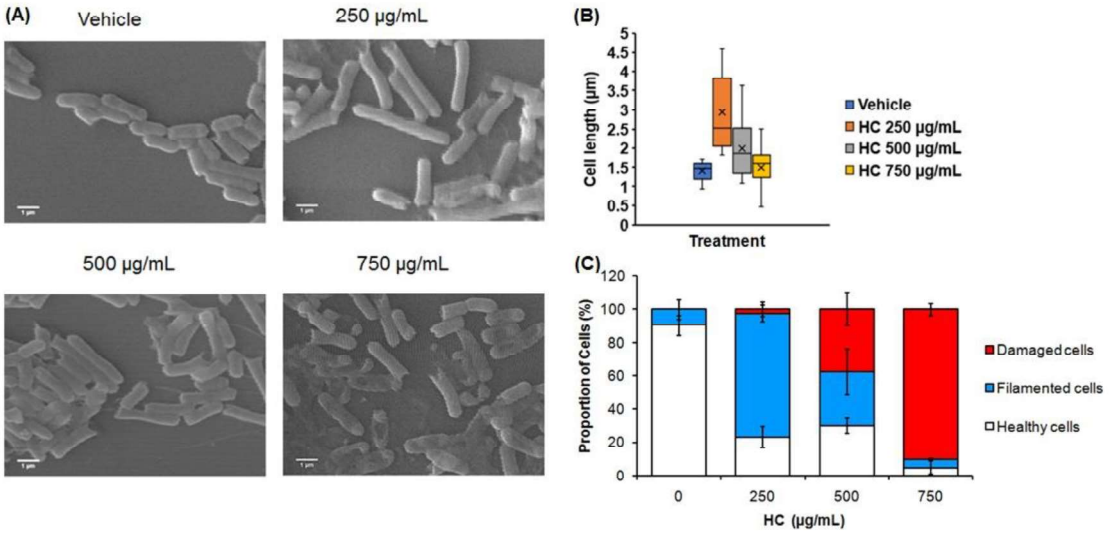

Figure 3.1.19. Quantification of phenotype induced by HC treatment. (A) Mid log cells were treated with HC for 3 h and the phenotype captured by scanning electron microscopy. The cell lengths were measured for each treatment with the associated software and plotted. (B) The proportion of the cells bearing different phenotypes after treatment with HC for 3 h. The values given are mean±SD.

Live cell imaging of HC treated *E. coli* cells (up to 3 h) revealed significant inhibition of cell growth as well as division at 500 µg/mL (Figure 3.1.20). At 750 µg/mL, the cells shrunk and lost granularity indicating broken cells and could not be observed properly under the microscope during the live cell imaging experiment. This could also be seen from the SEM picture of 750 µg/mL treated cells (Figure 3.1.19A). This indicated the death of cells caused by 750 µg/mL is sudden and the target is likely to be the membrane of the cell as evidenced from SEM and live cell imaging data.

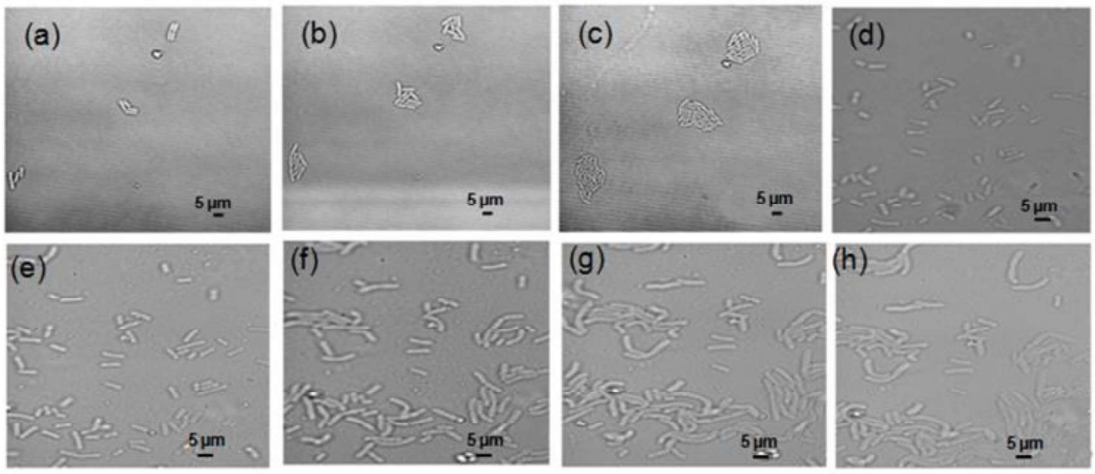

Figure 3.1.20. Effect of HC on the growth of E. coli cells by live cell imaging. Mid log cells were mixed with HC in molten Luria agar and overlaid on agarose coated slide and observed continuously up to 4 h for the effect on growth. (a-c) Vehicle treated samples: 0, 1 and 2 h, respectively. (d-h) HC (500 µg/mL) treated samples: 0, 1, 2, 3 and 4 h, respectively.

DNA damage leads to inhibition of cell division. We quantified the inhibition of growth and cell division by CFSE dye dilution and *sulA* expression. Untreated and vehicle treated cells grew normally leading to dilution of CFSE dye (~70% of original dye diluted) as shown in Figure 3.1.21A while HC treated cells retained the dye (~20% of original dye diluted and ~80% retained) as they did not divide. SulA, a protein under the control of SOS response inhibits cell division by inhibiting FtsZ ring formation [109] in response to genotoxic stress. We observed significant induction of *sulA* (9.04 ± 3.29) in response to HC treatment by q-RT PCR (Figure 3.1.21B).

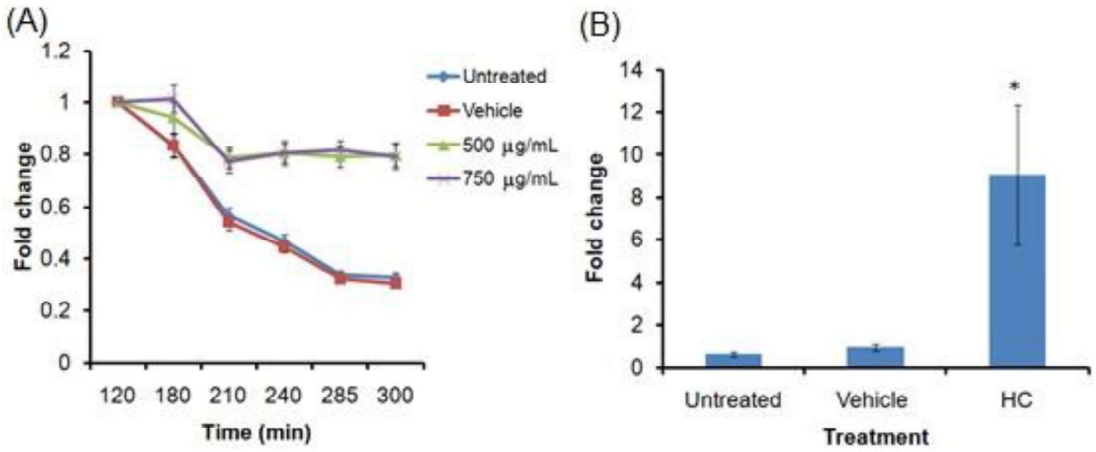

*Figure 3.1.21. HC inhibits cell division E. coli. Mid log culture of E. coli labelled with 10 µM CFSE dye and exposed to Vehicle and HC. (A) The fluorescence of CFSE dye was quantified at different time point by fluorescence plate reader and the mean is presented ±SD. (B) sulA gene expression was quantified in 3 h HC treated and vehicle treated sample by real time PCR. The experiment was done in triplicate and mean is presented ±SD. * refer significance difference ≤0.05.*

Apoptotic like death has been reported in prokaryotes previously [110] HC treated cells exhibited condensation of DNA as revealed by Hoechst staining, quantified by flow cytometry (Figure 3.1.22). Enhanced fluorescence upon Hoechst binding to condensed DNA detected by flow cytometry was taken as a mark of apoptosis like death in *E. coli* cells treated with HC. Untreated and vehicle treated cells revealed ~9-12% proportion of cells with condensed DNA while this increased significantly in HC treated cells. HC (750 µg/mL) treated sample exhibited 29.43 ± 3.12% proportion with condensed DNA revealing apoptosis like death.

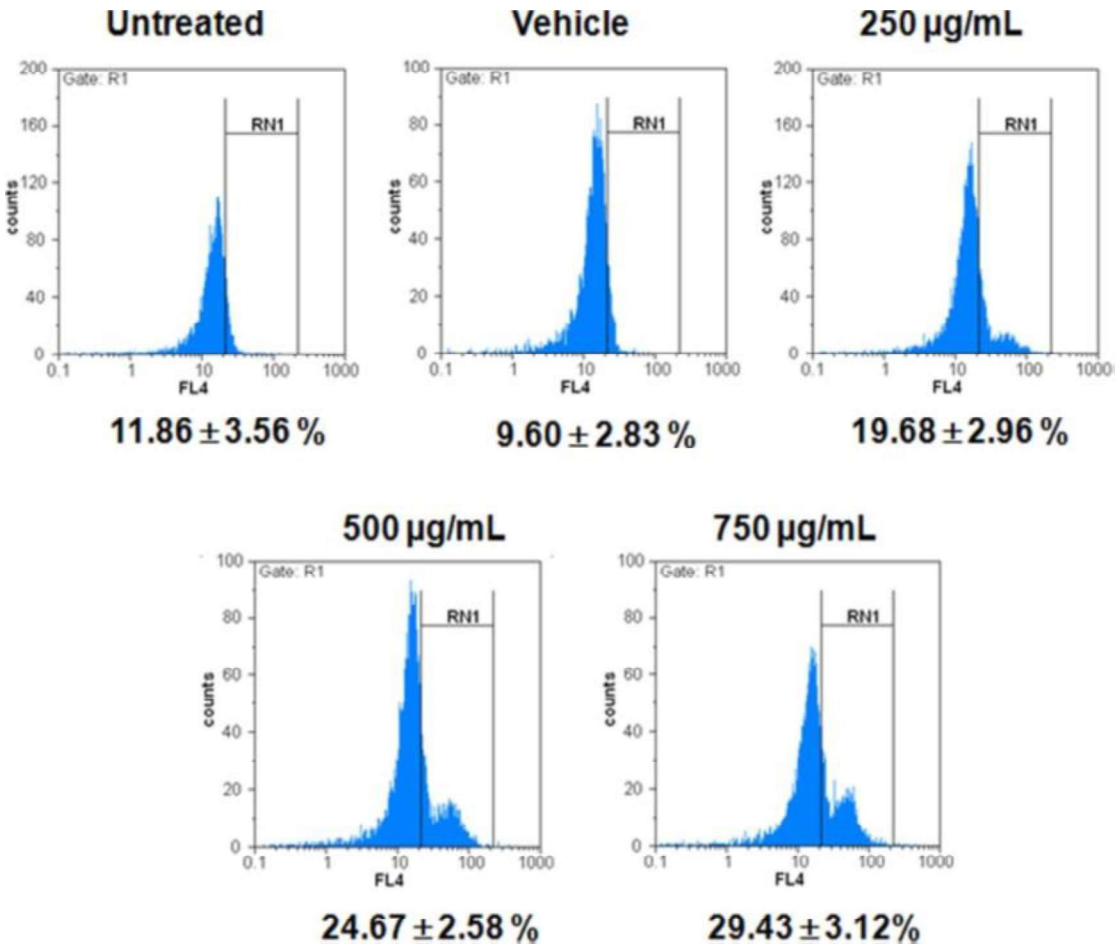

Figure 3.1.22. DNA condensation occurs in E. coli after treatment with HC. Mid log phase cells of E. coli were treated with vehicle or HC for 2 h. The cells were labelled with Hoechst 33342 (5 µg/mL) for 10 min in dark and fluorescence acquired by flow cytometry RN1 signifies Hoechst positive cells in that experiment. The experiment was done in triplicate. Data presented is representative histograms from one experiment. The experiment was done in triplicate and repeated twice (values = mean ± SD).

3.1.5. Role of membrane damage in the antibacterial activity of HC

We investigated the induction of membrane damage employing the PI uptake assay. We treated *E. coli* cells with HC and evaluated membrane damage by PI uptake. HC treated cells exhibited PI uptake after 1 h of treatment (Figure 3.1.23A and B). Evaluation of PI uptake at MBC revealed significant uptake at 15 min and thereafter (Figure 3.1.23C and D).

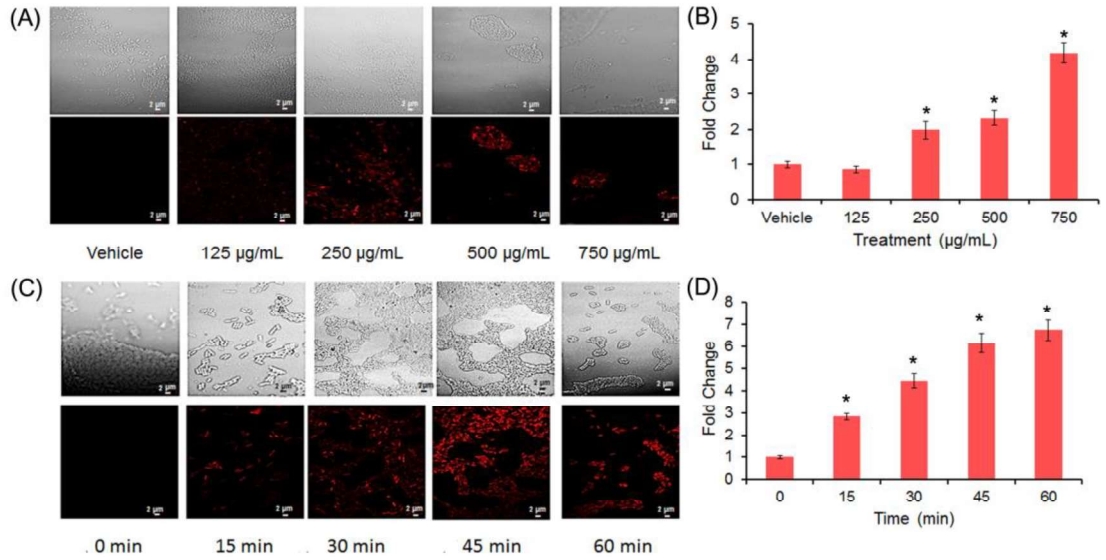

*Figure 3.1.23. Membrane damage induced by HC in E. coli. Mid log phase cells were treated with HC for 1 h after which the PI uptake was visualized by (A) microscopy and (B) quantified in a fluorescence plate reader. In a time kinetic assay, cells treated with HC (500 µg/mL) were processed at different time points for PI uptake either for visualization by microscopy (C) or quantified in a fluorescence plate reader (D). The values given are mean±SD. *indicates significant difference at $p<0.05$ (unpaired Student's t test). The experiment was done in triplicate and repeated thrice.*

This prompted us to check potassium and ATP leakage as markers of membrane damage. HC induced significant potassium leakage from cells (Figure 3.1.24A). Kinetic analysis revealed potassium leakage begins at 30 min (Figure 3.1.24B) after HC treatment.

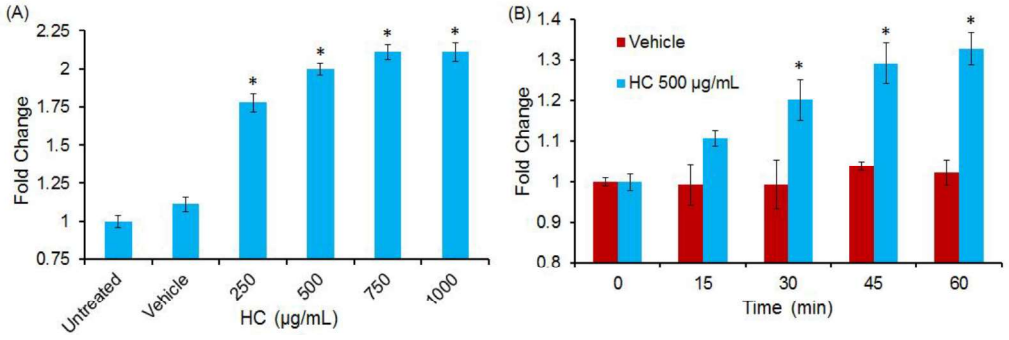

Figure 3.1.24. Estimation of potassium leakage from HC treated E. coli. Mid log cells were treated with (A) HC for 1 h (B) HC (500 µg/mL) for different time periods after which the amount of potassium leaked out of the cells was quantified by atomic absorption

*spectrometry. The values given are mean±SD. *indicates significant difference at p<0.05 (unpaired Student's t test). The experiment was done in triplicate and repeated thrice*

The lowest concentration of HC that induced leakage of ATP from *E. coli* cells was found to be 500 µg/mL after 1 h of treatment (Figure 3.1.25A). Similar to potassium leakage, cells treated with HC revealed significant ATP leakage at 30 min and beyond (Figure 3.1.25B).

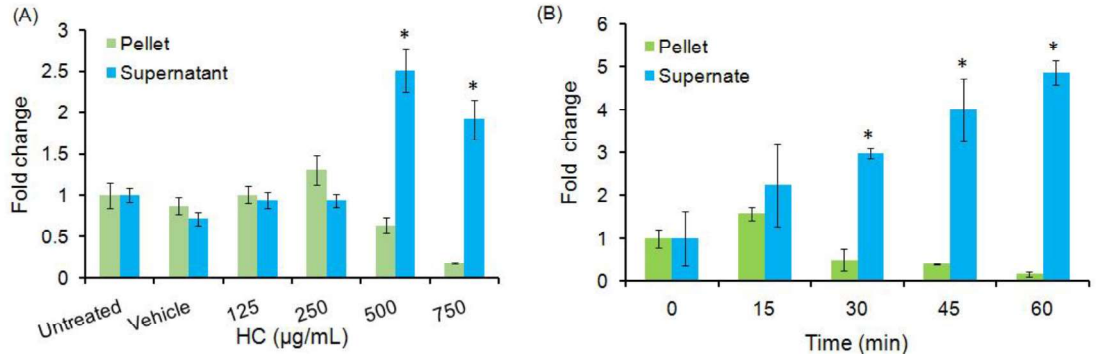

*Figure 3.1.25. Estimation of ATP leakage from HC treated E. coli. Mid log cells were treated with (A) HC for 1 h (B) HC (500 µg/mL) for different time periods after which the amount of ATP leaked out of the cells in supernate and residual ATP in the pellets was quantified by chemiluminescence. The values given are mean±SD. *indicates significant difference at p<0.05 (unpaired Student's t test). The experiment was done in triplicate and repeated thrice.*

A key feature of an intact bacterial membrane is the membrane polarity, with the intracellular milieu being relatively negative. Membrane damage results in ionic equilibration, causing membrane depolarization [111]. However, hyperpolarization has also been reported to accompany loss in viability [112]. Since membrane damage was detected after HC treatment we evaluated the membrane potential employing Rhodamine 123 [113]. As shown in Figure 3.1.26, significant membrane hyperpolarization was observed after 1 h of HC treatment. A time kinetic analysis revealed membrane hyperpolarization induced by HC (500 µg/mL) evident at 15 min after which it increased till the maximum time point observed (1 h) (Figure 3.1.26B).

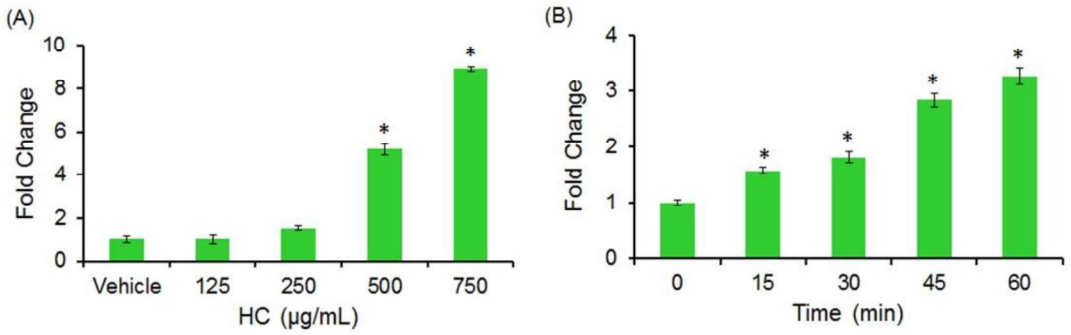

*Figure 3.1.26. Effect of HC treatment on the state of energy metabolism. Mid log cells were treated with (A) HC for 1 h (B) HC (500 µg/mL) for different time periods after which the fluorescence of rhodamine 123 was quantified in a plate reader. The values given are mean±SD. *indicates significant difference at $p<0.05$ (unpaired Student's t test). The experiment was done in triplicate and repeated thrice.*

When grown in the presence of a mild membrane lysing agent (0.1% SDS), higher rate of cell lysis was observed in case of HC (500 and 750 µg/mL) treated cells compared to vehicle treated cells. This showed that HC treated cells exhibited weakened membrane and was susceptible to treatment that would not affect healthy cells (Figure 3.1.27).

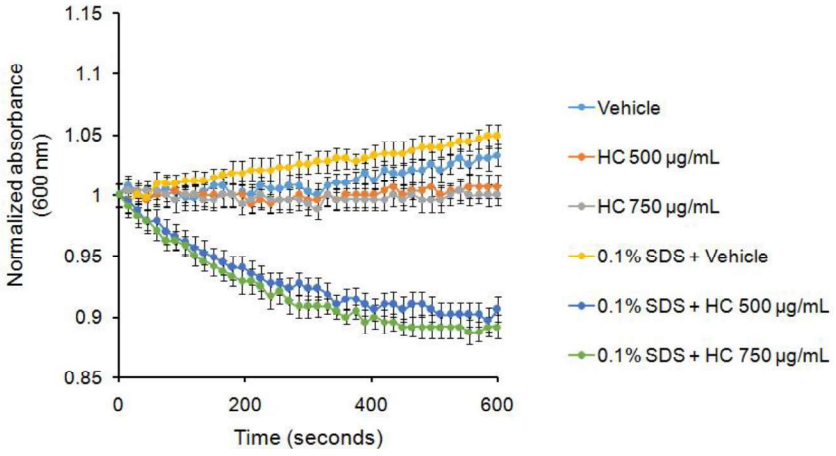

Figure 3.1.27. HC treated cells exhibit a higher rate of lysis. HC treated E. coli were washed and resuspended in LB. The rate of lysis was monitored continuously in the presence of 0.1% SDS at 600 nm in a plate reader. The experiment was conducted in triplicate and repeated thrice. As a representation, the mean values are provided.

There are different mechanisms by which membrane is damaged by antibacterial agents [114]. One of the mechanisms by which a small organic molecule might compromise a bacterial membrane is by stripping Mg^{2+} leading to collapse of the same [115]. We evaluated the effect of Mg^{2+} on HC induced growth inhibition and cytotoxicity in *E. coli*. External supplementation of Mg^{2+} protected cells from HC, resulting in higher growth (Figure 3.1.28A). Conversely, external addition of EDTA resulted in lower growth in presence of HC (Figure 3.1.29). External Mg^{2+} had an effect on MBC as revealed from the spot test (Figure 3.1.28B). However, EDTA only affected the extent of growth (lesser growth compared to HC alone) and not the MBC (Figure 3.1.29B). For e.g., no sensitization was observed in case of HC (200 µg/mL and 250 µg/mL) treatment in EDTA supplemented population (Figure 3.1.29). We further observed that the effect of Mg^{2+} on HC induced inhibition of growth did not hold true for gram positive bacterium *S. aureus*. External supplementation of Mg^{2+} did not have any effect on extent of growth as well as cytotoxicity induced by HC in *S. aureus* (Fig 3.1.28B and D). This data, coupled with the effects of Mg^{2+} and EDTA on HC induced membrane permeabilization suggests that HC destabilizes the outer membrane through cation abstraction.

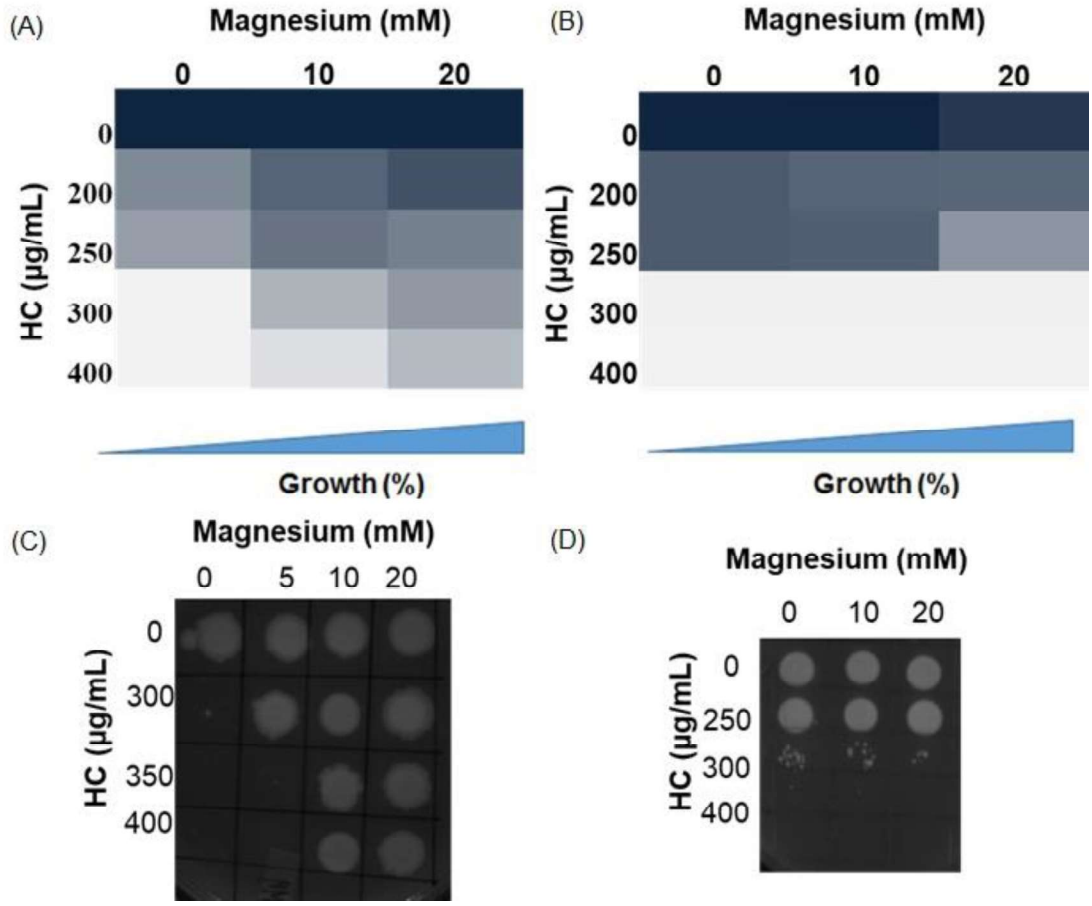

Figure 3.1.28. Effect of magnesium on HC mediated growth inhibition of E. coli. Mid log cells of E. coli and S. aureus were pretreated with Mg^{2+} before addition of HC. Extent of growth and viability was evaluated by absorbance and plating, respectively. Heat map based on the extent of growth in presence of Mg^{2+} in E. coli (A) and S. aureus (B) was generated. (C and D) Effect of Mg^{2+} on the viability of E. coli and S. aureus treated with HC.

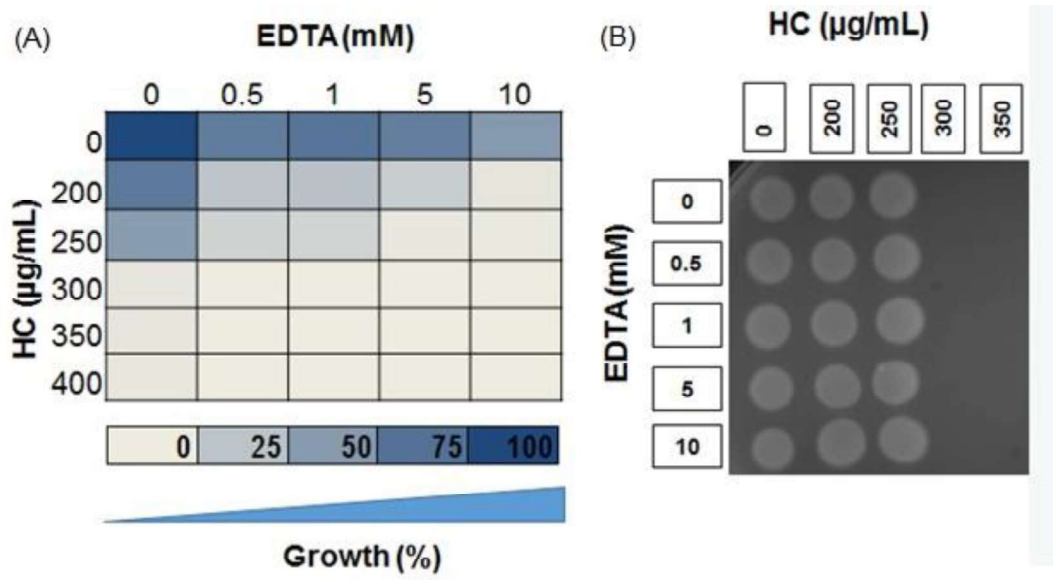

Figure 3.1.29. Effect of EDTA on HC mediated growth inhibition of E. coli. Mid log cells were pretreated with EDTA before addition of HC. Extent of growth and viability was evaluated by absorbance and plating, respectively. Heat map based on the extent of growth in presence of EDTA was generated. (C and D) Effect of EDTA on the viability of E. coli treated with HC.

3.1.6. Evaluation of the kinetics of damage to different molecular targets upon HC treatment

Because multiple targets were damaged after HC treatment, it is imperative to understand the relative temporal order of the events. We devised a method to simultaneously detect ROS generation and membrane damage after HC treatment, using DCFDA and PI uptake as a marker of ROS generation and membrane damage, respectively. DCFDA positive cells were detected as early as 10 min post HC treatment, while significant PI uptake was observed earliest at 30 min (Figure 3.1.30A). This data also agrees with the potassium and ATP leakage data. Quantitative analysis of the proportion of DCFDA positive, PI positive and double positive cells (Figure 3.1.30B) revealed DCFDA positive cells appeared at 10 min and peaked at 15 min, with significant proportion of cells remaining DCFDA positive even at 60 min. Significant proportion of PI positive was detected at 30 min and 60 min.

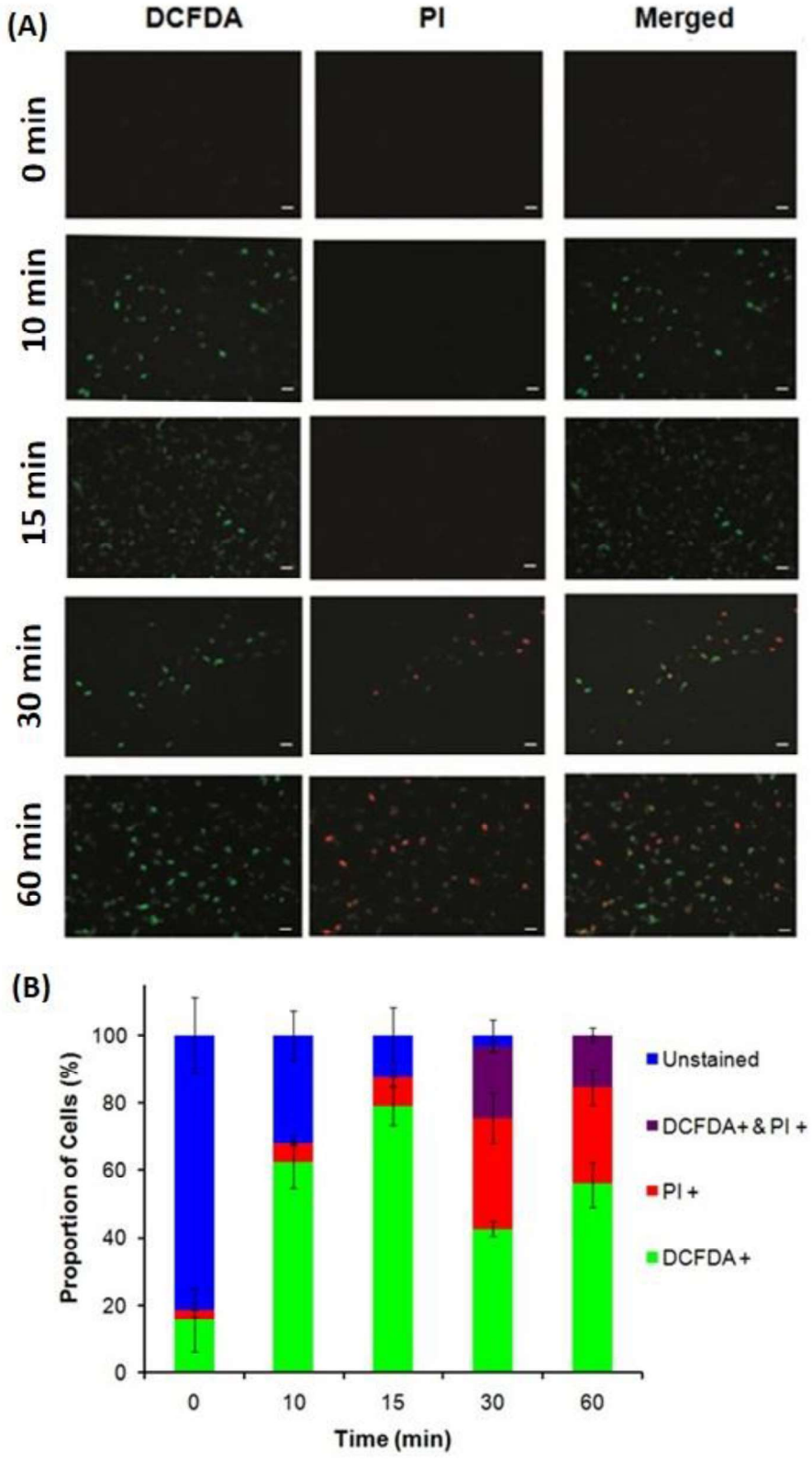

Figure 3.1.30. Simultaneous detection of ROS and membrane damage in HC treated cells. ROS by DCFDA and membrane damage by PI was detected simultaneously by prelabeling

cells with DCFDA before HC treatment. After HC treatment the cells were labeled with PI and observed under the fluorescence microscope (A). The scale bar in the figure represents 10 µm. Different fields were scanned and the unstained, DCFDA positive, PI positive and double positive cells were counted. For each sample at least 500 cells were counted before plotting the graph (B). The values are mean±SD. The experiment was conducted in triplicate and repeated thrice.

Physical damage to DNA in HC treated *E. coli* cells was visualized employing comet assay. No DNA damage was observed in cells treated with vehicle or 125 µg/mL, while significant DNA damage was observed at 250, 500 and 750 µg/mL (Figure 3.1.31).

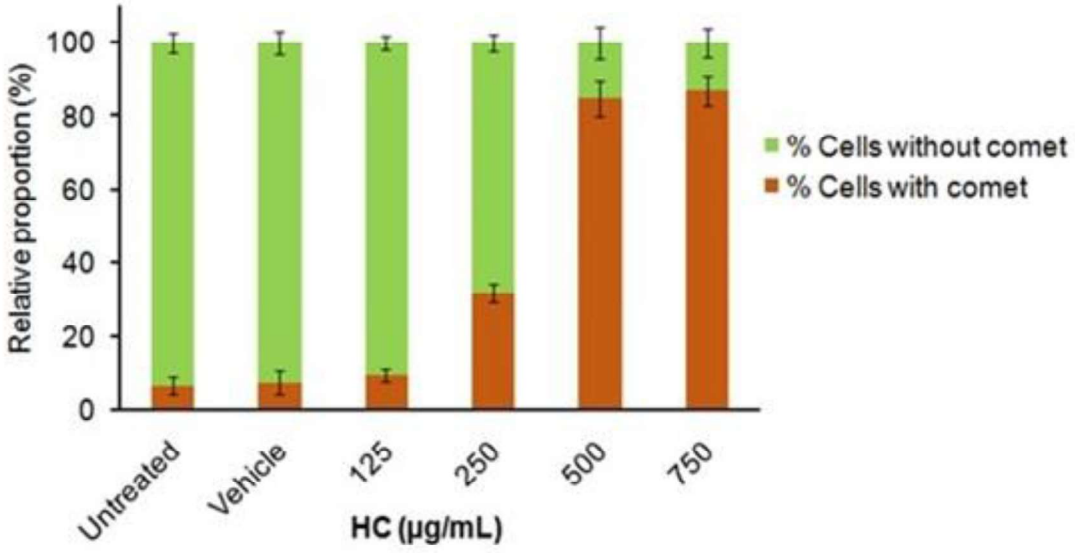

Figure 3.1.31. DNA damage induced by HC. Mid log cells were treated with HC and processed for comet assay. The number of comets in each sample was analyzed under the microscope and expressed as a proportion to that of normal cells.

Evaluation of the kinetics of the gene expression of DNA damage repair genes employing real time PCR revealed significant up regulation of *nth*, *nei*, *recN* and *dinB* genes. While *nth* was found to be up regulated after 40 min (Figure 3.1.32), *nei* and *recN* were found to be up regulated at 60 min. The up regulation of *dinB* was found to be at 120 min. The maximum up regulation of *nth* was found to be at 60 min. RecN is a member of the Structural Maintenance of Chromosome (SMC) class of proteins [116]. Oxidative DNA damage is repaired by Nth

and Nei [117], while DinB is a DNA polymerase involved in error prone DNA repair [118]. These data indicate oxidative DNA damage repair response to be optimally activated at 60 min. Interestingly, RecN has been recently implicated in filamentation in response to DNA damage [119], suggesting that induction of *recN* in response to HC treatment might have a bearing on HC induced cellular filamentation.

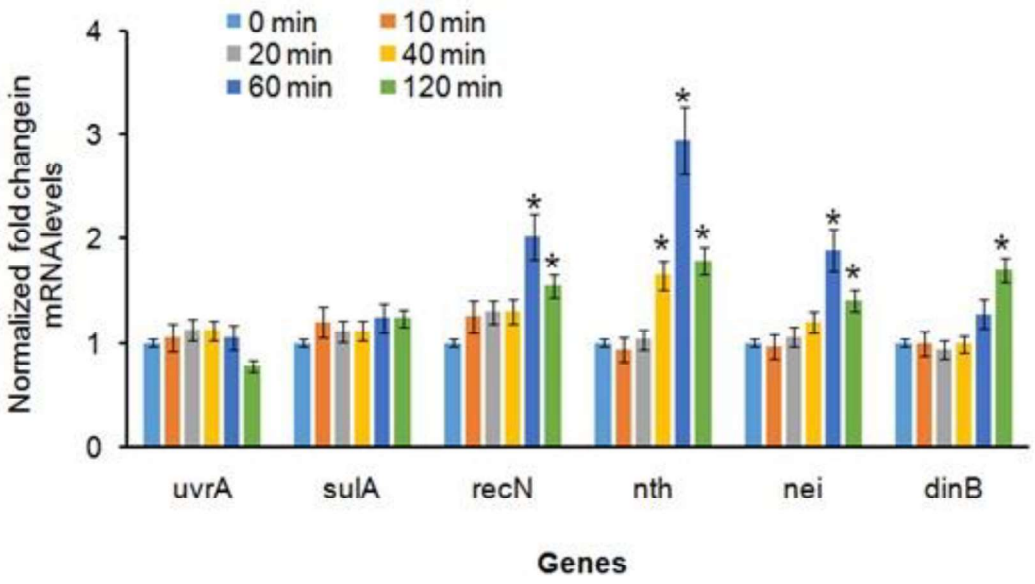

*Figure 3.1.32. Mid log cells were treated with HC (500 µg/mL) for different time points. RNA was extracted and cDNA prepared, followed by qPCR. Relative gene expression was obtained and plotted. The values given are mean±SD. *indicates significant difference at $p<0.05$*

All these kinetic experiments suggested that HC 500 µg/mL treatment induced in ROS induction (15 min) which followed by membrane damage (30 min) and DNA damage (60 min).

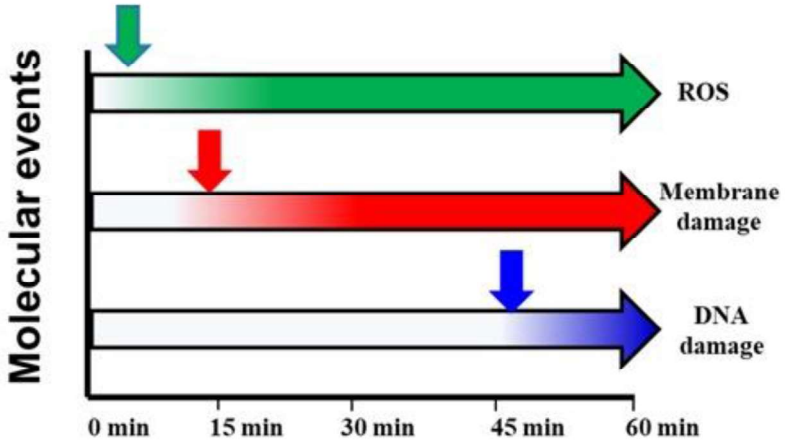

Figure 3.1.33. A graphical representation of kinetic events that occur after HC 500 µg/mL treatment in E. coli.

3.1.7. Evaluation of predisposition of gram negative bacteria by HC to hydrophobic antibiotics.

To test if HC induced membrane damage would enhance the sensitivity of *E. coli* to hydrophobic antibiotics, cells were pretreated with HC (250, 500 and 750 µg/mL) for 1 h. The pretreatment alone did not affect growth and viability. But when challenged with different antibiotics, the pretreated cells exhibited higher sensitivity compared to cells that were not pretreated with HC. Compared to cells that were pretreated with vehicle HC pretreated cells exhibited less growth as well as viability with each of the antibiotics tested (Figure 3.1.34A to H).

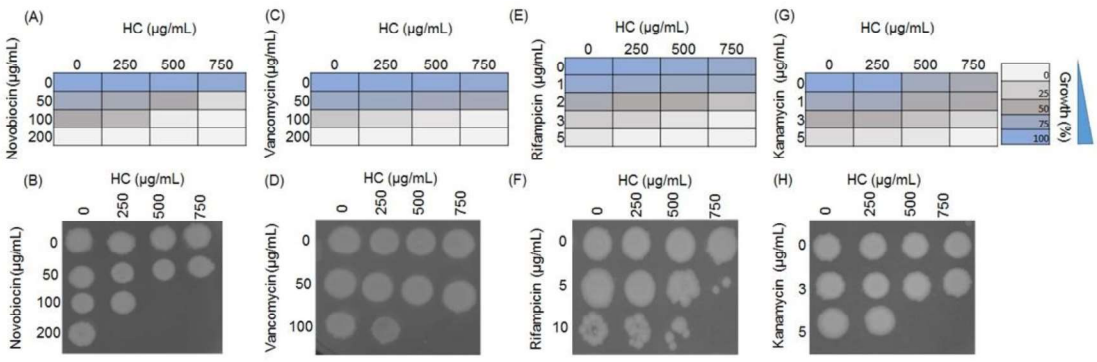

Figure 3.1.34. Sensitization of E. coli by HC to hydrophobic antibiotics. Cells were pretreated with HC for 1 h and washed before exposure to different antibiotics. Extent of

growth and viability was evaluated by absorbance and plating, respectively. Heat map (A, C, E, G) based on the extent of growth was generated. Effect of the treatment on viability was evaluated by spotting (B, D, F, H) an aliquot after 18 h incubation on MH agar. The growth on plates was observed after 24 h of spotting.

To test the efficacy of HC against different bacteria with varied antibiotic sensitivity profiles, we obtained bacteria from the Department of Pathology, BARC Hospital that was isolated from patients during the course of clinical investigation. As shown in Table 3.1.2 the MIC and MBC values of HC against these bacteria were in the range that was comparable to the laboratory strains. The clinical symptoms and antibiotic resistance profile of each pathogen is provided in Table 3.1.2. Fourteen *E. coli* samples were tested against HC. The MIC was either 250 µg/mL or 500 µg/mL while MBC was found to be either 500 µg/mL or 750 µg/mL (except one isolate where the MBC was 1000 µg/mL). Differences in standard antibiotic resistance profiles did not bear an effect on susceptibility to HC as observed in clinical *E. coli* samples. This was also true in case of other pathogens like *K. pneumoniae*, *P. aeruginosa* and *P. vulgaris* (Table 3.1.2).

Table 3.1.2. List of clinical isolates employed in the investigation of antibacterial activity of HC.

S. No.	Name of the organism	Clinical source	Clinical symptoms	Age/ Gender	Sensitive to	Resistant to	MIC vs HC	MBC vs HC
1.	*E. coli*	Urine	Known case of HT on treatment No h/o DM, however, his sugars had been on the higher side He had retention of urine with prostate of 70 gm	73 Yr/ Male	Tigecycline, Colistin	Meropenem, Ertapenem, Amoxyclav, Cefuroxime, Ceftazidime, Cefotaxime, Ceftriaxone, Cefepime, Nitrofurantoin, Co-trimoxazole, Ciprofloxacin, Ceftriaxone/ Tazobactam, Aztreonam, Imipenem,	250 µg/mL	500 µg/mL
2.	*E. coli*	Urine	C/o dysuria	92 Yr/ Female	Ciprofloxacin, Ampicillin/ Sulbactam, Norfloxacin, Ceftazidime, Cefepime, Ceftriaxone, Cefotaxime, Ceftriaxone/ Tazobactam, Co-trimoxazole, Ofloxacin, Piperacillin/ Tazobactam, Cefoperazone/ Sulbactam, Amikacin Gentamicin, Nalidixic Acid.	Amoxyclav, Cefuroxime, Nitrofurantoin	250 µg/mL	500 µg/mL
3.	*E. coli*	Urine	Fever	71 Yr / Female	Cefepime, Ceftriaxone, Co-trimoxazole, Ceftriaxone/ Tazobactam, Piperacillin/ Tazobactam, Cefuroxime, Ampicillin /Sulbactam, Gentamicin, Amikacin, Nitrofurantoin, Cefoperazone/ Sulbactam .	Nalidixic Acid, Ciprofloxacin, Norfloxacin, Amoxyclav, Ofloxacin, Amoxyclav	250 µg/mL	500 µg/mL
4.	*E. coli*	Urine	Pyelonephritis	68 Yr/ Female	Piperacillin/ Tazobactam, Ceftazidime, Ampicillin /Sulbactam, Ceftriaxone/	Ciprofloxacin, Ofloxacin, Amoxyclav, Ceftriaxone, Norfloxacin, Cefuroxime,	250 µg/mL	500 µg/mL

					Tazobactam, Cefepime, Gentamicin, Amikacin, Cefoperazone/ Sulbactam, Nitrofurantoin.	Cefotaxime, Co-trimoxazole, Nalidixic Acid.		
5.	*E. coli*	Urine	C/o of post turp, incontinence.	86 Yr/ Male	Tigecycline, Colistin	Imipenem, Meropenem, Ertapenem, Levofloxacin, Aztreonam, Cefoperazone/ Sulbactam, Amikacin, Gentamicin, Nalidixic Acid, Nitrofurantoin, Piperacillin/ Tazobactam, Cotrimoxazole, Cefepime, Ceftazidime, Ofloxacin, Cefuroxime, Ceftriaxone, Norfloxacin, Ceftriaxone/ Tazobactam, Amoxyclav, Ciprofloxacin, Cefotaxime, Piperacillin/ Tazobactam	250 µg/mL	500 µg/mL
6.	*E. coli*	Urine	Na	72 Yr/ Male	Amikacin, Gentamicin, Co-trimoxazole, Tigecycline, Colistin	Meropenem, Levofloxacin, Amoxyclav, Ampicillin/ Sulbactam, Cefuroxime, Ceftazidime, Cefotaxime, Ceftriaxone, Cefepime, Nalidixic Acid, Norfloxacin, Nitrofurantoin, Piperacillin/ Tazobactam, Cefoperazone/ Sulbactam, Ceftriaxone/ Tazobactam, Cotrimoxazole, Ciprofloxacin, Imipenem	250 µg/mL	500 µg/mL
7.	*E. coli*	Sputum	C/o blood vomiting	78 Yr/ Male	Amikacin, Cefoperazone/ Sulbactam	Ampicillin, Amoxyclav, Cefuroxime, Ceftazidime, Cefotaxime, Cefuroxime, Ceftazidime, Cefotaxime, Ceftriaxone, Cefepime, Gentamicin, Piperacillin/	500 µg/mL	500 µg/mL

						Tazobactam, Ceftriaxone/ Tazobactam, Ciprofloxacin, Ofloxacin, Levofloxacin, Co-trimoxazole		
8.	*E. coli*	Wound swab	Wound	48 Yr/ Male	Amikacin, Gentamicin, Cefepime.	Ampicillin, Amoxyclav, Cefuroxime, Ceftazidime, Cefotaxime, Ceftriaxone, Cefepime, Ciprofloxacin, Ofloxacin, Levofloxacin, Piperacillin/ Tazobactam, Cefoperazone/ Sulbactam, Ceftriaxone/ Tazobactam, Cotrimoxazole	500 µg/mL	1000 µg/mL
9.	*E. coli*	Urine	C/o body ache 1 day	42 Yr/ Male	Amikacin, Gentamicin, Cefuroxime, Ceftazidime, Cefotaxime, Ceftriaxone, Cefepime, Co-trimoxazole, Piperacillin/Tazobactam, Cefoperazone/Sulbactam Ceftriaxone/Tazobactam, Ciprofloxacin, Norfloxacin.	Amoxyclav, Ampicillin/ Sulbactam, Nitrofurantoin, Nalidixic Acid	500 µg/mL	500 µg/mL
10.	*E. coli*	Urine	Pain in epigastric region since last one month	72 Yr/ Male	Amikacin, Imipenem, Meropenem, Ertapenem, Colistin, Tigecycline, Levofloxacin	**Interm**: Piperacillin/ Tazobactam, Cefoperazone/ Sulbactam. **Resistant**: Amoxyclav, Ampicillin/ Sulbactam, Cefuroxime, Ceftazidime, Cefotaxime, Ceftriaxone, Cefepime, Nalidixic Acid, Norfloxacin, Nitrofurantoin, Ciprofloxacin, Co-trimoxazole, Ceftriaxone/ Tazobactam, Gentamicin, Aztreonam	500 µg/mL	750 µg/mL

11.	*E. coli*	Urine	Primi with pog 38 wks with prom	25 Yr/ Male	Amikacin, Gentamicin, Nalidixic Acid, Norfloxacin, Ciprofloxacin, Piperacillin/ Tazobactam, Cefoperazone/ Sulbactam	Amoxyclav, Ampicillin/ Sulbactam, Cefuroxime, Ceftazidime, Ceftriaxone, Cefepime, Ceftriaxone/ Tazobactam, Co-trimoxazole	250 µg/mL	500 µg/mL
12.	*E. coli*	Urine	C/o dm with htn and anaemia	57 Yr/ Male	Tigecycline, Ciprofloxacin, Piperacillin/ Tazobactam, Amikacin, Gentamicin, Norfloxacin, Cefoperazone/ Sulbactam, Ofloxacin, Colistin, Ceftriaxone/ Tazobactam, Ceftazidime, Ertapenem	Cefotaxime, Nitrofurantoin, Amoxyclav	500 µg/mL	750 µg/mL
13.	*E. coli*	Urine	High risk preg conceived by ivf	41Yr/ Female	Ceftazidime, Cefuroxime, Norfloxacin, Amikacin, Gentamicin, Nalidixic Acid, Nitrofurantoin, Ampicillin/ Sulbactam, Ofloxacin, Ciprofloxacin, Ceftriaxone, Piperacillin/ Tazobactam, Ceftriaxone/ Tazobactam, Cefepime. Cefoperazone/ Sulbactam	Amoxyclav, Co-trimoxazole	500 µg/mL	750 µg/mL
14.	*E. coli*	Urine	UTI k/c/o DM	63 Yr/ Female	Norfloxacin, Cefuroxime, Ceftazidime, Ampicillin / Sulbactam, Ofloxacin, Cefepime, Ceftriaxone, Cefotaxime, Piperacillin/ Tazobactam, Cefoperazone/ Sulbactam, Ciprofloxacin, Ceftriaxone/ Tazobactam. Amikacin, Gentamicin.	Amoxyclav, Co-trimoxazole, Nalidixic Acid, Nitrofurantoin	250 µg/mL	500 µg/mL
15.	*K.*	Sputum	cough x 1 mth Feb thr	54 Yr/	Cefotaxime, Ceftriaxone/ Tazobactam, Ciprofloxacin,	Ampicillin, Amoxyclav,	500 µg/mL	1000

	pneumoniae		cong + rs clear	Female	Piperacillin/ Tazobactam Ofloxacin, Levofloxacin, Meropenem, Cefepime, Ceftriaxone, Imipenem Cotrimoxazole, Amikacin, Gentamicin, Cefoperazone/ Sulbactam, Ceftazidime, Ceftazidime/ Clavulanic Acid	Cefuroxime		µg/mL
16.	*K. pneumoniae*	Urine	A 70 years old female came to SOPD with complaints of Pain over the bilateral lower limb with difficulty in walking Patient was a/a till few days ago after which she started developing pain over bilateral iliac region with difficulty in doing day to day activity.	70 Yr/ Female	Tigecycline, Colistin	Meropenem, Levofloxacin, Imipenem, Ertapenem, Amoxyclav, Cefuroxime, Ceftazidime, Cefotaxime, Ceftriaxone, Cefepime, Nalidixic Acid, Norfloxacin, Nitrofurantoin, Piperacillin/Tazobactam, Cefoperazone/Sulbactam, Ceftriaxone/Tazobactam, Cotrimoxazole, Ciprofloxacin.	500 µg/mL	750 µg/mL
17.	*K. pneumoniae*	Sputum	NA	62 Yr/ Female	Cefuroxime, Ceftazidime, Cefotaxime, Ceftriaxone, Cefepime, Ciprofloxacin, Ofloxacin, Levofloxacin, Piperacillin/ Tazobactam, Cefoperazone/ Sulbactam, Ceftriaxone/ Tazobactam, Cotrimoxazole.	Ampicillin, Amoxyclav	500 µg/mL	1000 µg/mL
18.	*K. pneumoniae*	Catheter tip Culture	Breathlessness & Secretion	48 Yr/ Male	Amikacin, Gentamicin, Levofloxacin, Cefoperazone/ Sulbactam, Piperacillin/ Tazobactam	Ampicillin, Amoxyclav, Cefuroxime, Ceftazidime, Cefotaxime, Ceftriaxone, Cefepime, Ceftriaxone/ Tazobactam, Ciprofloxacin, Ofloxacin, Cotrimoxazole	500 µg/mL	1000 µg/mL

19.	*K. pneumoniae*	c/o throat pain and fever for 3 days c/o dysphagia fever decreased no ear nose complaints	Throat Swabs	34 Yr/ Male	Cefuroxime, Ceftazidime, Cefotaxime, Ceftriaxone, Levofloxacin, Ciprofloxacin, Ofloxacin, Piperacillin/ Tazobactam, Cefoperazone/ Sulbactam, Ceftriaxone/ Tazobactam, Cotrimoxazole, Gentamicin	Ampicillin, Amoxyclav, Cefepime, Amikacin	500 µg/mL	1000 µg/mL
20.	*K. pneumoniae*	NA	Urine	23 Yrs / Female	Amikacin, Gentamicin, Nalidixic Acid, Norfloxacin,	Amoxyclav, Ampicillin/ Sulbactam, Cefuroxime, Ceftazidime, Cefotaxime, Ceftriaxone, Cefepime, Piperacillin/ Tazobactam, Cefoperazone/ Sulbactam, Ceftriaxone/ Tazobactam, Nitrofurantoin, Co-trimoxazole	500 µg/mL	1000 µg/mL
21.	*K. pneumoniae*	In FU for recurrent UTI. At present c/o minor dysuria	Urine	82 Yrs / Male	Ertapenem, Tigecycline, Meropenem, Imipenem, Levofloxacin, Colistin	Amoxyclav, Ampicillin/ Sulbactam, Cefuroxime, Ceftazidime, Cefotaxime, Ceftriaxone, Cefepime, Nalidixic Acid, Norfloxacin, Nitrofurantoin, Co-trimoxazole, Piperacillin/ Tazobactam, Ciprofloxacin, Aztreonam, Ceftriaxone/ Tazobactam, Cefoperazone/ Sulbactam	500 µg/mL	1000 µg/mL
22.	*K. pneumoniae*	68 YRS P3L3 K/C/O DM,	Sputum	68 Yr/ Female	Ciprofloxacin, Ofloxacin, Cefoperazone/ Sulbactam, Amikacin, Gentamicin.	Intermediate : Levofloxacin Resistant to: Ampicillin, Amoxyclav, Cefuroxime, Ceftazidime, Cefotaxime,	500 µg/mL	1000 µg/mL

		HTN, Hypothyroidism, ca endometrium operated as TAH WITH BSO WITH B/L pelvic LN dissection in 2016 at TMH.				Ceftriaxone, Cefepime, Piperacillin/ Tazobactam, Ceftriaxone/ Tazobactam, Cotrimoxazole.		
23.	*K. pneumoniae*	severe haematuria with uti	Urine	64 Yr/ Male	Tigecycline, Meropenem, Ertapenem, Levofloxacin.	Resistant to: Imipenem, Aztreonam. Cefuroxime, Norfloxacin, Amoxyclav, Ciprofloxacin, Piperacillin/ Tazobactam, Cotrimoxazole, Ceftazidime, Gentamicin, Nalidixic Acid, Nitrofurantoin, Amikacin, Cefepime, Ofloxacin, Ampicillin/ Sulbactam, Cefotaxime, Ofloxacin, Ceftriaxone, Ceftriaxone/ Tazobactam	500 µg/mL	1000 µg/mL
24.	*P. aeruginosa* *Highly*	c/o jerky movements since	Urine	88 Yr/ Male	Imipenem, Colistin	Amoxyclav, Cefuroxime, Ceftriaxone, Ceftazidime, Cefepime, Piperacillin/ Tazobactam, Cefoperazone/ Sulbactam, Ceftriaxone/	>1000 µg/mL	>1000 µg/mL

	swarming	evening				Tazobactam, Ciprofloxacin, Levofloxacin, Ofloxacin, Co-trimoxazole, Meropenem, Tigecycline		
25.	*P. aeruginosa*	Throat pain & fever persists. Throat= Congestion ++	Throat Swabs	15 Yrs / Male	Amikacin, Gentamicin, Tobramycin, Netilmicin, Cefoperazone/Sulbactam, Levofloxacin	Ampicillin, Amoxyclav, Cefuroxime, Ceftriaxone, Cefepime, Co-trimoxazole, Ciprofloxacin, Ofloxacin, Piperacillin/Tazobactam, Ceftriaxone/Tazobactam	500 µg/mL	500 µg/mL
26.	*P. aeruginosa*	Breathlessness & Secretion	Catheter tip	48 Yr / Male	Amikacin, Ciprofloxacin, Levofloxacin, Meropenem	Ampicillin, Amoxyclav, Cefuroxime, Ceftriaxone, Cefepime, Ceftazidime, Piperacillin/Tazobactam, Cefoperazone/Sulbactam Ceftriaxone/Tazobactam, Ofloxacin, Co-trimoxazole, Imipenem	>1000 µg/mL	>1000 µg/mL
27.	*P. aeruginosa* *Highly swarming*	with h/o recurrent uti since past 4-5 months.	Urine Culture	49 Yr / Female	Aztreonam, Imipenem, Colistin.	Tigecycline, Levofloxacin, Ceftriaxone, Ceftazidime, Co-trimoxazole, Cefotaxime, Cefoperazone/Sulbactam Amoxyclav, Gentamicin, Meropenem, Netilmicin, Levofloxacin, Cefuroxime, Amikacin, Ceftriaxone/Tazobactam, Cefepime, Tobramycin, Piperacillin/Tazobactam	>1000 µg/mL	>1000 µg/mL
28.	*P. mirabilis*	C/O injectio	Wound Swabs	42 Yr/ Female	Ampicillin, Amoxyclav, Cefuroxime, Ceftazidime,		750 µg/mL	>1000 µg/mL

		n site abscess on rt gluteal region adv: i&d under la			Cefotaxime, Ceftriaxone, Cefepime, Piperacillin/ Tazobactam, Cefoperazone/ Sulbactam, Ceftriaxone/ Tazobactam, Amikacin, Gentamicin, Co-trimoxazole, Ciprofloxacin. Ofloxacin, Levofloxacin			
29.	*P. mirabilis*	c/o pain in the Penis foreskin not retractin g	Urine	3 Yr/ Male	Amikacin, Cefuroxime, Ceftazidime, Cefotaxime, Ceftriaxone, Cefepime, Piperacillin/ Tazobactam, Cefoperazone/ Sulbactam, Ceftriaxone/ tazobactam	Gentamicin, Amoxyclav, Ampicillin/ Sulbactam, Nitrofurantoin, Nalidixic Acid, Norfloxacin, Ciprofloxacin, Cotrimoxazole	750 µg/mL	>1000 µg/mL
30.	*P. mirabilis*	Gluteal tissue from bedsore	Tissue for culture	28 Yr/ Male	Ceftriaxone/Tazobactam, Amikacin, Ceftazidime, Cefotaxime, Ceftriaxone, Ceftazidime/Clavulanic Acid, Cefepime, Co-trimoxazole, Imipenem, Cefuroxime, Ampicillin, Ciprofloxacin, Gentamicin, Ofloxacin, Levofloxacin		1000 µg/mL	>1000 µg/mL
31.	*Salmonella species*	loose motion since 3-4days fever for 2days vomitin g for 1day	Blood	2 Yr/ Female	Ampicillin, Amoxyclav, Cefotaxime, Ceftriaxone, Cefpodoxime, Cefepime, Piperacillin/Tazobactam, Cefoperazone/Sulbactam Co-trimoxazole.	Nalidixic Acid, Ciprofloxacin, Levofloxacin, Ofloxacin, Amikacin, Gentamicin.	750 µg/mL	1000 µg/mL

3.1.8. Evaluation of toxicity of HC in mice

The toxicity of HC was evaluated employing Swiss mice. HC was administered either orally or intraperitoneally. HC was observed to be safe up to 75 mg/kg body weight when administered intraperitoneally. HC was found to be safe up to 750 mg/kg body weight when administered orally.

3.1.9. Evaluation of HC in a peritonitis infection model

To evaluate *in vivo* protective effect of HC, a peritonitis mice infection was employed.

Peritonitis was induced by injecting 10^8 cells of *E. coli* in 4% mucin in saline solution. The untreated mice were visibly sick in 12 h and mortality ensued within 48 h. For intervention, HC was administered either orally (250 mg/kg body weight) or intraperitoneally (10, 25 or 50 mg/kg body weight). The HC treatment by either of the routes of administration did not protect the mice against mortality.

In untreated mice the bacteria were recovered from kidney, liver and spleen after 24 h of infection. When the mice were treated with HC intraperitoneally (50 mg/kg body weight) or orally (250 mg/kg body weight) the bacterial numbers in different organs did not reduce significantly as shown in Table 3.1.3.

Table 3.1.3. Effect of HC treatment on the bacteria recovered from different organs in mice after infection in a peritonitis model.

Sr. No.	Treatment	Liver (cfu/g)	Kidney (cfu/g)	Spleen(cfu/g)
1	Uninfected	0 ± 0	0 ± 0	0 ± 0
2	Infected	$6.5\times10^6\pm1.5\times10^6$	$3\times10^4\pm2.15\times10^4$	$2\times10^5\pm1.85\times10^5$
3	Infected + HC orally	$2.5\times10^7\pm1.8\times10^7$	$4\times10^5\pm1.93\times10^5$	$1\times10^6\pm1.98\times10^6$
4	Infected + HC intraperitoneally	$1.5\times10^7\pm1.2\times10^7$	$3\times10^5\pm2.06\times10^5$	$4\times10^6\pm2.12\times10^6$

3.1.10. Discussion

The detrimental consequences of the evolution of antibiotic resistance in bacteria have forced researchers to look for successful antibacterial chemotherapy. The magnitude of the problem of antibacterial resistance is increasing at an alarming rate as highlighted by the general and scientific news. HC is an active component of leaves of the climber *Piper betle*. Since the mechanism of action of HC against bacteria is not understood clearly we investigated the events leading to cell death in *E. coli* after HC treatment. In eukaryotic cells HC has been reported to exert its activity by interfering with redox balance [120]. In *E. coli* too HC generated copious quantities of ROS within a short span of treatment. External supplementation of antioxidants reduced HC induced cell death as well as decreased the amount of ROS generated. Role of ROS in cell death remains a subject of grey area without clarity regarding cause or effect phenomenon. Many molecules have been shown to increase intracellular ROS and this has been assigned an important role in inducing cell death [77]. Production of ROS in cells has also been observed to have an impact on survival. Tuneable ROS induction in bacteria to make them susceptible to cell death was mooted recently [121]. Catechin, a well known phytochemical mediates bacterial cell death by production of ROS. It increases the levels of antioxidant enzymes SOD and catalase and decreases the intracellular glutathione concentration [74]. On the contrary, not all phytochemicals mediate bacterial cell death by ROS production. Bromo-cinnamaldehyde was shown to kill *E. coli* in a ROS independent mechanism and ROS scavenging seems to sensitize *E. coli* to Bromo-cinnamaldehyde [122]. Our data suggest the antibacterial property exerted by HC is mediated at least, in part via oxidative stress. This is due to the fact that HC treatment results in ROS generation that correlates to the kinetics of loss of cell viability and antioxidants like GSH and Thiourea protect the cells against HC induced lethality. Antioxidants also vary in their ability to protect against drugs that kill bacteria by ROS generation. For e.g. Catechin

induced cell death in *E. coli* is inhibited by N-acetyl cysteine while catalase did not offer any protection [76]. In case of HC, both thiourea and GSH protected *E. coli* and, GSH deficient cells were more sensitive to HC compared to wild type cells. In the presence of thiourea or GSH reduced ROS was observed. Thiourea exerts its action purely by radical scavenging and GSH acts both directly and indirectly by providing reductant to enzymes like glutathione peroxidase and regenerating other antioxidants. However, HC induced ROS in *E. coli* was more subdued by GSH (1.29 fold from 1.84 fold) than by thiourea (1.56 fold from 1.84 fold). It has been observed GSH protects *E. coli* against fluoroquinolone ciprofloxacin by acting as an antioxidant as well as playing a role in efflux of the antibiotic [123]. Similar to that observation, GSH may play a dual role in protecting *E. coli* against HC. This assumes more significance especially in the light of the fact that efflux mutant of *E. coli Δtolc* is hypersensitive to HC compared to wild type. Glutathione has been also observed to play an important role in protecting other cell types against HC [124]. In *in vitro* experiments HC is conjugated to glutathione in rat hepatocytes thereby protecting them [125]. The observation that *gshA* mutant did not exhibit higher ROS compared to wild type cells, yet, exhibited a hypersensitive phenotype to HC treatment may suggest a more complex role of GSH, in addition to its function as an antioxidant. Many molecules can switch the type of pathway to induce cell death under different conditions or induce cell death by more than one mechanism [126]. This only goes to show, the induction of cell death by phytochemicals is a complex phenomenon that has not been understood completely. This could also account for why complete protection is not observed when a single process contributing to death is inhibited. In bacteria, ROS accumulation can arrest cell growth or trigger death by directly inhibiting specific essential metabolic enzymes and by causing DNA damage [127]. Induction of genes involved in DNA damage repair by HC reveals DNA damage occurring upon exposure to HC. This is reiterated by the fact that DNA damage deficient mutants are hypersensitive to

HC. Taken together, HC upon entering the cells induces ROS, damages DNA and inhibits cell division. Further this results in cell death as shown by DNA condensation. HC binds to DNA *in vitro* (albeit not to the magnitude of standard intercalator doxorubicin) and cleaves it in presence of copper. Since this process was inhibited by thiourea, EDTA or neocuproine it is reasonable to assume HC induces ROS to cleave DNA that is amenable to antioxidants and the process involves reduction of copper. The iron sulfur proteins mutants data suggests, ROS generated by HC not only damages DNA but also other targets and leakage of iron from some of these targets may further amplify the ROS produced inside the cells by Fenton Chemistry [128]. Given that the mutants that lack iron sulfur proteins are less sensitive to HC compared to the wild type and these mutants exhibit reduced levels of ROS upon HC treatment, reiterates the importance of these proteins in amplification of ROS inside the cells [128]. HC has been reported to get converted into monoglucuronide, monosulfate and monoglutathione conjugates in liver cells [125]. Two independent studies have observed HC to be non-toxic up-to 500 mg/kg body weight when given by oral route [129, 130]. Further 2% HC did not exhibit any acute dermal toxicity in guinea pigs [129]. A 0.5% HC solution was found to completely kill fungal cells in an animal model when applied topically [129]. Salivary concentration of HC during betel quid chewing is reported to be 4.6 mM (~700 µg/mL) that is effective against different bacteria [125]. Formulations for mouth rinse with HC up to 2.5 mg/mL did not have any unpleasant reaction on human subjects [131]. These observations along with the high abundance of HC in *Piper betle* [131] warrant further work to develop HC as an anti-infection agent. Since pathogenic bacteria use a wide array of processes to overcome the effects of different antibacterial molecules that may be absent in laboratory strains we challenged patient isolated strains with HC. Evaluation of HC against 14 *E. coli*, 9 *K. pneumoniae*, 4 *P. aeruginosa* and 3 *P. Mirabilis* isolated from patients undergoing pathological investigation revealed, the MIC and MBC was comparable to that of laboratory

strains. Differences in standard antibiotic resistance profile did not have a bearing on the efficacy of HC. It is reasonable to assume this could be because of the difference in mechanism of action of HC compared to the standard antibiotics used. Hence the susceptibility to HC remained unaffected irrespective of the presence or absence of those factors that have a bearing on the outcome of standard antibiotics. This raises the hope that HC could be used as a component in our fight against infectious bacteria either as a standalone drug or in combination with other antibiotics.

The generation of ROS is considered a key effecter of cell death in mammalian as well as prokaryotic cells. Many plant derived molecules have been shown to function against cancer cells by tipping the balance of oxidative stress in the cell [132]. Prokaryotic cells, including infectious bacteria, are susceptible to oxidative stress and molecular damage due to them. ROS has also been shown to induce apoptosis-like cell death in bacteria [133, 134]. A common ROS mediated pathway underlying bacterial cell death treated with various antibiotics have been repeatedly proposed and contested [70, 71, 135]. This shows that the mechanism and importance of ROS generation by antibacterial agents are not very well understood. Infectious bacteria have steadily acquired resistance to different clinically used antibiotics by a variety of mechanisms, resulting in frequent failure of established treatment regimens. In the context of ROS, though oxidative stress was detected within 10 min of exposure to HC, induction of DNA damage repair genes, *nth* and *nei* that are typically involved in the repair of oxidative damage peaked at 60 min. Plant derived molecules have been known to exhibit cytotoxicity through complex multiple pathways affecting different targets [136]. Hence we investigated if membrane compromise could be a phenomenon contributing to cell death by HC in addition to ROS induced DNA damage. Outer membrane of gram negative bacteria physically excludes many antibacterial compounds. Poor efficacy of plant derived antibacterial compounds in gram negative bacteria compared to gram

positive bacteria has been recorded previously [137]. In this context a phytochemical that damages the membrane is desirable. The ability of HC to damage membrane revealed by uptake of PI and leakage of intracellular ATP and potassium was thus interesting. Because no oxidative lipid end products were observed, we investigated the mechanism underlying this membrane compromise induced by HC i*n E. coli*. Our results demonstrated that HC destabilizes the outer membrane through cation abstraction. Membrane active phytochemicals have been reported previously and their mechanism of action has been found to be diverse [138]. A general mechanism common for different phenolic phytochemicals affecting the membrane bilayer of bacteria thereby compromising functions of different proteins was proposed recently [139]. A similar phenomenon occurring in case of HC is most likely. However, the high amount of oxidative stress detected after HC treatment is also intriguing. Hence, for all the different findings those support a common mechanism for phenolic antibacterial, subtle differences do exist in the events that lead to death of a bacterial cell. It is important to understand these differences from the point of scientific curiosity as well as to better exploit these molecules as antibacterial agents.

Outer membrane permeabilization has been identified as a strategy to make bacteria susceptible to different antibiotics [140, 141]. Our study provides strong evidence towards membrane compromising activity of HC (in the form of susceptibility to SDS, sensitization by EDTA, and protection by Mg^{2+}) resulting in hyperpolarization of the membrane. Further, this event alone may not explain the antibacterial activity as oxidative stress in the cells and DNA damage were also detected. Their contribution towards cell death could not be undermined. Cell death thus could be a result of damage to multiple targets after HC treatment. To our knowledge, events at the membrane level have not been given sufficient priority as a potential target to kill bacteria. Recently, a lot of focus has been on the events occurring at the membrane after treatment with different antimicrobial compounds [114, 142,

143]. To exploit the membrane compromise induced by HC we tested if pretreatment with HC could sensitize the cells to clinically used hydrophobic antibiotics. Cells pretreated with HC exhibited higher sensitivity to clinically used antibiotics such as vancomycin, novobiocin, rifampicin and kanamycin. Previously, phytochemicals such as thymol and gallic acid have also been observed to permeabilize membrane of gram negative bacteria sensitizing them to clinically used antibiotics [141]. To this end, our work extensively establishes the mechanism of action of the antibacterial activity of HC and kinetics of damage to different targets in the cell. The upshot of the mechanistic understanding is the use of HC as a helper compound with antibiotics that do not work against gram negative bacteria. This sensitization has a very important potential towards combating different gram negative bacteria such as Klebsiella spp, Pseudomonas spp, Proteus spp etc. Further this finding also augments the application of hydrophobic antibiotics towards combating infections. Considering HC functions at a higher concentration it may be an appropriate candidate to be used as a topical antibacterial agent. Coupled with the wound healing activity of HC [144] it could potentially be used to treat wounds in diabetic patients after further investigation.

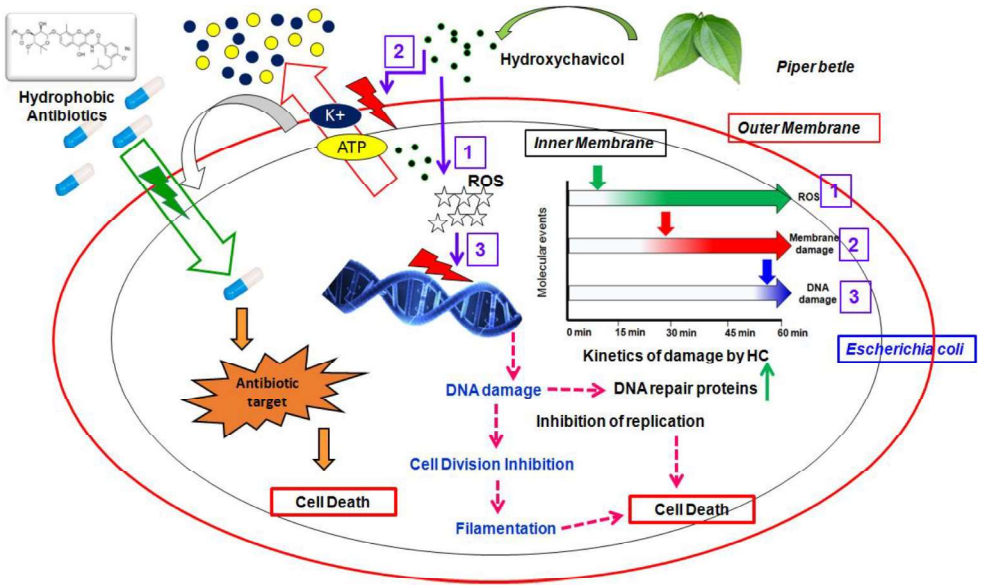

Figure 3.1.35. Graphical representation of HC antibacterial mechanism in E. coli.

3.2. Evaluation of antibacterial activity of stilbenes: A structure-activity relationship study and co-operativity between Stilbenes and antibiotics.

3.2.1. Structure antibacterial activity relationship in stilbenes: A quest towards improvement over Resveratrol

3.2.1.1. Rationale behind selection of different stilbenes

Among all Stilbenes, resveratrol is a very well acclaimed molecule for its health benefits. Recent reports from our group [145] as well as others have investigated the mechanisms behind the antibacterial action of resveratrol [146, 147]. Resveratrol (**1**) possess a 1,3 dihydroxy function on ring 1 and a 4' hydroxy function on ring 2 that is deemed essential for anticancer activity [148]. We selected a number of stilbenes with reference to resveratrol to answer the necessity of some of the substitutions towards antibacterial activity and the changes in the underlying mechanisms as explained below. Analogue **2** provides the effect of introduction of a halogen in place of hydroxy group (4'). Analogue **3** provides information on removal of 4' hydroxy group while analogue **4** provides information on absence of 1 and 3 hydroxy groups (instead a single hydroxy present at 4 position). Addition of an extra hydroxy group at 3' results in analogue **5**, while change in the position of hydroxy group from 4' to 2' yields analogue **6**. Analogue **5** and **6** together provide information on having additional hydroxy groups and at different positions. It has been reported that **1** is converted to analogue **5** by cytochrome P450 enzyme CYP1B1 [149]. Effect of conversion of OH to OMe at position 3 of 1 is provided by analogue **7** while both 3 and 5 OH groups are converted to OMe in case of analogue **8**. In case of analogues **9** and **10** all the 3 OH groups of **1** are replaced by OAc and OMe respectively. Dimerized and oligomerized resveratrol as well as that of other stilbenes have been reported to be biologically important [150]. Hence analogue **11**, the dimer of analogue **4** was also incorporated in the current investigation with an

objective to evaluate the function of a dimeric stilbene. The structure of all stilbenes employed in the current investigation with their common names is depicted in Figure 3.2.1.

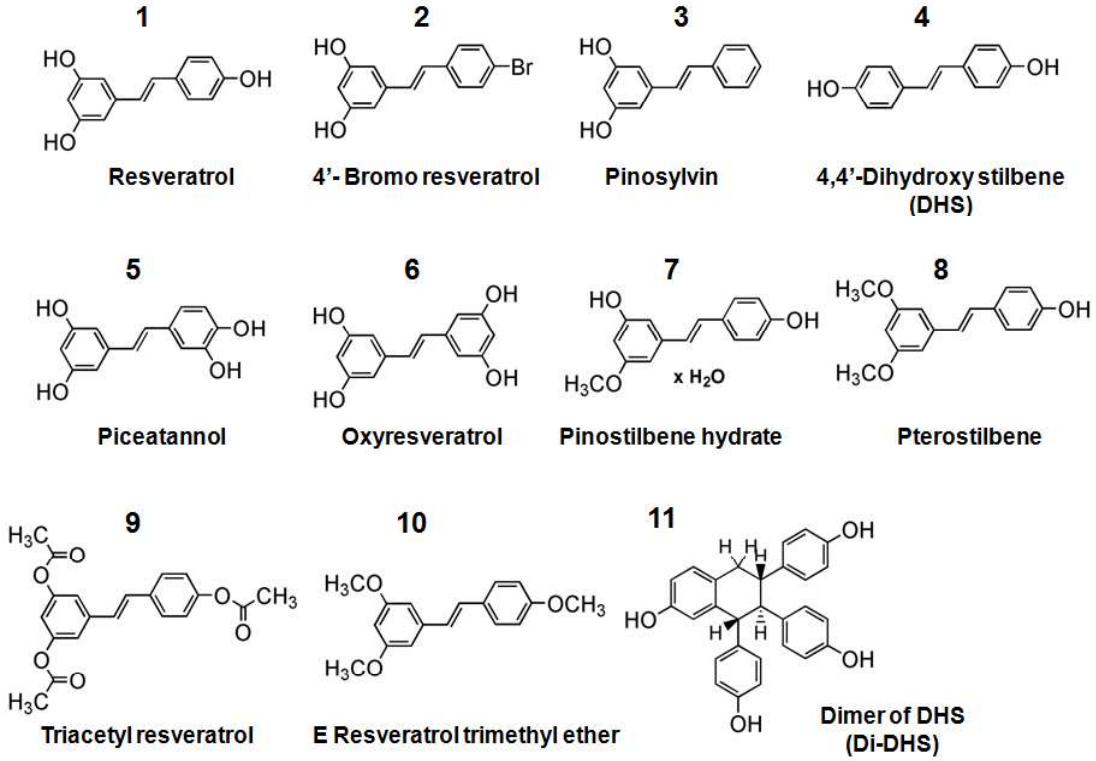

Figure 3.2.1. Structure of different stilbenes employed in the current investigation with their common names.

3.2.1.2. Antibacterial activity of Stilbenes

Resveratrol (**1**) and its structural analogues were evaluated against a panel of gram negative and gram positive bacteria. Plant antimicrobials exhibit antibacterial activity in the range of 100 to 1000 µg/mL [137]. Higher concentrations, greater than few hundreds of µg/mL are not easily achievable pharmacologically and hamper the successful application [137]. Based on our previous work on resveratrol and the reported antibacterial concentrations of other phytochemicals [151, 152] we selected 100 µg/mL to compare different stilbenes for their antibacterial activity [145]. In case of gram negative bacteria **1** was more effective against the enteric bacteria *P. vulgaris* and *S. typhimurium* (~45% in both cases) compared to other bacteria tested. The analogues **2** and **3** exhibited higher inhibition than **1**, when evaluated

against gram negative bacteria (>80% against **3** bacteria), while analogue **7** exhibited comparable activity (Figure 3.2.2). All other analogues exhibited lesser activity when compared to **1**.

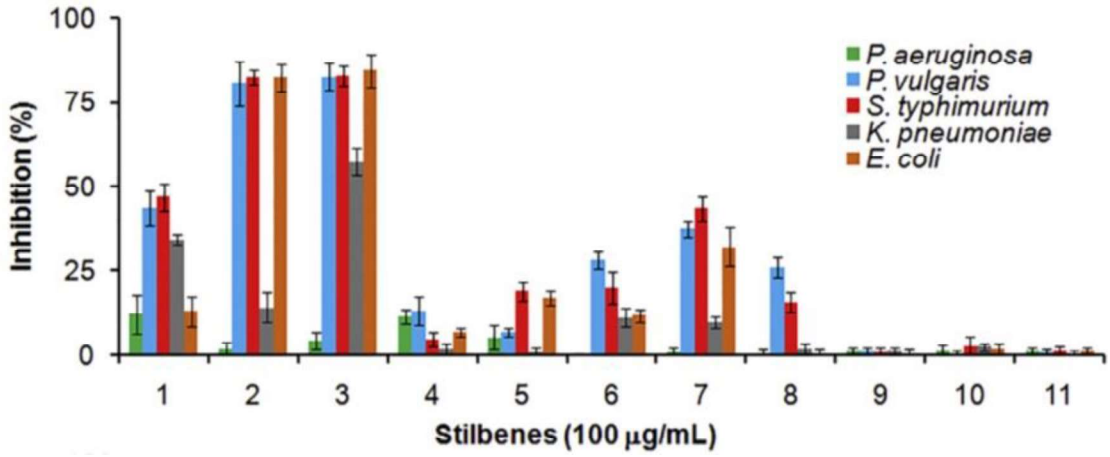

Figure 3.2.2. Antibacterial activity of stilbenes against gram negative bacteria. The extent of inhibition was determined by growing the bacteria in presence of vehicle and different stilbenes as per CLSI guidelines. The experiment was done in triplicate and repeated thrice. The data presented is mean ± SD.

In case of gram positive bacteria analogues **2**, **3**, **7**, **8** and **11** exhibited higher activity than **1**. Resveratrol (**1**) inhibited *S. aureus* by 71.50 ± 2.90% at 100 µg/mL while analogues **2**, **3** and **8** exhibited >80% inhibition at 100 µg/mL. Based on this we employed *S. aureus* as a model organism for further investigation with special focus on analogues **2**, **3**, **7**, **8** and **11** along with **1**.

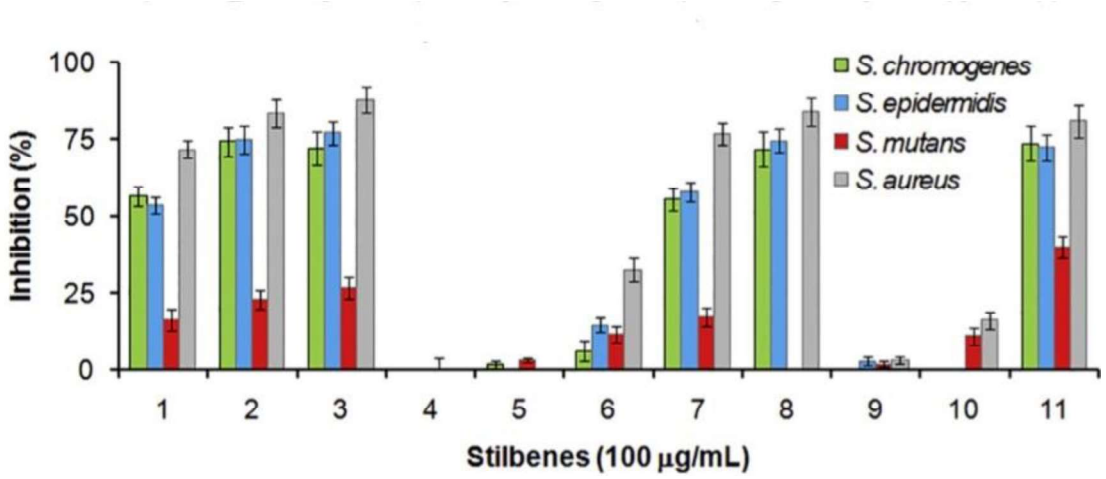

Figure 3.2.3. Antibacterial activity of stilbenes against gram positive bacteria. The extent of inhibition was determined by growing the bacteria in presence of vehicle and different stilbenes as per CLSI guidelines. The experiment was done in triplicate and repeated thrice. The data presented is mean ± SD.

3.2.1.3. Efficacy of stilbenes against efflux mutant *E. coli ΔtolC*

The efficacy of resveratrol analogues was different in gram negative and gram positive bacteria. For e.g. analogues **8** and **11** were completely ineffective in case of gram negative bacteria while in case of gram positive bacteria they were better than resveratrol. The analogues that were effective against gram negative bacteria were equally effective against gram positive bacteria (**2**, **3**, and **7**). The efficacy of different phytochemicals being less against gram negative bacteria has been attributed to the presence of efflux pumps [137]. To test if the difference in efficacy could be due to the efflux pump(s) present in gram negative bacteria, we analysed the antibacterial activity of the stilbenes against *E. coli* wild type BW25113 and its efflux mutant *ΔtolC* that lacks efflux function. As shown in Figure. 3.2.4, the antibacterial activity of all analogues except **4**, **9** and **10** were considerably higher in *ΔtolC* compared to wild type bacteria. In case of **4**, **9** and **10** no antibacterial activity was observed either in *ΔtolC* or the wild type *E. coli*. In case of **1**, **5**, **6** and **7** the efficacy against *ΔtolC* was significantly higher than wild type. Analogues **8**, **11** did not exhibit any activity

against wild type while their activity against *ΔtolC* was comparable to **2** and **3**, the two analogues that were most active against wild type *E. coli*. Analogues **2** and **3** were least affected while analogues **8**, **11**, **7** and **1** were most affected by the presence of efflux pump at the concentration tested (100 µg/mL).

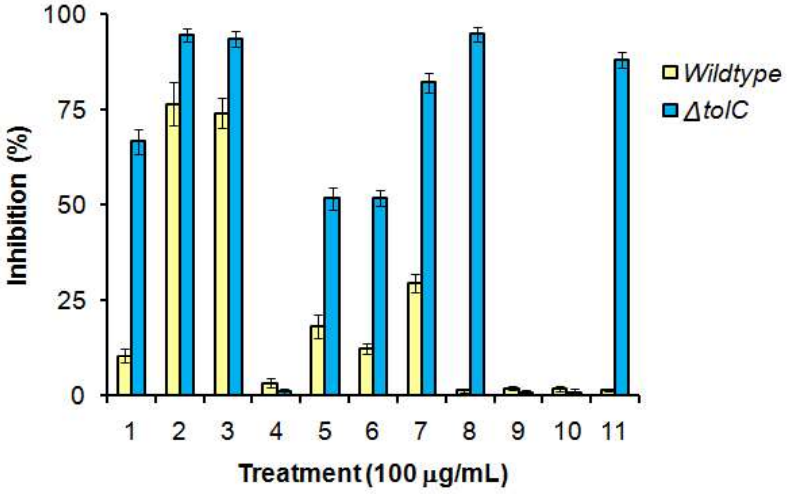

Figure 3.2.4. Comparative efficacy of stilbenes in wild type E. coli and ΔtolC mutant. The extent of inhibition was determined by growing the bacteria in presence of vehicle and different stilbenes as per CLSI guidelines. The experiment was done in triplicate and repeated thrice. The data presented is mean ± SD.

Comparative MIC values of selected stilbenes against wild type and efflux mutant is provided in Table 3.2.1.

Table 3.2.1. MIC values of different stilbenes evaluated against E. coli K-12 strain BW25113 *and its efflux mutant ΔtolC. The MIC was determined by broth dilution method as per CLSI guidelines. The experiment was done in triplicate and repeated thrice.*

Stilbene	***E. coli* BW25113 MIC (µg/mL)**	***E. coli* BW25113 *ΔtolC* MIC (µg/mL)**
1	>100	100
2	>100	25
3	>100	100
7	>100	100
8	>100	25
11	>100	10

3.2.1.4. Quantification of oxidative stress

Small organic molecules containing catechol have a tendency to produce semiquinone and quinone in presence of metal ions. In this process, superoxide anion is generated that subsequently leads to production of other reactive oxygen species (ROS) via Fenton reaction and spontaneous dismutation [105]. Oxidative stress was quantified in *S. aureus* cells treated with different stilbenes employing two different dyes. In case of both the dyes, *S. aureus* treated with analogues **2**, **8** and **11** exhibited higher fluorescence compared to other stilbenes. Analogues **2**, **8** and **11** exhibited 4.8, 3.4 and 3.9 fold increase respectively, compared to untreated sample when evaluated for hydroxyl radical production detected by HPF (Figure 3.2.5A). In case of superoxide production, the same analogues exhibited 4.1, 4.3 and 4.3 fold increase respectively detected by DHE (Figure 3.2.5B). Other analogues did not produce either of the oxygen radical species at the concentration tested.

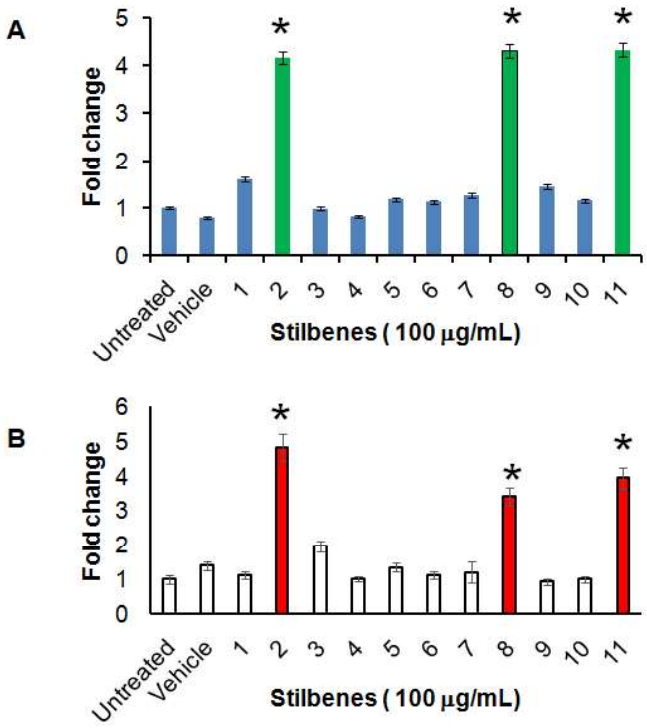

*Figure 3.2.5. Oxidative stress induced by stilbenes. After treatment with different stilbenes for 1 h, oxidative stress was quantified with A) HPF or B) DHE in S. aureus. The fold increase was calculated based on the value obtained for untreated sample. The experiment was done in triplicate and repeated thrice. The data presented is mean ± SD. Significant difference at *p ≤ 0.01 compared to untreated sample.*

3.2.1.5. Quantification of DNA cleavage and DNA binding

Stilbenes and other phytochemicals have been long known to induce DNA damage in presence of metal ions [101]. DNA cleavage activity of the different stilbenes in presence of copper revealed that the DNA cleaving property varies among this class of molecules with minor modifications in their structure. As reported previously **1** cleaved plasmid DNA in presence of copper [101]. Maximum cleavage was observed in case of analogue **5** followed by **2**. Stilbenes **11** and **6** followed closely revealed by the conversion of supercoiled form of DNA to open circle form (Figure 3.2.6). No significant cleavage was observed in case of **3**, **4**, **7**, **8**, **9** and **10**.

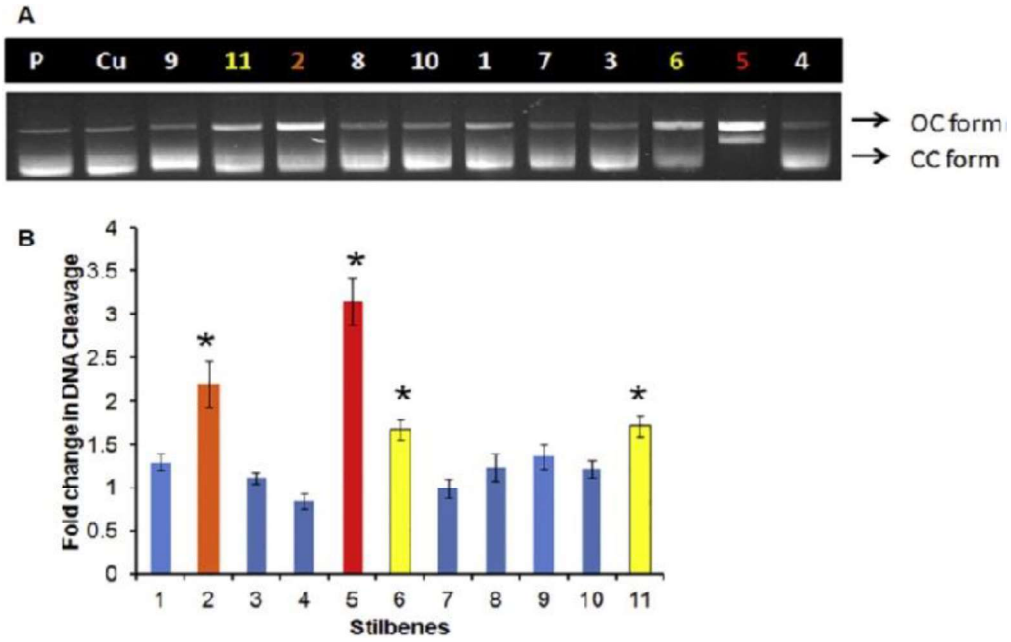

*Figure 3.2.6. DNA cleavage by different stilbenes. (A) Gel electrophoresis of plasmid DNA after incubation with stilbenes and copper. P- plasmid DNA alone (150 ng); Cu- plasmid DNA + Cu (50 µM); All other lanes had plasmid DNA and copper along with the mentioned stilbene (50 µg/mL) incubated for 1 h. (B) Quantification of the extent of damage by imageJ. Fold increase in OC/linear form of DNA quantified by imageJ. The experiment was conducted thrice. The data presented is mean ± SD. *Significant difference at $p \leq 0.01$ compared to untreated sample ('p' in Figure 3.2.6A).*

3.2.1.6. DNA binding activity of stilbenes

Among these stilbenes, **7** and **10** bound very well to DNA while **4** exhibited moderate binding and **3**, **8**, **9** did not bind well to DNA (Table 3.2.2). The best DNA cleaving molecules, **5** exhibited high binding to DNA (54.99 ± 3.17%) and **2** exhibited moderate binding (26.48 ± 2.17%). The analogues **6** and **11**, did not possess any DNA binding ability at all (Table 3.2.2; Nil and 1.5 ± 0.09% respectively). Yet, **6** and **11** exhibited DNA cleavage activity. It is reasonable to conclude DNA binding may not be a pre-requisite to cleave DNA. Generation of diffusible oxygen radicals by these molecules could explain damage to DNA in the absence of binding directly to the target.

Table 3.2.2. Binding efficiency of different stilbenes to plasmid DNA. To a fixed concentration of each stilbene plasmid DNA was added and the spectra were recorded. The experiment was done in triplicate and repeated thrice. The data presented is mean ± SD.

Stilbene	% change at λ_{max}	Type of change
1	4.00 ± 0.20	Hypochromicity
2	26.48 ± 2.17	Hyperchromicity
3	2.28 ± 0.11	Hypochromicity
4	21.25 ± 2.36	Hyperchromicity
5	54.99 ± 3.17	Hypochromicity
6	None	None
7	47.39 ± 3.22	Hyperchromicity
8	11.09 ± 0.58	Hypochromicity
9	15.33 ± 0.77	Hypochromicity
10	62.84 ± 3.75	Hypochromicity
11	1.50 ± 0.09	Hyperchromicity

3.2.1.7. Quantification of membrane damage

Membrane damage to *S. aureus* was evaluated by PI uptake. Maximum membrane compromise was detected in *S. aureus* treated with analogue **8** as revealed by the uptake of PI (Figure 3.2.7A). Compared to vehicle treated sample **8** treated sample exhibited 114.38 ± 29.14 fold higher PI uptake revealing membrane damage. Stilbenes **2** and **11** were the other analogues that exhibited membrane damage as revealed by 62.71 ± 15.59 and 15.74 ± 3.71 fold increase in PI uptake respectively. None of the other stilbenes including **1** exhibited membrane damage in this assay (Figure 3.2.7A). The positive control (70% isopropanol for 30 min) exhibited 69.78 ± 17.18 fold increase compared to untreated sample. When evaluated by an alternate method (calcein leakage) similar result was observed in case of stilbene **8** which outperformed all other stilbenes and exhibited the least retention of calcein (Figure

3.2.7B). Stilbenes **2** and **11** exhibited lesser retention of calcein compared to vehicle treated and other stilbenes treated samples, confirming the damage to membrane as well as supplementing the data obtained in the PI uptake experiment.

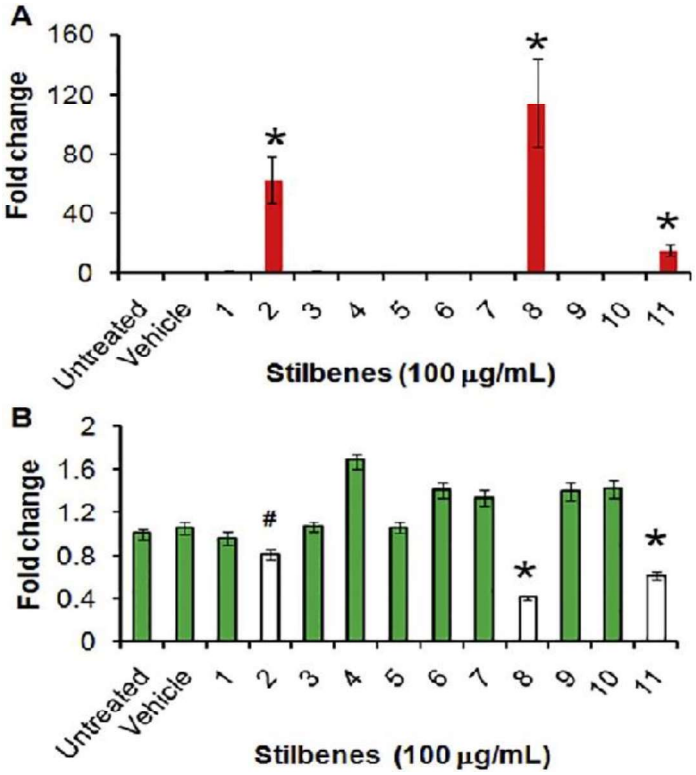

*Figure 3.2.7. Membrane compromise induced by stilbenes. A) PI uptake B) Calcein leakage. PI uptake was quantified in S. aureus treated with stilbenes by measuring the fluorescence of PI inside the cells. In a separate experiment calcein labelled S. aureus cells were treated with stilbenes and the amount of calcein retained in the cells was quantified by measuring the fluorescence. The fold change was calculated compared to the untreated sample. The experiment was done in triplicate and repeated thrice. The data presented is mean ± SD. *Significant difference at $p \leq 0.01$ and # at $p \leq 0.05$ compared to untreated sample.*

3.2.1.8. Cell surface perturbations induced by stilbenes

Damage to the exterior surface on the cell wall has been observed in *S. aureus* after treatment with antibacterial compounds [153]. Previous studies have shown peeling off of cell wall, blebs etc as a mark of damage to the cell surface in *S. aureus* after treatment with antibacterial agents [153, 154]. Similar to those observations a strong blebbing and roughness

was observed in case of cells treated with **2**. Physical damage to cell surface was also observed in case of cells treated with **11**, **1**, **8** and **3** (Figure 3.2.8). Punctured cells were maximally observed in case of treatment with **8** that was in agreement with PI uptake data. Very few cells could be observed in case of **2** and **11** due to high inhibitory activity of these stilbenes.

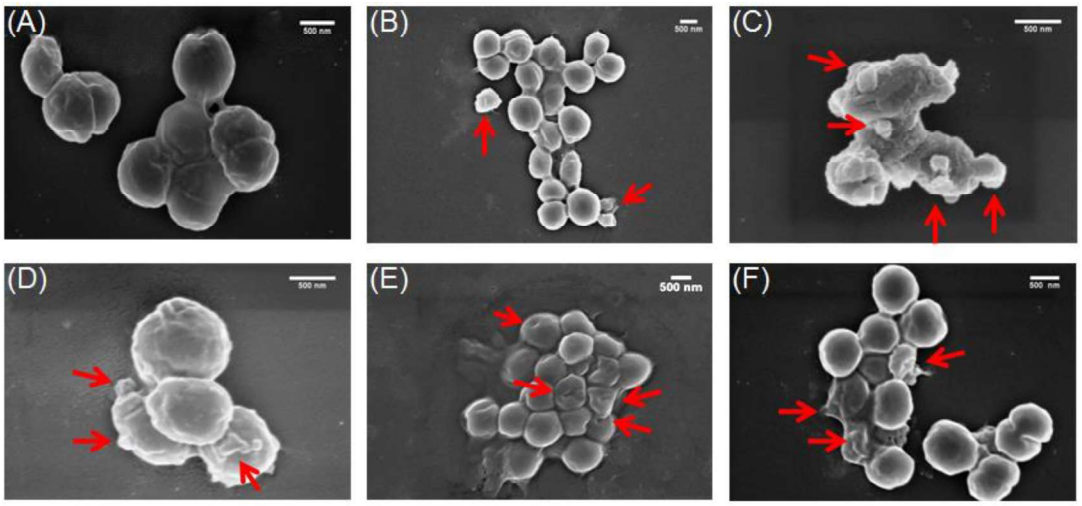

Figure 3.2.8. Surface perturbations induced by stilbenes. S. aureus was treated with different stilbenes for 6 h after which the samples were fixed, dehydrated and gold coated before viewing in a scanning electron microscope. The arrows indicate the different perturbations induced by stilbenes on the cell wall of S. aureus. (A-F) S. aureus treated with vehicle, 1, 2, 11, 8 and 3 respectively. Determination of MIC and MBC against S. aureus.

We determined the MIC and MBC values of the selected analogues against *S. aureus*. The MIC of **1** was found to be 100 µg/mL while that of **3** and **7** was also found to be 100 µg/mL. The MIC of analogues **2** and **8** was 25 µg/mL while in case of **11** it was 10 µg/mL. The MBC of **1** was 200 µg/mL, while **3** and **7** possessed MBC >100 µg/mL. In case of **2** and **8** the MBC was 50 µg/mL, while in case of **11** it was 25 µg/mL (Table 3.2.3).

Table 3.2.3. Inhibitory activity of stilbenes against S. aureus. The MIC and MBC values were determined by broth dilution method and viable count plating method respectively as per CLSI guidelines. The experiment was done in triplicate and repeated thrice.

Stilbene	MIC (µg/mL)	MBC (µg/mL)
1	100	150
2	25	50
3	100	150
7	100	200
8	25	50
11	10	25

The data reiterated the fact that analogues **2**, **8** and **11** were better than **1** against *S. aureus* while **3** and **7** were comparable to **1**. The molecular weight of stilbenes is in the range of 200-250 g/mole and a 100 µg/mL solution of stilbene translates to 400-500 µM which is at the higher end of pharmacological considerations. Hence a concentration of 100 µg/mL or less would be most appropriate for antibacterial applications. However, since there are reports about mechanism of action of **1** being concentration dependent [155, 156], we also assessed selected stilbenes in this study at their respective MBC.

We determined the effect of selected stilbenes at their respective MBC in two representative assays viz oxidative stress by DHE and membrane permeability by PI uptake assay. When different stilbenes were evaluated at their respective MBC, the most effective stilbenes in generating oxidative stress were **2**, **8** and **11** (Figure 3.2.9). This result was similar to the observation when all stilbenes were evaluated at a single concentration (100 µg/mL, Figure 3.2.5). Only difference observed was in case of resveratrol (**1**). Compared to 1 at 100 µg/mL, higher amount of oxidative stress was observed at its MBC (150 µg/mL; Figure 3.2.9).

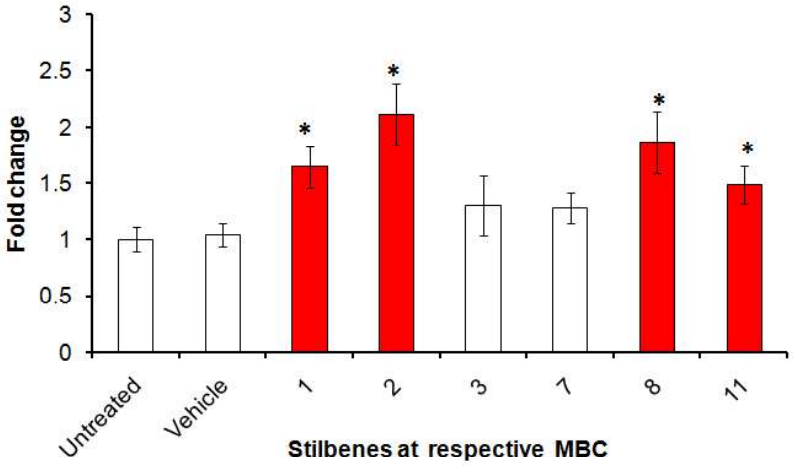

*Figure 3.2.9. Oxidative stress induced by stilbenes at MBC. After treatment with different stilbenes for 1 h at MBC (1= 150 µg/mL; 2= 50 µg/mL; 3= 150 µg/mL; 7= 200 µg/mL; 8= 50 µg/mL; 11= 25 µg/mL) oxidative stress was quantified with DHE in S. aureus. The fold increase was calculated based on the value obtained for untreated sample. The experiment was done in triplicate and repeated thrice. The data presented is mean ± SD. * Significant difference at $p \leq 0.05$ compared to untreated sample.*

In case of PI uptake assay the results obtained with MBC were similar (Figure 3.2.10) to the data obtained at 100 µg/mL (Figure 3.2.7). Stilbenes 2 and 8 scored the highest and way above other stilbenes in both the cases. In case of 11 at 100 µg/mL 15.74 ± 3.70 fold increase was observed while at its MBC (25 µg/mL) only 2.74 ± 0.71 fold increase was observed. All other stilbenes exhibited less PI uptake compared to these three stilbenes.

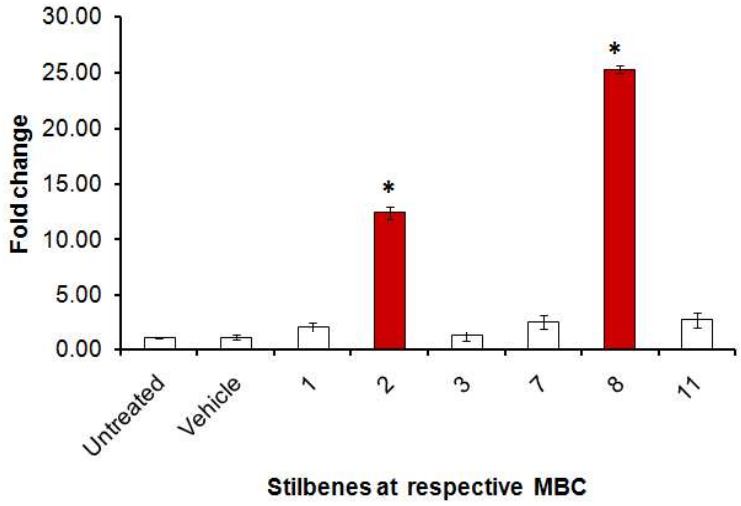

*Figure 3.2.10. Membrane compromise induced by stilbenes at MBC. After treatment with different stilbenes for 1 h at MBC (1= 150 µg/mL; 2= 50 µg/mL; 3= 150 µg/mL; 7= 200 µg/mL; 8= 50 µg/mL; 11= 25 µg/mL) PI uptake was quantified in S. aureus. The experiment was done in triplicate and repeated thrice. The data presented is mean ± SD. *Significant difference at p ≤0.01 compared to untreated sample.*

2.2.1.9. Toxicity and bioavailability of Stilbenes

The toxicity and bioavailability of resveratrol (**1**) as well as other stilbenes is well investigated. Resveratrol is tolerated at a dose of 3 g/kg/day in rats for 4 weeks without any apparent ill effect [157]. In humans, 5 g/70 kg single intake dose and 0.9 g/kg iterative dose were reported to be devoid of any serious adverse effects [157]. Resveratrol suffers from poor bioavailability [158]. Recently pterostilbene (**8**) was found to be more metabolically stable and exhibited stronger pharmacological activities than that of resveratrol [159]. Pterostilbene (**8**) is generally safe for use in humans at doses up to 250 mg per day [160]. Pinosylvin undergoes extensive glucuronidation upon intravenous administration similar to resveratrol and also exhibits poor bioavailability [161]. The Maximum tolerated dose of Pinosylvin (**3**) is not known in animals or humans, however at 10 mg/kg body weight i.p administration, it reduces tumor burden in mice [162]. Pinostilbene (**7**) is metabolically unstable and possesses limited bioavailability [163]. In mice fed with pterostilbene (**8**), pinostilbene (**7**) arises in

colonic cells as a metabolite [164]. The dimer of resveratrol vinferin possesses pharmacological properties similar to that of resveratrol. After oral administration of the same (70 mg/kg body weight), it was metabolized rapidly to glucuronide and sulfate conjugates [165]. Different Stilbenes were evaluated for their effect on cell proliferation on mouse fibroblast cell line L929 and human cervical cell line INT 407. Concentrations ranging from 10 to 100 µg/mL of each stilbene was tested. The IC_{50} value of each stilbene was calculated for both the cell lines employed. The IC_{50} value of each stilbene did not vary widely among these two cell lines (Figure 3.2.11). Further the pattern of toxicity also did not differ, for e.g. the least toxic molecule in both the cell lines was **8** (IC_{50} of 99 and 100 µg/mL), while most toxic was **1** (IC_{50} of 21 and 28 µg/mL). The toxicity of **2** was comparable to that of **1**.

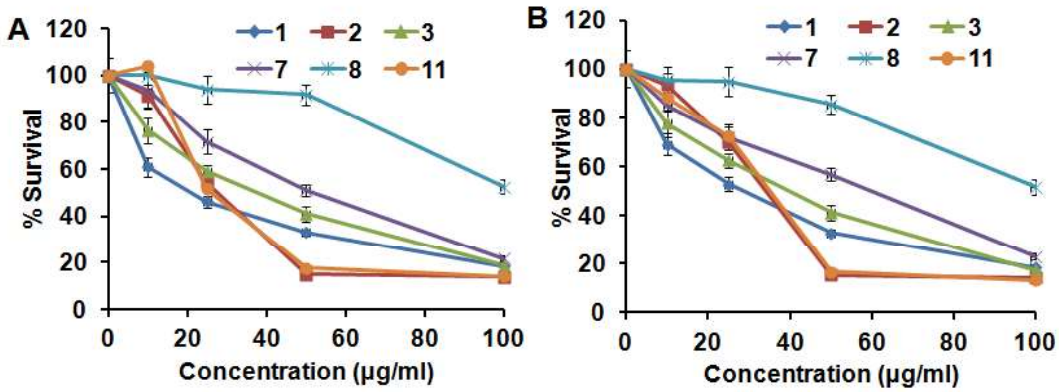

Figure 3.2.11. Cell line cytotoxicity of stilbenes 1, 2, 3, 7, 8 and 11. (A) Mouse fibroblast cell line L929 and (B) human cervix cell line INT 407 were incubated with different concentrations of stilbenes for 24 h. The number of viable cells after 24 h was quantified by MTT assay. The experiment was done in hexaplicate. The data presented is mean ± SD.

The therapeutic index (TI) of all stilbenes was calculated as the ratio of MIC against *S. aureus* and cytotoxicity in human cell line INT407 (Table 3.2.4). The stilbene with the best TI was **8** (3.96) followed by **11** (3.20). Further study in rodent model is required to compare the pharmacology parameters of **2** and **11** with other stilbenes.

Table 3.2.4. Therapeutic index (TI) value of the stilbenes calculated based on their MIC against S. aureus and cytotoxicity towards INT407 (human) cell line.

Stilbene	MIC (µg/mL)	IC_{50} (µg/mL)	TI
1	100	21	0.21
2	25	28	1.12
3	100	38	0.38
7	100	52	0.52
8	25	99	3.96
11	10	32	3.20

Figure 3.2.12. Ranking of different stilbenes was based on the score of their activity in different parameters employing S. aureus as a model organism.

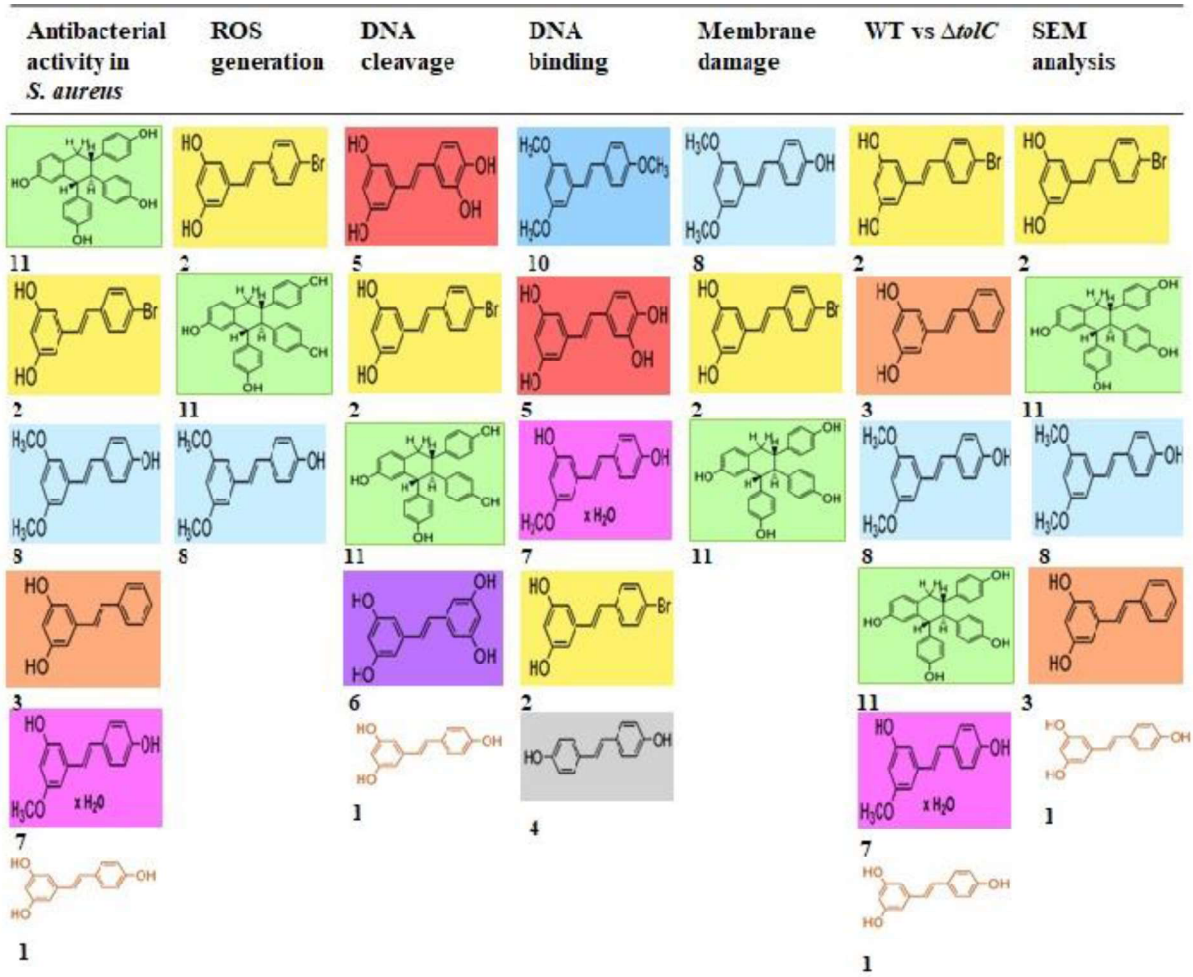

3.2.2. Evaluation of the antibacterial activity of DS and its synergistic potential with clinically used antibiotics.

3.2.2.1. Effect of DS on the growth of *S. aureus*

A profound effect of DS was observed on the growth of *S. aureus*. At a concentration of 10 µg/mL the growth of *S. aureus* was completely inhibited (Figure 3.2.13A).

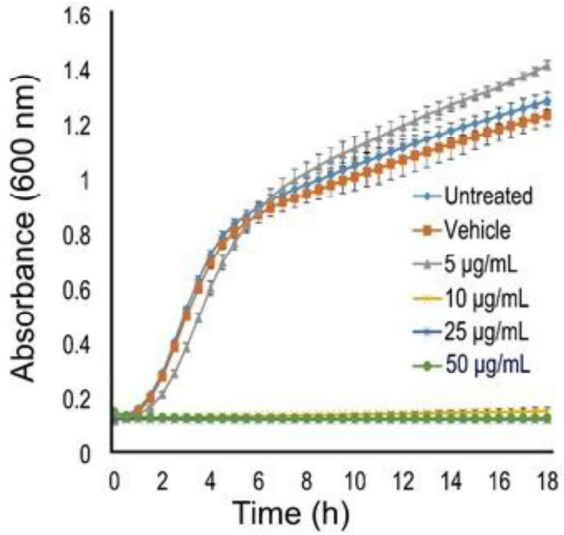

Figure 3.2.13. Effect of DS on growth of S. aureus. S. aureus was inoculated in NB medium with vehicle or DS and absorbance was continuously monitored at 37 °C in a plate reader equipped with temperature control. The experiment was done in triplicate and repeated twice. Data presented is mean ± SD.

When pre-grown *S. aureus* cells were incubated with DS, loss in viability was observed at 20 µg/mL. The rate of loss of viability was very rapid at 50 µg/mL (Figure 3.2.14).

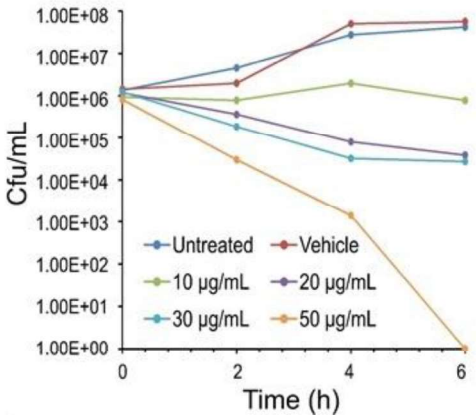

Figure 3.2.14. Time dependent killing of S. aureus by DS. Time dependent killing was monitored by exposing mid log phase cells to DS and enumerating the viable cell number by dilution and plating. The experiment was done in triplicate and repeated twice. Data presented is mean ± SD.

We also evaluated the post exposure effect (1 h) of DS on *S. aureus*. As shown in the results Figure 3.2.15A the vehicle treated cells started growing exponentially after 8 h while DS treated (10 µg/mL; MIC) cells exhibited a further lag of 2 h before growing exponentially. However, the cells treated with DS (2× MIC and 5× MIC) did not grow at all as seen in the growth curve. Further the lag was also confirmed by the viable count seen in case of vehicle and DS treated cells (Figure 3.2.15B). The 2× MIC (DS) treated cells did show growth after 20 h while in case of 5× MIC no viable cells could be recovered even after 20 h.

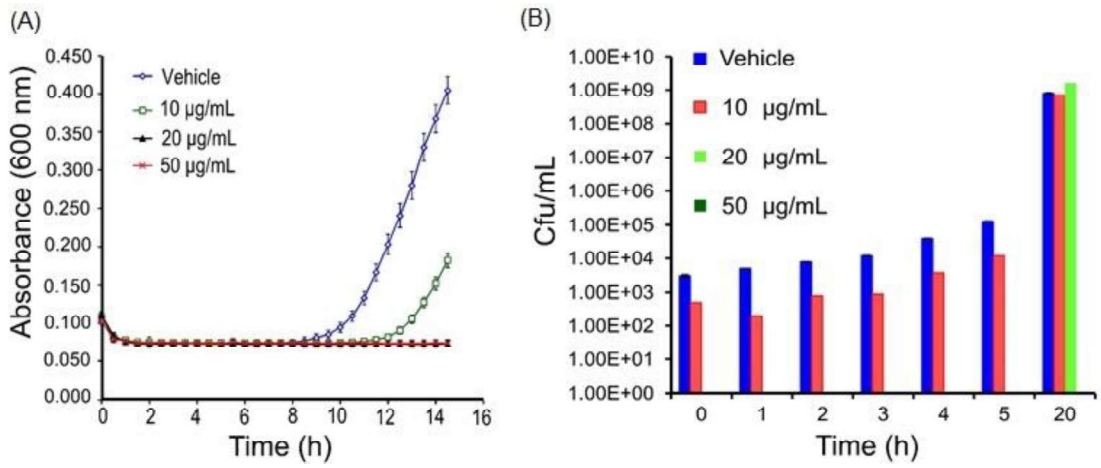

Figure 3.2.15. Post exposure effect of DS on S. aureus. Mid log cells were exposed to vehicle and different concentrations of DS for 1 h in 1% glucose saline. These cells were further diluted (1:100) in fresh NB medium and growth was monitored by measuring the absorbance in a multiwell plate reader (A) and counting viable cells by plating at different time intervals (B). The experiment was done in triplicates and repeated twice. Data presented in mean ±SD.

3.2.3. Screening for co-operativity between DS and antibiotics

Phytochemicals have been known to function co-operatively with clinical antibiotics [166, 167]. Since DS inhibited growth of *S. aureus* at a low concentration we envisaged the utility of this molecule could be larger if it exhibited a positive co-operativity with existing clinical antibiotics. DS pretreated and vehicle treated cells were plated on MH agar plates and a strip containing an antibiotic with increasing concentrations was placed and observed after incubation for 18 h. Our results revealed co-operative behavior of DS with several antibiotics that inhibit protein synthesis (Table 3.2.5). The result obtained by this screen was taken up for further detailed investigation.

Table 3.2.5. The co-operativity between DS and clinical antibiotics was obtained by E-test. Values represent the MIC of antibiotics (µg/mL) in S. aureus cells that preincubated (1h) with vehicle or DS (5 µg/mL).

Sr. No.	Antibiotics	Mechanism of action	Vehicle	DS 5 µg/mL	Co-operativity
1	Amikacin	Cell wall, β-lactam	1.75	1.75	None
2	Amoxicillin	Cell wall, β-lactam	0.16	0.16	None
3	Oxacillin	Cell wall, β-lactam	-	-	None
4	Cefazolin	Cell wall, β-lactam	0.25	0.25	None
5	Fosfomycin	Cell wall, non β-lactam	1.5	2.0	Antagonist
6	Kanamycin	Proteins synthesis, Aminoglycosides	1	0.75	**Exist**
7	Gentamicin	Proteins synthesis, Aminoglycosides	0.64	0.64	None
8	Tobramycin	Proteins synthesis, Aminoglycosides	1	0.5	**Exist**
9	Chloramphenicol	Proteins synthesis	3.5	2	**Exist**
10	Clindamycin	Proteins synthesis	0.16	0.16	None
11	Tetracycline	Proteins synthesis	1	0.75	**Exist**
12	Streptomycin	Proteins synthesis	2-1.5	1.5	**Exist**
13	Muciporin	Proteins synthesis	0.5	0.38	**Exist**
14	Linezolid	Proteins synthesis	1.5	1.5	None
15	Minocycline	Proteins synthesis, tetracycline class	0.25	0.25	None
16	Nalidixic acid	DNA gyrase replication	4	4	None
17	Nitrofurantoin	Multiple target, protein synthesis	8	12	Antagonist
18	Trimethoprim	Metabolism	0.5	0.5	None
19	Rifampicin	RNA synthesis	0.016	0.016	None
20	Norfloxacin	DNA gyrase replication	0.5	0.5	None
21	Moxifloxacin	DNA gyrase replication	0.23	0.23	None
22	Ciprofloxacin	DNA gyrase replication	0.23	0.23	None
23	Clarithromycin	Protein synthesis macrolide	0.125	0.125	None
24	Erythromycin	Protein synthesis macrolide	0.38	0.3	**Exist**

3.2.4. Test for co-operativity between DS and antibiotics affecting protein synthesis

We chose tetracycline, kanamycin, erythromycin, streptomycin and chloramphenicol for detailed investigation based on the screening. *S. aureus* was grown in the presence of different concentrations of these antibiotics and DS. Tetracycline inhibited the growth of *S. aureus* in a concentration dependent manner. A checker board assay revealed combination of sub-lethal concentrations of both the molecules could inhibit the growth of *S. aureus* significantly (Figure 3.2.16). Accordingly, the FIC value of DS and tetracycline combination was found to be 0.9. This value indicates additive relation between the two co-operating entities.

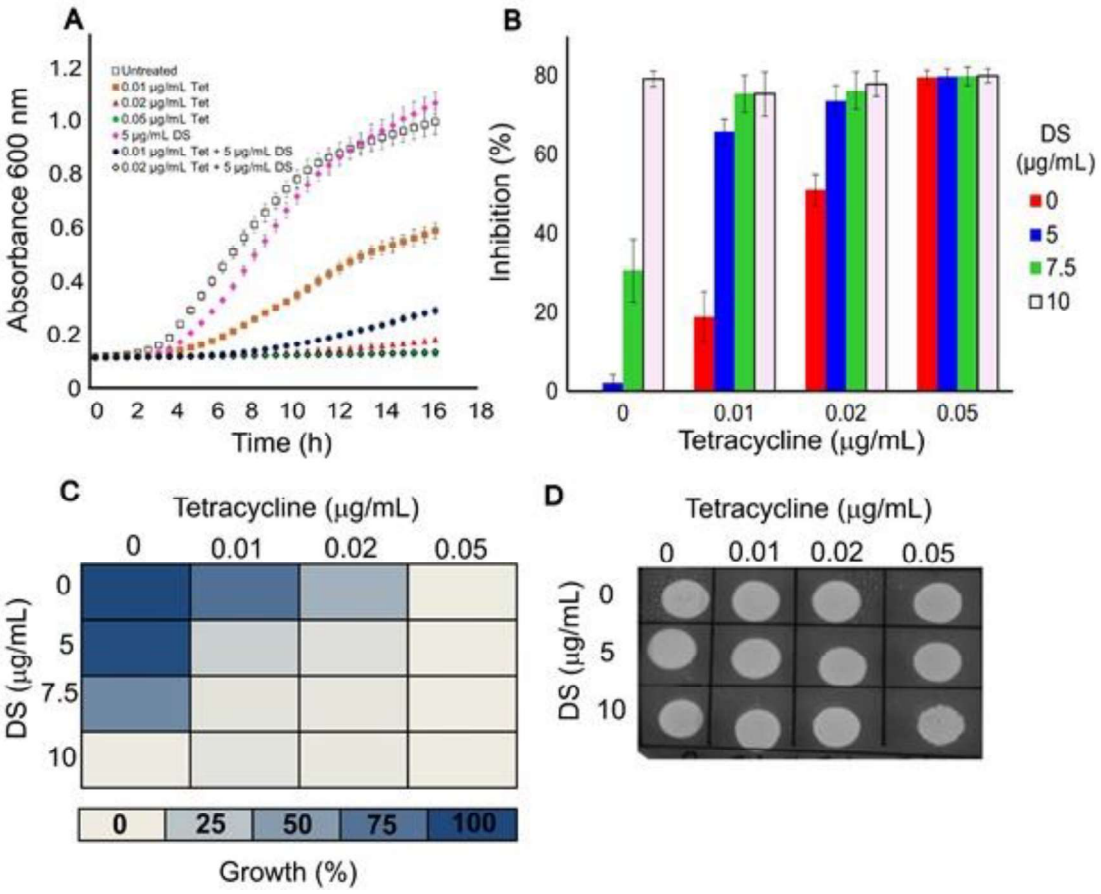

Figure 3.2.16. DS exhibits co-operativity with tetracycline. The co-operativity between DS and tetracycline was evaluated against S. aureus. Mid log phase cells were incubated with different concentrations of DS, tetracycline or combination of both. The growth curve was

monitored in a microplate reader equipped with temperature control (A). The extent of inhibition (B) was calculated after 16 h and represented as a heat map (C). The viability of the cells (D) at the end of the experiment was evaluated by spotting (10 µL) on an agar plate and observed after 24 h.

Similar to tetracycline, a co-operative phenomenon was observed with kanamycin (Figure 3.2.17), erythromycin, streptomycin and chloramphenicol (Figure 3.2.18-20) also.

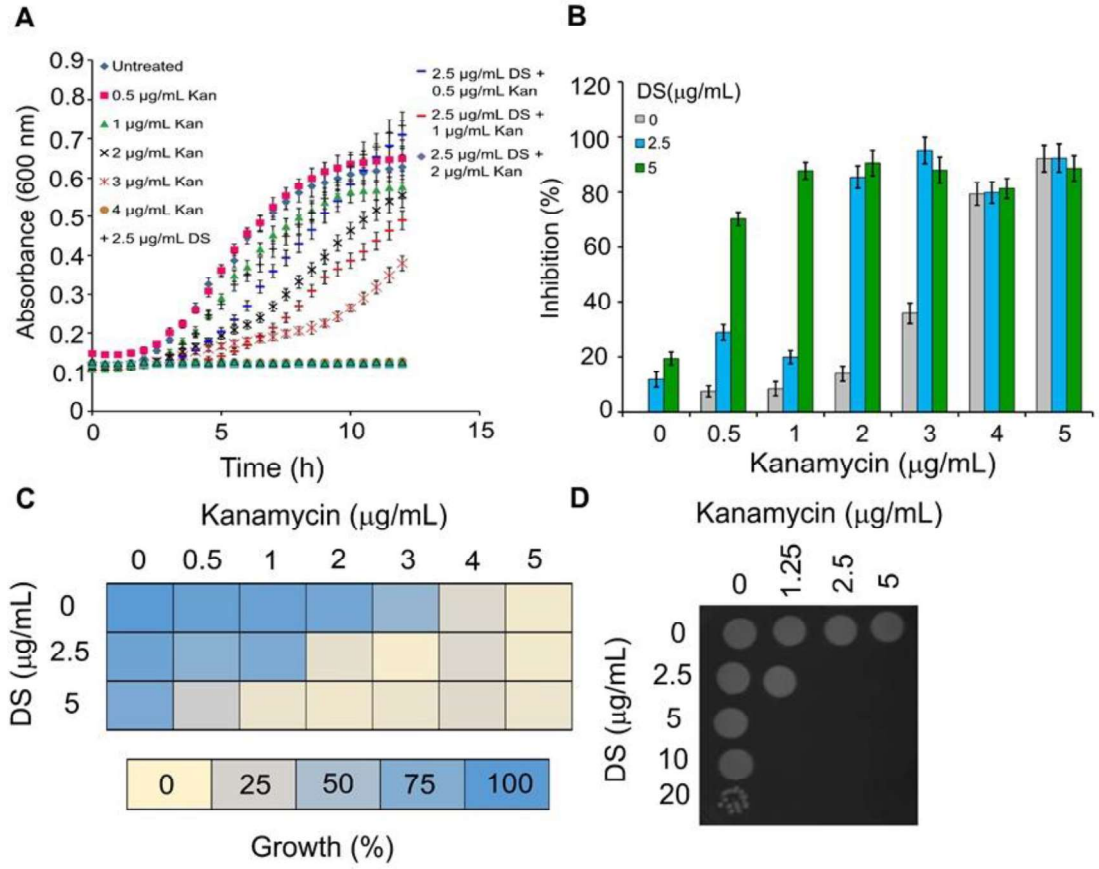

Figure 3.2.17. DS exhibits co-operativity with kanamycin. The co-operativity between DS and kanamycin was evaluated against S. aureus. Mid log phase cells were incubated with different concentrations of DS, kanamycin or combination of both. The growth curve was monitored in a microplate reader equipped with temperature control (A). The extent of inhibition (B) was calculated after 16 h and represented as a heat map (C). The viability of the cells (D) at the end of the experiment was evaluated by spotting (10 µL) on an agar plate and observed after 24 h.

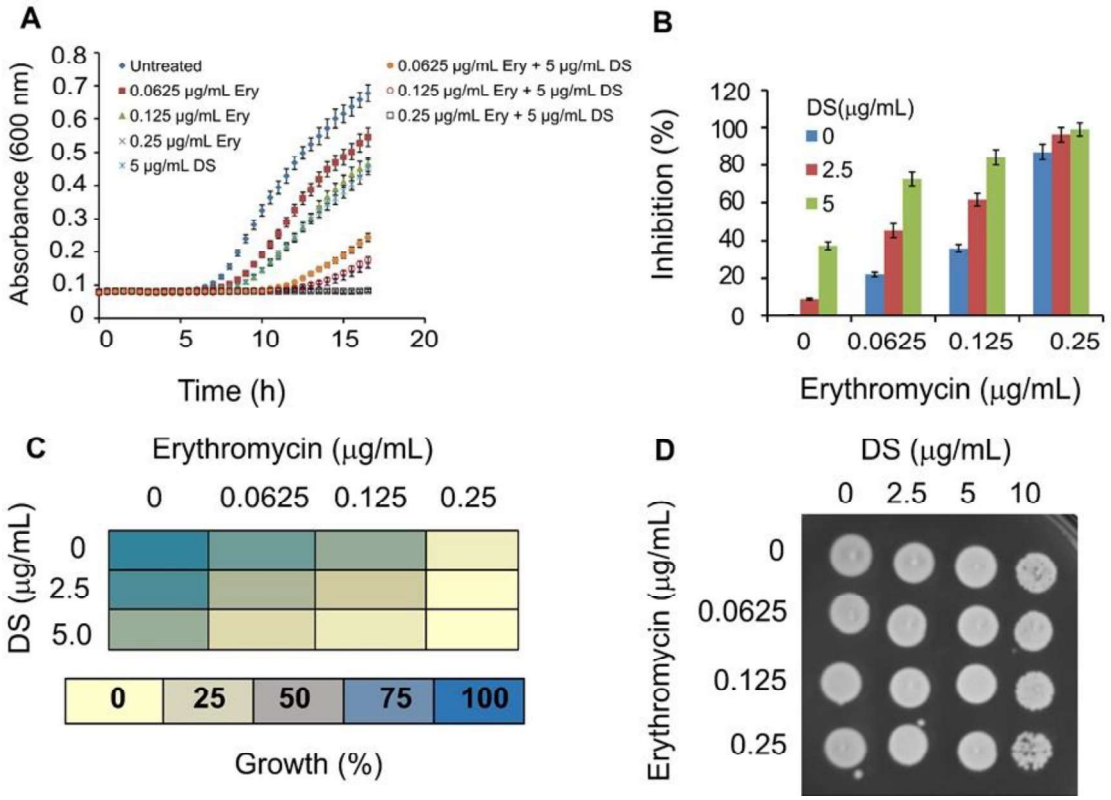

Figure 3.2.18. DS exhibits co-operativity with erythromycin. The co-operativity between DS and erythromycin was evaluated against S. aureus. Mid log phase cells were incubated with different concentrations of DS, erythromycin or combination of both. The growth curve was monitored in a microplate reader equipped with temperature control (A). The extent of inhibition (B) was calculated after 16 h and represented as a heat map (C). The viability of the cells (D) at the end of the experiment was evaluated by spotting (10 µL) on an agar plate and observed after 24 h.

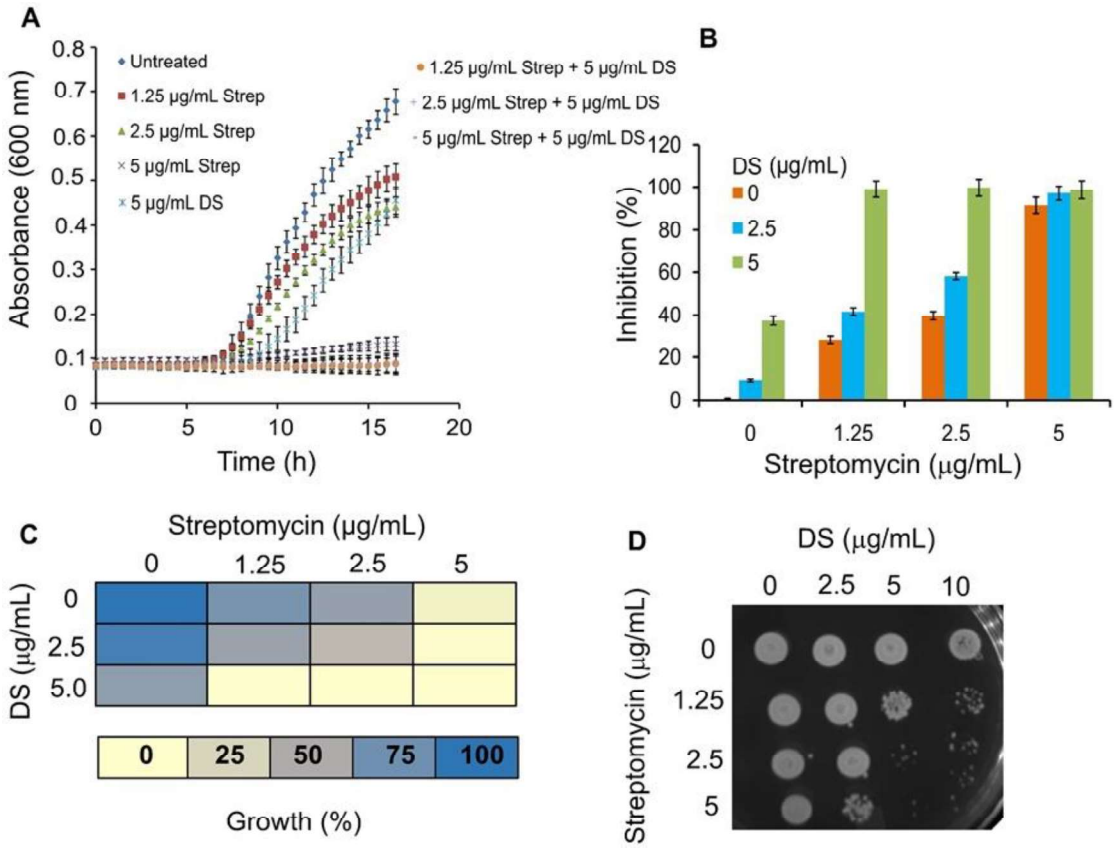

Figure 3.2.19. DS exhibits co-operativity with streptomycin. The co-operativity between DS and streptomycin was evaluated against S. aureus. Mid log phase cells were incubated with different concentrations of DS, streptomycin or combination of both. The growth curve was monitored in a microplate reader equipped with temperature control (A). The extent of inhibition (B) was calculated after 16 h and represented as a heat map (C). The viability of the cells (D) at the end of the experiment was evaluated by spotting (10 µL) on an agar plate and observed after 24 h.

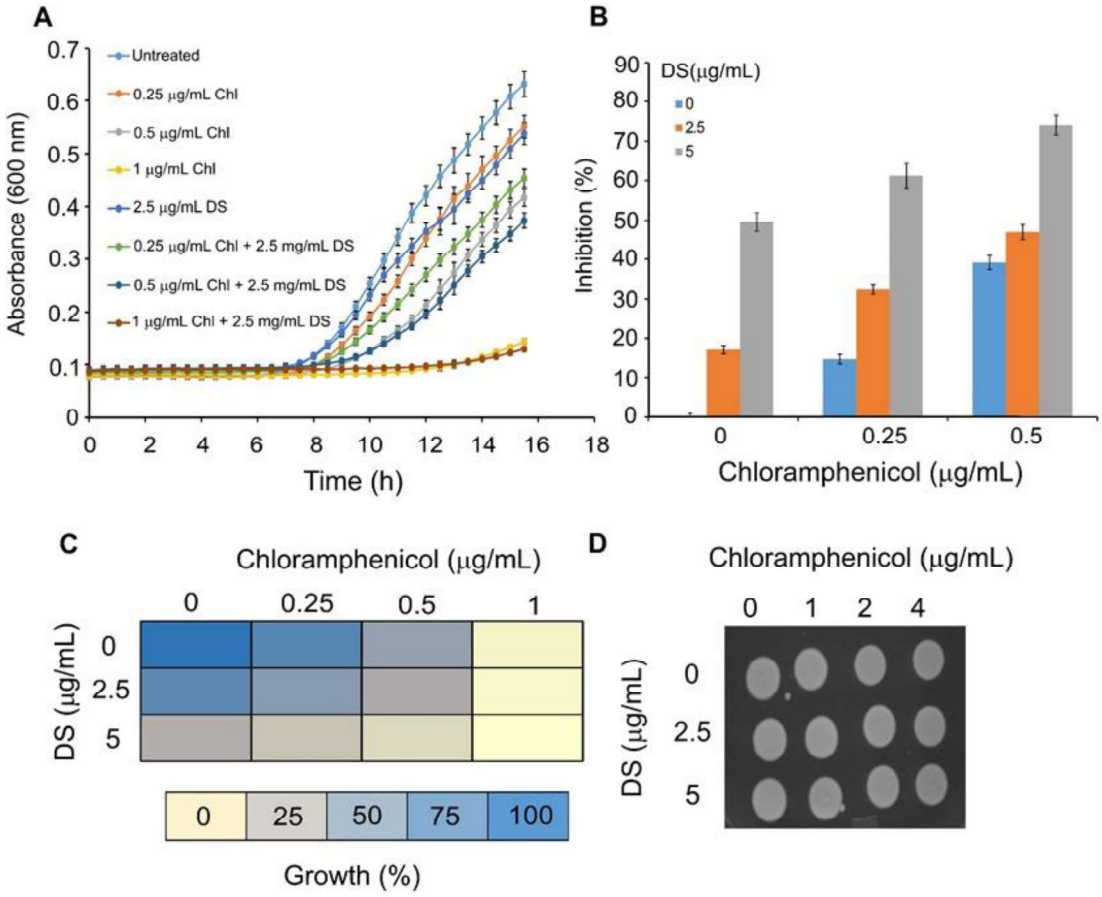

Figure 3.2.20. DS exhibits co-operativity with chloramphenicol. The co-operativity between DS and chloramphenicol was evaluated against S. aureus. Mid log phase cells were incubated with different concentrations of DS, chloramphenicol or combination of both. The growth curve was monitored in a microplate reader equipped with temperature control (A). The extent of inhibition (B) was calculated after 16 h and represented as a heat map (C). The viability of the cells (D) at the end of the experiment was evaluated by spotting (10 µL) on an agar plate and observed after 24 h.

3.2.5. Co-operativity of antibiotics with antibacterial stilbenes

Due to our longstanding interest in stilbene class of molecules [82, 145] we also tested other antibacterial stilbenes for co-operative behavior with kanamycin and tetracycline. Our work had previously identified pinosylvin, bromoresveratrol, pinostilbene and pterostilbene as potent antibacterial molecules [12]. As shown in figure 5 pterostilbene, pinosylvin, bromoresveratrol and pinostilbene exhibited antibacterial activity against *S. aureus* and sensitized *S. aureus* towards tetracycline treatment.

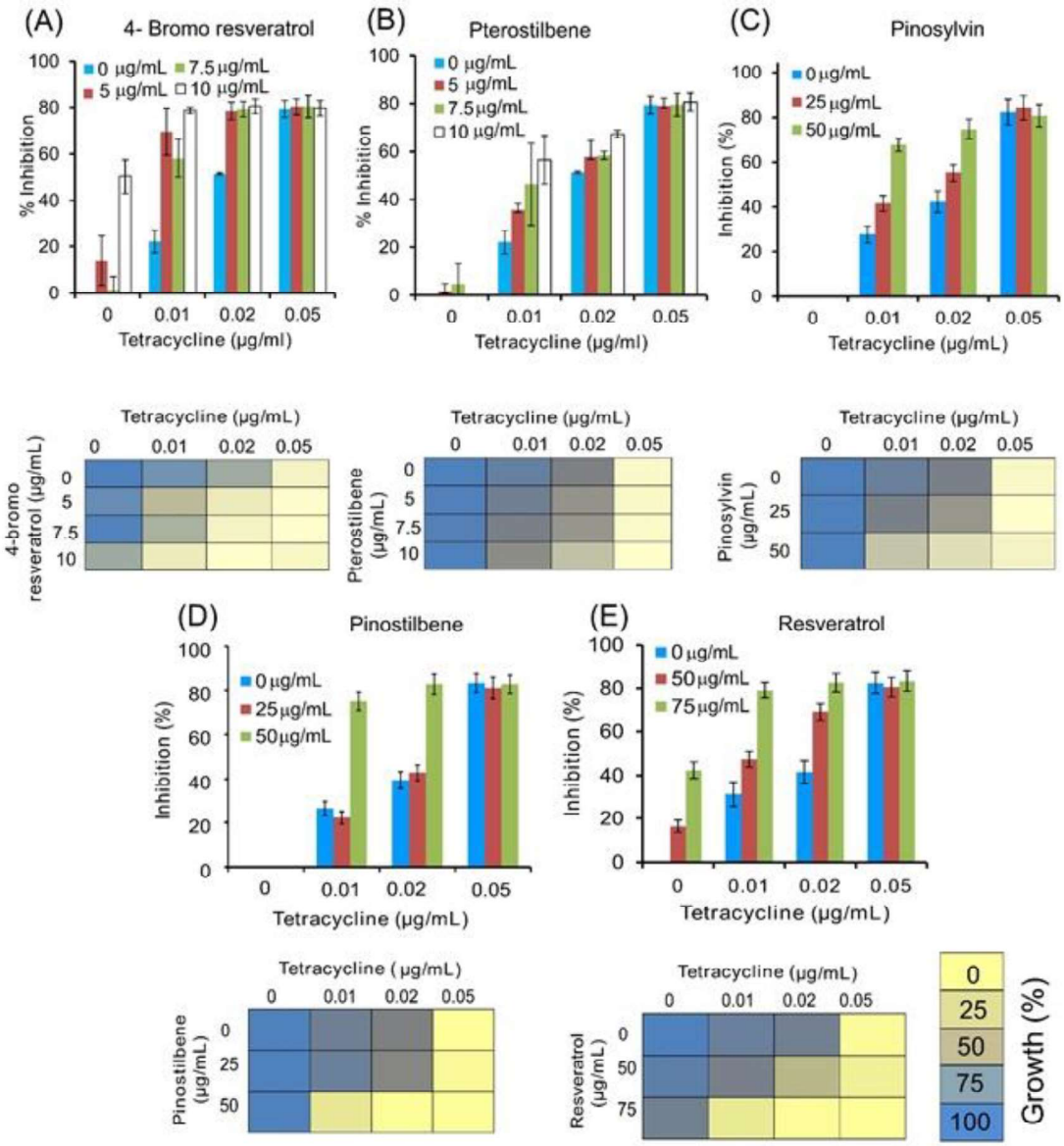

Figure 3.2.21. Stilbenes exhibits co-operativity with tetracycline. The co-operativity between stilbenes and tetracycline was evaluated against S. aureus. Mid log phase cells were incubated with different concentrations of stilbenes, tetracycline or combination of both in a microplate and incubated at 37 ºC for 16 h. The extent of inhibition was calculated and represented as a heat map. A-E represents the extension of inhibition and the heat map representation of the data obtained in case of bromo resveratrol, pterostilbene, pinosylvin, pinostilbene and resveratrol respectively. The experiment was done in triplicates and repeated twice. Data represented is mean±SD.

Similarly all the selected stilbenes sensitized *S. aureus* to kanamycin (Figure 3.2.22).

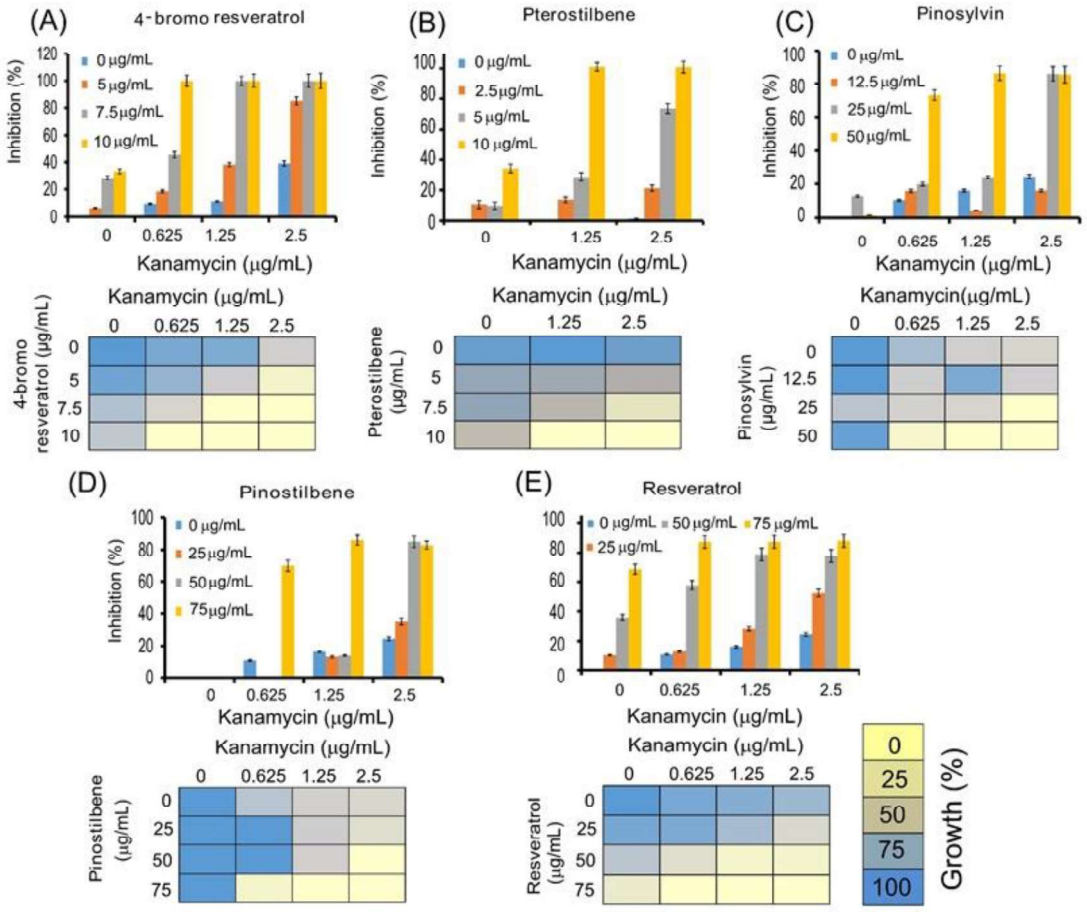

Figure 3.2.22. Stilbenes exhibits co-operativity with kanamycin. The co-operativity between stilbenes and kanamycin was evaluated against S. aureus. Mid log phase cells were incubated with different concentrations of stilbenes, kanamycin or combination of both in a microplate and incubated at 37 ^{o}C for 16 h. The extent of inhibition was calculated and represented as a heat map. A-E represents the extension of inhibition and the heat map representation of the data obtained in case of bromo resveratrol, pterostilbene, pinosylvin, pinostilbene and resveratrol respectively. The experiment was done in triplicates and repeated twice. Data represented is mean±SD.

The nature of co-operativity between different stilbenes and tetracycline, kanamycin is summarized in below Table 3.2.6.

Table 3.2.6. FICI value of selected stilbenes with kanamycin and tetracycline was determined by checkerboard assay.

Stilbenes	FICI with Tetracycline	FICI with Kanamycin
Resveratrol	0.95 (A)	0.9 (A)
Pterostilbene	0.8 (A)	0.65 (PS)
Pinostilbene hydrate	0.7(PS)	0.75 (PS)
Pinosylvin	0.9 (A)	1 (A)
4 Bromo resveratrol	0.6 (PS)	2 (IN)
DS	0.9 (A)	0.65 (PS)

3.2.6. Generation of resistance to DS and kanamycin, evaluation of cross resistance

Repeated growth of *S. aureus* either in the presence of DS or kanamycin resulted in resistance to kanamycin while resistance to DS was not observed (Figure 3.2.23). However, kanamycin resistant cells thus obtained, were found to be susceptible to DS (Figure 3.2.23). Cells exposed to DS for multiple generations (10 passage) were found to have the same sensitivity towards kanamycin, showing they have not accumulated random mutations resulting in resistance to other antibiotics. This shows no cross resistance between kanamycin and DS exists. One possible suggestion could be the targets of these two molecules are different.

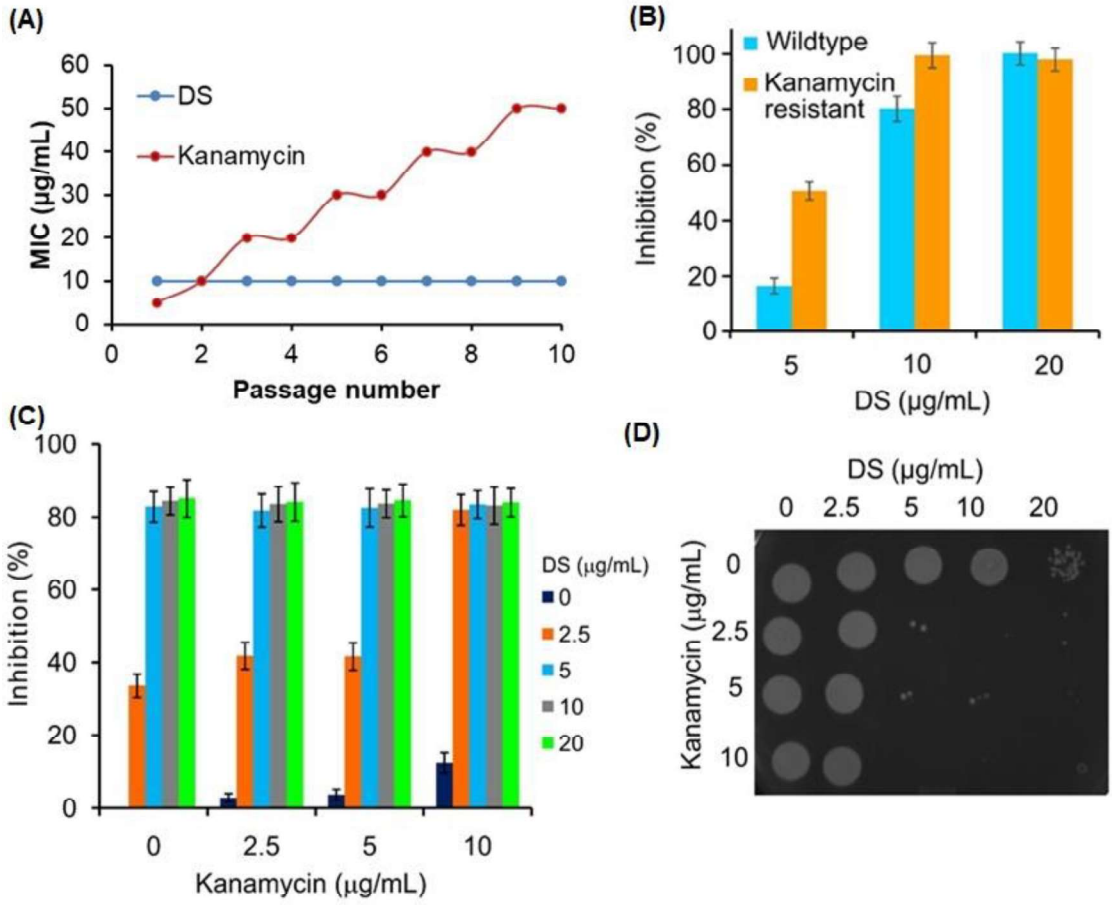

Figure 3.2.23. Evaluation of generation of resistance to kanamycin and DS in S. aureus. MIC of DS and kanamycin was determined after growing S. aureus in the presence of different concentrations of either of these compounds. The population of that survived the highest concentration of the test compound was used to determine MIC in the next cycle of experiment. (A) MIC values of S. aureus after exposure to DS or kanamycin over 10 passages. (B) Comparative study of inhibition activity of DS on wild type cells and kanamycin resistant cells (C) Co-treatment with DS renders kanamycin resistant cells susceptible to kanamycin. Mid log phase cells were incubated with different concentrations of DS, kanamycin or combination of both in a microplate and incubated at 37 ^{o}C for 16 h. The extent of inhibition was calculated. The viability of the cells (D) at the end of the experiment was evaluated by spotting (10 µL) on an agar plate and observed after 24 h. Experiment was done in triplicates and repeated twice. Data presented is mean±SD.

3.2.7. Efficacy of DS and its synergy with kanamycin on clinical isolates.

Clinical strains isolated from patients were tested for kanamycin sensitivity and were found to be resistant up to 500 µg/mL (highest concentration of kanamycin tested). DS was effective against clinical strains irrespective of their antibiotic resistance profile (Table 3.2.7). DS restored kanamycin susceptibility in kanamycin resistant clinical strains (Figure 3.2.24).

Table 3.2.7. List of clinical isolates employed in the investigation of antibacterial activity of DS.

	Name of the organism	**Clinical source**	**Clinical symptoms**	**Age/ Gender**	**Sensitive to**	**Resistant to**	**MIC vs DS**	**MBC vs DS**
1.	*MRSA*	Wound Swab	c/o left upper arm swelling with pain since1 week, gradually increasing in size associated with redness and discomfort. no comorbidities at presently	86 Yr/ Male	Cefuroxime, Cefoperazone, Ciprofloxacin, Clindamycin, Levofloxacin, Linezolid, Tetracycline, Co-trimoxazole, Gentamicin	Cefepime, Cloxacillin, Amoxyclav, Erythromycin, Vancomycin, Novobiocin, Azithromycin, Teicoplanin	10 µg/mL	20 µg/mL
2.	*MRSA*	Ear swab	Lt. EAC shows copious mucopurulent dx swab sent, suctioned out, TM central perforation seen in anterior quadrant with severe inflammation in remaining part of TM	25 Yr / Male	Vancomycin, Teicoplanin, Linezolid, Tetracycline, Co-trimoxazole, Clindamycin, Levofloxacin, Ciprofloxacin.	Amoxyclav, Cloxacillin, Linezolid, Cefadroxil, Cefuroxime, Cefotaxime, Ceftriaxone, Erythromycin.	10 µg/mL	20 µg/mL
3.	*MSSA*	Wound Swabs	Having right palm abscess. Augmentin is on	57 Yr / Male	Cefazolin, Cefuroxime, Cefotaxime, Ceftriaxone, Co-trimoxazole, Ciprofloxacin, Levofloxacin, Vancomycin, Teicoplanin, Linezolid,	Amoxyclav, Cloxacillin, Erythromycin	10 µg/mL	20 µg/mL

					Gentamicin, Clindamycin.			
4.	*MSSA*	Wound Swabs	c/o left thigh abscess associated with pus discharge since 4 days o/e ruptured posterior left thigh abscess with induration and seropululent discharge expressed out.iandd done under la	22 Yr / Male	Cefuroxime,/ Cefoperazone, Levofloxacin, Linezolid, Erythromycin, Gentamicin, Vancomycin, Novobiocin, Mupirocin, Clindamycin, Teicoplanin, Ampicillin, Amoxyclav, Cefuroxime, Ceftazidime, Cefotaxime, Ceftriaxone, Cefepime, Piperacillin/Tazobactam, Cefoperazone/Sulbactam, Ceftriaxone /Tazobactam, Amikacin, Gentamicin, Co-trimoxazole, Ciprofloxacin. Ofloxacin, Levofloxacin	Ciprofloxacin Cefepime, Cloxacillin, Amoxyclav, Co-trimoxazole, Azithromycin.	10 µg/mL	20 µg/Ml
5.	*MSSA*	Wound Swabs	Abscess at upper aspect of lt thigh	48 Yr / Male	Cefuroxime, Cefotaxime, Ceftriaxone, Cefoperazone, Vancomycin, Teicoplanin, Linezolid, Clindamycin, Gentamicin, Co-trimoxazole	Amoxyclav, Cloxacillin, Ciprofloxacin, Erythromycin, Levofloxacin	10 µg/mL	20 µg/Ml
6.	*MSSA*	Ear swab	c/o left ear scanty yellowish mp, foul-smelling, nfs dx since 3-4days h/o tympanoplasty 1yr back in pvt after which dx stopped and hearing improved	24 Yr / Female	Cefazolin, Cefadroxil, Cefuroxime, Cefotaxime, Ceftriaxone, Cefoperazone, Erythromycin, Clindamycin, Vancomycin, Teicoplanin, Linezolid.	Resistant to: Ampicillin, Amoxyclav, Cloxacillin, Levofloxacin, Ciprofloxacin, Tetracycline	10 µg/mL	20 µg/Ml

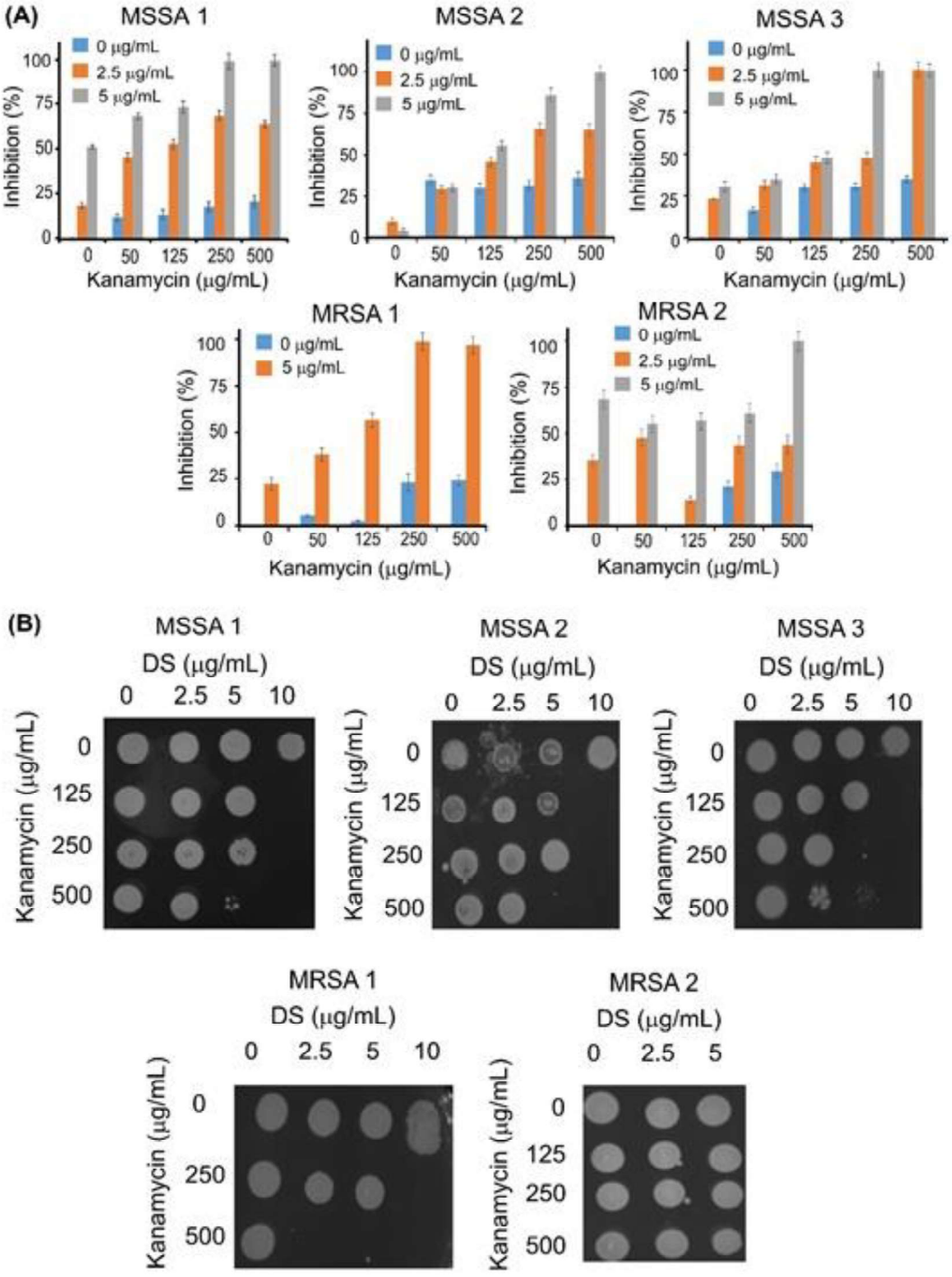

Figure 3.2.24. Co-treatment with DS renders kanamycin resistant clinical isolates susceptible to kanamycin. Mid log phase cells were incubated with different concentrations of DS, kanamycin or combination of both in a microplate and incubated at 37 ºC for 16 h. The extent of inhibition was calculated (A). The viability of the cells (B) at the end of the

experiment was evaluated by spotting (10 µL) on an agar plate and observed after 24 h. Experiment was done in triplicates and repeated twice. Data presented is mean±SD.

3.2.8. DS effectively eradicates infection in mice as a standalone drug and potentiates the effect of kanamycin

Neutropenic mice injected with *S. aureus* in thigh exhibited limited movement within 12 h and died between 24 to 48 h. DS toxicity evaluated in neutropenic mice up to 100 mg/kg b.wt. by subcutaneous injection. DS was observed to be safe up to 100mg/kg weight. Treatment in the form of either DS (25 mg/kg b. wt) or kanamycin (12.5 mg/kg body weight) administered subcutaneously protected the mice from death, while lower concentrations of either drug did not protect the mice from mortality (Figure 3.2.25A and B). Mice were also protected from when non protective doses of DS and kanamycin were combined (Figure 3.2.25C). The result confirmed the *in vitro* synergy observed between kanamycin and DS.

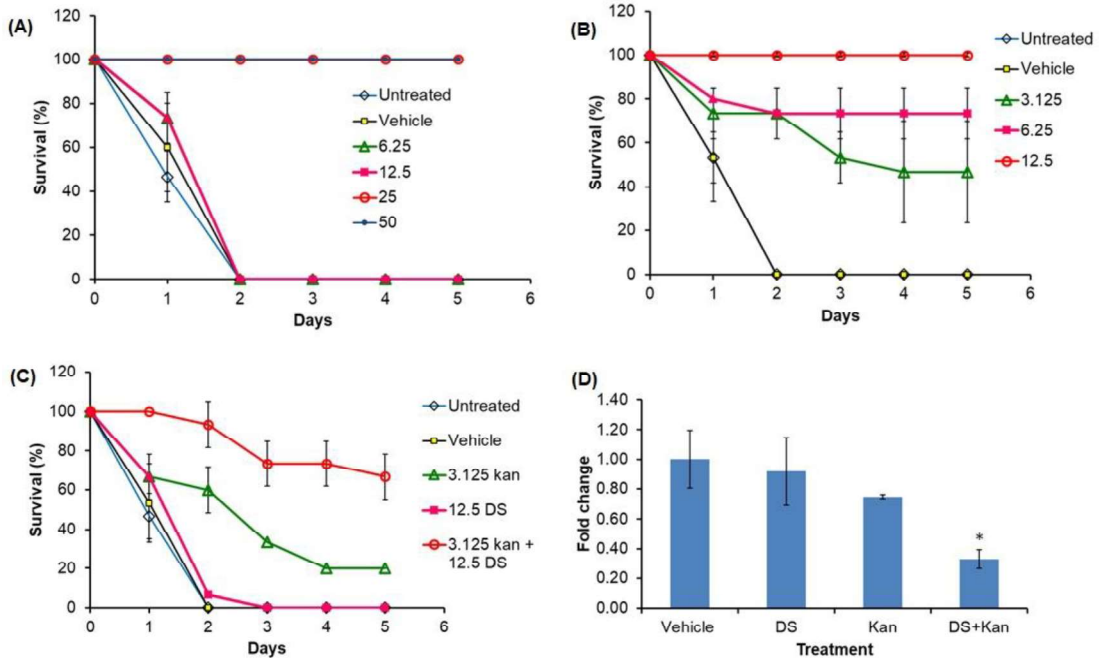

Figure 3.2.25. Effect of DS, kanamycin and combination on S. aureus induced thigh infection in mice. Neutropenic mice infected with S. aureus were treated with different concentrations of DS (A), kanamycin (B) or a combination of both (C) and monitored for 5 days for survival. The bacterial load in the thigh of the mice treated with DS, kanamycin or a combination was

*enumerated 24 h post infection (D). Each group contained 5 mice and the experiment was repeated thrice. Data presented is mean±SD. *indicates significant difference at p<0.05.*

3.2.9. Discussion

Stilbenes are a class of compounds of intense research due to their various biological activities [168, 169]. The most well-known molecule of this class is resveratrol which is not devoid of limitations [170, 171]. Hence a constant effort to identify analogues of resveratrol with better bioactivity has been the endeavor of many research groups [170, 172, 173]. Intake of resveratrol in forms of natural food is low. For e.g. consumption of 300-600 mL of red wine results in intake of 0.25 to 1.92 mg of trans-resveratrol [174]. However, for therapeutic purpose/nutritional supplement higher quantities of resveratrol in the form of tablets are commercially available. Resveratrol intake followed by peak plasma concentration has been studied after different routes of administration and doses. Although a low amount of resveratrol was found in plasma (539 ng/mL), it was present abundantly (20 fold more) in conjugated forms [175]. Metabolites have been observed to retain the biological activity of the parent in conjugated phenols similar to resveratrol[176, 177]. From this perspective as well as considering the fact that resveratrol (**1**) exhibits >50 % inhibitory activity against the panel of gram positive bacteria selected, the concentration selected for the SAR study in the current investigation is 100 µg/mL. In our study, five stilbenes exhibited better/equivalent antibacterial activity against gram positive bacteria compared to resveratrol (**1**).

If all the hydroxy groups are converted to OAc or OMe the antibacterial activity diminished drastically (**1** vs **9** or **10**). This shows the importance of the hydroxy group for antibacterial activity. However, increasing the number of hydroxy groups did not result in better antibacterial activity (**1** vs **5** or **6**). Since 4' hydroxy group is considered important in stilbenes [148, 178], we investigated the role of this in antibacterial activity. Presence of 4’ hydroxy group does not necessarily render the molecule active (as in analogue **4**, **5**) nor its absence

abolishes it completely (as in analogue **3**). However, it is important to notice that the best molecules of the series (**2**, **3**, **7**, **8** and **11** along with **1**) possess 4' OH group in conjunction with other substitutions. Hence it is prudent to look at this functionality "in toto" rather than in isolation. Partial modification of OH group to others resulted in better antibacterial activity (**1** vs **2**, **7** or **8**). In case of gram negative bacteria, the trend remained the same, except **8** and **11**.

It has been observed previously phytochemicals are less active against gram negative bacteria due to the efflux activity [137]. Our results show that all the stilbenes tested are substrates of efflux pump. This is in agreement with a previous observation employing resveratrol [137]. However, it is surprising that stilbenes **2** and **3** were significantly effective even in presence of efflux pump which was not the case with other analogues. This could either be due to one of the following reasons: (1) stilbenes **2** and **3** are poor substrates for the efflux pump or (2) these molecules induce damage in a very short span of time wherein they cause damage before being effluxed out. Conclusive statements about these possibilities necessitate further investigation. Since the antibacterial activity of the stilbenes was restored in *ΔtolC* mutant, it raises the possibility of using them in conjunction with efflux pump inhibitors for therapeutic success [179] especially against gram negative pathogens. Further investigation of different parameters that could contribute to cell cytotoxicity revealed a direct correlation between antibacterial activity and oxidative stress, DNA cleavage, membrane damage and physical perturbation in case of the most effective stilbenes **2** and **11** (Figure 3.2.12). All stilbenes that exhibited better (or equivalent) activity than resveratrol (**1**) scored over it in at least one among the several parameters investigated. In case of stilbene **8**, its activity was in direct correlation with oxidative stress and membrane damage. Recently **8** has been reported to damage membrane of *S. aureus* leading to leakage of cytosolic contents [180]. This is in agreement with our observation. Stilbene **8** did not exhibit any DNA binding

or DNA cleavage activity. Stilbenes **5** and **6** exhibited DNA cleavage but did not possess remarkable antibacterial activity. Among these two stilbenes, **6** exhibited better antibacterial activity than **5**. Higher number of hydroxy group contributed to more DNA cleavage. Partial or complete conversion of OH to OMe abolishes DNA cleavage activity. Increase in the number of OH groups did not result in higher antibacterial activity while partial conversion of OH to OMe resulted in improvement of antibacterial activity.

Our data on DNA cleavage is in agreement with a previous study that reported DNA cleavage activity of different stilbenes in presence of copper [181]. In our study there was no direct correlation between DNA cleavers and DNA binders. Further, these two parameters did not directly correlate to antibacterial activity. However, our study revealed ROS generation by **8** inside the cells while *in vitro* it did not exhibit any DNA cleavage. Quantification of DNA damage inside the cells by additional experiments for all the stilbenes would further strengthen our understanding and the DNA cleavage data should be taken as a suggestive evidence towards that effect.

Investigation of membrane damage revealed the most active stilbenes in terms of activity also scored highest in this parameter (**8**, **2** and **11**). This was also observed in case of surface damage to *S. aureus* cells revealed by SEM. All these correlations except DNA binding and to a smaller extent DNA cleavage reveals, there exists a direct relation between antibacterial activity and the parameters investigated. A straight forward explanation to this could be, these mechanisms underlie the antibacterial activity of stilbenes. However, more than one mechanism resulting in pleiotropic effects on targets is not novel in case of phytochemicals and has been reported earlier [182].

Pterostilbene (**8**) has already been shown to possess better pharmacokinetic characteristics compared to resveratrol [169]. Pharmacokinetic parameters of **4**, **8** were reported to be better than that of resveratrol while **8** was also found to exhibit higher lipophilicity [169]. This

could also explain the observation that **8** selectively damages membrane of *S. aureus*. Further it has been observed **3** and **7** possess different pharmacological characteristics [173] compared to **1** and this may be exploited to make them better drugs as these two analogues exhibit similar anti Staphylococcal activity compared to **1**. Halogenation of ring A resulting in 2-bromo resveratrol and 2-chloro resveratrol exhibited better activity than resveratrol against Candida [183]. However, there are no reports of the effect of halogenation on ring B. Our study shows that halogenation in ring B also results in higher antimicrobial activity and better TI value. However, halogenation has been found to increase cytotoxicity in other studies [184]. A thorough investigation of **2** and **11** is warranted in animal model. Overall our data significantly contributes towards newer insights into the antibacterial activity of stilbene class of molecules.

Three stilbenes were identified that possess higher anti-bacterial activity than resveratrol while two other stilbenes were comparable to it. Though hydroxy group is considered important for cytotoxicity, presence of methoxy group along with hydroxy group resulted in higher antibacterial activity. Halogenation and dimerization resulted in enhanced antibacterial property. Stilbenes that possess better antibacterial activity than resveratrol scored higher in all the mechanistic parameters investigated except DNA binding. Binding to DNA is not an essential parameter to exhibit antibacterial activity in case of stilbenes.

Phytochemicals are an important reservoir of potential molecules for health benefits. They have also contributed towards very important parent structures that have been modified later to different derivatives resulting in drugs that have benefitted human kind [185, 186]. However, not all molecules see the light of the day in the form of drugs due to failure at several stages of development. This has led to a constant effort in our search for molecules that could be put to use for health benefits. One such molecule is resveratrol that belongs to the stilbene class reported in 1997 [187] for its ability to cure cancer. Further this molecule

was hailed as a miracle molecule that was shown to possess several health benefits like anti-inflammatory, anti-aging, antioxidant to name a few [187]. Antibacterial activity of resveratrol was also reported and its efficacy was established in an animal model of infection [188]. In the event of growing threat from multidrug resistant bacteria a renewed interest in search for molecules with antibacterial activity, an ability to modulate the resistance or potentiate the efficacy of an existing clinical antibiotic betided [189, 190]. The renewed interest has resulted in research culminating in clinical trials of some phytochemicals against infectious bacteria [191-193]. Investigations towards understanding fundamental mechanisms operating at the molecular level with an objective to exploit these findings clinically have also progressed [194]. To this end the information on resveratrol as a helper molecule to combat infectious bacteria remains divided. Reports have suggested resveratrol to act in a co-operative manner with some antibiotics [195] while others have suggested a role of resveratrol in protecting the target bacteria during antibiotic treatment [196]. The existing gap in the understanding about the co-operativity between stilbenes and clinical antibiotics remains a hindrance to their application as antibacterial molecules. DS exhibited 20 times more potency than resveratrol against *S. aureus*. Our results exhibit a promising strategy towards overcoming drug resistance in *S. aureus* by combination of DS and antibiotics like kanamycin, tetracycline and streptomycin. Further the same strategy was shown to work successfully against kanamycin resistant laboratory strain and kanamycin resistant clinical strains. *S. aureus* infections remain a major concern in the post-operative care of a variety of medical procedures [197]. Failure towards treatment of *S. aureus* infections results in very high mortality and morbidity [197, 198]. The standard treatment options for *S. aureus* infections remain β-lactam antibiotics for methicillin sensitive *S. aureus* while for methicillin resistant *S. aureus* combination treatments are employed [199]. A 2018 study places MRSA in a high priority group that threatens human health [200]. Various strategies have been

conceived towards successful treatment of MRSA. One of the important components of this combat has been the use of natural molecules that could sensitize the antibiotic resistant bacteria to existing antibiotics [201]. Such strategies have shown promise for e. g. hypericin from *Hypericum perforatum* sensitizes *S. aureus* to β-lactam antibiotics by reducing the expression of virulent genes [202]. Berberine, a plant derived alkaloid exhibits synergistic activity with β-lactam antibiotics against MRSA [203]. Further, synergistic activity of chloramphenicol, ampicillin, gentamicin, tetracycline, and oxacillin with the methanolic extracts of *Punica granatum* (L.) results in anti-MRSA activity and the inhibition of efflux pumps, promoting antibiotic efficacy [204]. In this context the finding of synergy between DS and kanamycin an other is exciting. More interestingly this property is not unique only to DS but is a general property of different stilbenes as our study has revealed. In our previous study we had revealed how the properties contributing towards cell death change with changes in some structural components in stilbene class of molecules. Irrespective of these changes, the current investigation reveals all stilbenes exhibit co-operativity with antibiotics targeting protein synthesis. For e.g. the membrane targeting pterostilbene (predominant target) also exhibits this cooperative behavior. This indicates a unifying event at the cellular level that is common to all stilbenes. Further investigation in this phenomenon would give as a better insight about the mechanism of behind the co-operative behavior between stilbenes and antibiotics targeting protein synthesis.

CHAPTER 4 REFERENCES

1. WHO, World health statistics overview 2019: monitoring health for the SDGs, sustainable development goals, 2019, World Health Organization: Geneva.

2. CDC, Antibiotic resistance threats in the United States 2019., 2019, Atlanta, GA:U.S. Department of Health and Human Services, CDC

3. Agrawal, V., et al., Pivotal role of Pharmacovigilance Programme of India in containment of antimicrobial resistance in India. Perspectives in Clinical Research, 2019. **10**(3): p. 140.

4. Sumanth, G., et al., Scoping Report on Antimicrobial Resistance in India. Washington, DC: Center for Disease Dynamics, Economics & Policy., 2017.

5. Adedeji, W., The treasure called antibiotics. Annals of Ibadan postgraduate medicine, 2016. **14**(2): p. 56.

6. Arias, C.A. and B.E. Murray, Antibiotic-resistant bugs in the 21st century--a clinical super-challenge. N Engl J Med, 2009. **360**(5): p. 439-43.

7. Mayor, S., Antibiotic resistant bacteria cause nearly one in five infections in wealthy countries, report warns, 2018, British Medical Journal Publishing Group.

8. Klein, E.Y., et al., Global increase and geographic convergence in antibiotic consumption between 2000 and 2015. Proceedings of the National Academy of Sciences, 2018. **115**(15): p. E3463-E3470.

9. Ito, H., et al., Plasmid-mediated dissemination of the metallo-beta-lactamase gene blaIMP among clinically isolated strains of Serratia marcescens. Antimicrob Agents Chemother, 1995. **39**(4): p. 824-9.

10. Queenan, A.M. and K. Bush, Carbapenemases: the versatile beta-lactamases. Clin Microbiol Rev, 2007. **20**(3): p. 440-58, table of contents.

11. Daikos, G.L., et al., Prospective observational study of the impact of VIM-1 metallo-β-lactamase on the outcome of patients with Klebsiella pneumoniae bloodstream infections. Antimicrobial agents and chemotherapy, 2009. **53**(5): p. 1868-1873.

12. Nordmann, P., et al., Does broad-spectrum β-lactam resistance due to NDM-1 herald the end of the antibiotic era for treatment of infections caused by Gram-negative bacteria? Journal of Antimicrobial Chemotherapy, 2011. **66**(4): p. 689-692.

13. WHO, Community-based surveillance of antimicrobial use and resistance in resource-constrained settings: report on five pilot projects, 2009, World Health Organization.

14. Laxminarayan, R. and R.R. Chaudhury, Antibiotic resistance in India: drivers and opportunities for action. PLoS medicine, 2016. **13**(3): p. e1001974.

15. CDDEP, ResistanceMap Washington DC, 2015, Center for Disease Dynamics, Economics & Policy; [August 20, 2015]. http://www.resistancemap.org." CDDEP.

16. Datta, S., et al., A ten year analysis of multi-drug resistant blood stream infections caused by Escherichia coli & Klebsiella pneumoniae in a tertiary care hospital. The Indian journal of medical research, 2012. **135**(6): p. 907.

17. Chatterjee, D., et al., A questionnaire-based survey to ascertain the views of clinicians regarding rational use of antibiotics in teaching hospitals of Kolkata. Indian journal of pharmacology, 2015. **47**(1): p. 105.

18. Van Boeckel, T.P., et al., Global antibiotic consumption 2000 to 2010: an analysis of national pharmaceutical sales data. Lancet Infect Dis, 2014. **14**(8): p. 742-750.

19. Singh, S., et al., Surgical site infection rates in six cities of India: findings of the International Nosocomial Infection Control Consortium (INICC). International health, 2015. **7**(5): p. 354-359.

20. Rhomberg, P.R. and R.N. Jones, Summary trends for the meropenem yearly susceptibility test information collection program: a 10-year experience in the United States (1999–2008). Diagnostic microbiology and infectious disease, 2009. **65**(4): p. 414-426.

21. Walia, K., et al., Establishing antimicrobial resistance surveillance & research network in India: journey so far. The Indian Journal of Medical Research, 2019. **149**(2): p. 164.

22. Hutchings, M.I., A.W. Truman, and B. Wilkinson, Antibiotics: past, present and future. Current Opinion in Microbiology, 2019. **51**: p. 72-80.

23. Blair, J. and M. Webber, Baylay AJ, Ogbolu DO. Piddock LJ. Molecular mechanisms of antibiotic resistance. Nat Rev Microbiol, 2015. **13**(1): p. 42-51.

24. Smith, T., K.A. Wolff, and L. Nguyen, Molecular biology of drug resistance in Mycobacterium tuberculosis. Curr Top Microbiol Immunol, 2013. **374**: p. 53-80.

25. Petchiappan, A. and D. Chatterji, Antibiotic resistance: current perspectives. Acs Omega, 2017. **2**(10): p. 7400-7409.

26. Burian, J., et al., The mycobacterial transcriptional regulator whiB7 gene links redox homeostasis and intrinsic antibiotic resistance. Journal of Biological Chemistry, 2012. **287**(1): p. 299-310.

27. Fridman, O., et al., Optimization of lag time underlies antibiotic tolerance in evolved bacterial populations. Nature, 2014. **513**(7518): p. 418-421.

28. Mauldin, P.D., et al., Attributable hospital cost and length of stay associated with health care-associated infections caused by antibiotic-resistant gram-negative bacteria. Antimicrob Agents Chemother, 2010. **54**(1): p. 109-15.

29. Neidell, M.J., et al., Costs of healthcare- and community-associated infections with antimicrobial-resistant versus antimicrobial-susceptible organisms. Clin Infect Dis, 2012. **55**(6): p. 807-15.

30. Fair, R.J. and Y. Tor, Antibiotics and bacterial resistance in the 21st century. Perspect Medicin Chem, 2014. **6**: p. 25-64.

31. Shrestha, P., et al., Enumerating the economic cost of antimicrobial resistance per antibiotic consumed to inform the evaluation of interventions affecting their use. Antimicrob Resist Infect Control, 2018. **7**: p. 98.

32. Allegranzi, B., et al., Burden of endemic health-care-associated infection in developing countries: systematic review and meta-analysis. Lancet, 2011. **377**(9761): p. 228-41.

33. Paphitou, N.I., Antimicrobial resistance: action to combat the rising microbial challenges. Int J Antimicrob Agents, 2013. **42 Suppl**: p. S25-8.

34. Boucher, H.W., et al., Bad bugs, no drugs: no ESKAPE! An update from the Infectious Diseases Society of America. Clin Infect Dis, 2009. **48**(1): p. 1-12.

35. Diaz-Torres, M.L., et al., Determining the antibiotic resistance potential of the indigenous oral microbiota of humans using a metagenomic approach. FEMS Microbiol Lett, 2006. **258**(2): p. 257-62.

36. de Castro, A.P., R. Fernandes Gda, and O.L. Franco, Insights into novel antimicrobial compounds and antibiotic resistance genes from soil metagenomes. Front Microbiol, 2014. **5**: p. 489.

37. Nichols, D., et al., Use of ichip for high-throughput in situ cultivation of "uncultivable" microbial species. Appl Environ Microbiol, 2010. **76**(8): p. 2445-50.

38. Ling, L.L., et al., A new antibiotic kills pathogens without detectable resistance. Nature, 2015. **517**(7535): p. 455-9.

39. Neilands, J.B., Siderophores: structure and function of microbial iron transport compounds. J Biol Chem, 1995. **270**(45): p. 26723-6.

40. Wencewicz, T.A., et al., Is drug release necessary for antimicrobial activity of siderophore-drug conjugates? Syntheses and biological studies of the naturally occurring salmycin "Trojan Horse" antibiotics and synthetic desferridanoxamine-antibiotic conjugates. Biometals, 2009. **22**(4): p. 633-48.

41. Miller, M.J., et al., Utilization of microbial iron assimilation processes for the development of new antibiotics and inspiration for the design of new anticancer agents. Biometals, 2009. **22**(1): p. 61-75.

42. Ferreras, J.A., et al., Small-molecule inhibition of siderophore biosynthesis in Mycobacterium tuberculosis and Yersinia pestis. Nat Chem Biol, 2005. **1**(1): p. 29-32.

43. Challis, G.L. and D.A. Hopwood, Synergy and contingency as driving forces for the evolution of multiple secondary metabolite production by Streptomyces species. Proc Natl Acad Sci U S A, 2003. **100 Suppl 2**(Suppl 2): p. 14555-61.

44. Cherian, P.T., et al., New β-lactam - Tetramic acid hybrids show promising antibacterial activities. Bioorg Med Chem Lett, 2018. **28**(18): p. 3105-3112.

45. Wang, K.K., et al., A Hybrid Drug Limits Resistance by Evading the Action of the Multiple Antibiotic Resistance Pathway. Mol Biol Evol, 2016. **33**(2): p. 492-500.

46. Hu, Y.Q., et al., 4-Quinolone hybrids and their antibacterial activities. Eur J Med Chem, 2017. **141**: p. 335-345.

47. Baker, S.J., et al., Technologies to address antimicrobial resistance. Proc Natl Acad Sci U S A, 2018. **115**(51): p. 12887-12895.

48. Bode, M. and U. Payyappallimana, Evidence based traditional medicine: for whom and to what end? eJournal of Indian Medicine, 2013. **6**(1): p. 1-20.

49. Gundala, S.R. and R. Aneja, Piper betel leaf: a reservoir of potential xenohormetic nutraceuticals with cancer-fighting properties. Cancer Prev Res (Phila), 2014. **7**(5): p. 477-86.

50. Atanasov, A.G., et al., Discovery and resupply of pharmacologically active plant-derived natural products: A review. Biotechnol Adv, 2015. **33**(8): p. 1582-1614.

51. Compant, S., et al., Use of plant growth-promoting bacteria for biocontrol of plant diseases: principles, mechanisms of action, and future prospects. Appl Environ Microbiol, 2005. **71**(9): p. 4951-9.

52. Lewis, K. and F.M. Ausubel, Prospects for plant-derived antibacterials. Nat Biotechnol, 2006. **24**(12): p. 1504-7.

53. Hammerschmidt, R., PHYTOALEXINS: What Have We Learned After 60 Years? Annu Rev Phytopathol, 1999. **37**: p. 285-306.

54. Mamedov, N., Medicinal plants studies: history, challenges and perspective. Med Aromat Plants, 2012. **1**(8): p. e133.

55. Seukep, A.J., et al., Plant-derived secondary metabolites as the main source of efflux pump inhibitors and methods for identification. Journal of Pharmaceutical Analysis, 2019.

56. Kagan, I.A. and R. Hammerschmidt, Arabidopsis ecotype variability in camalexin production and reaction to infection by Alternaria brassicicola. J Chem Ecol, 2002. **28**(11): p. 2121-40.

57. Dixon, R.A., Natural products and plant disease resistance. Nature, 2001. **411**(6839): p. 843-7.

58. Gibbons, S., Anti-staphylococcal plant natural products. Nat Prod Rep, 2004. **21**(2): p. 263-77.

59. Sangwan, P.L., et al., Piperine analogs as potent Staphylococcus aureus NorA efflux pump inhibitors. Bioorg Med Chem, 2008. **16**(22): p. 9847-57.

60. Hamilton-Miller, J.M. and S. Shah, Activity of the tea component epicatechin gallate and analogues against methicillin-resistant Staphylococcus aureus. J Antimicrob Chemother, 2000. **46**(5): p. 852-3.

61. Nicolson, K., G. Evans, and P.W. O'Toole, Potentiation of methicillin activity against methicillin-resistant Staphylococcus aureus by diterpenes. FEMS Microbiol Lett, 1999. **179**(2): p. 233-9.

62. Khameneh, B., et al., Review on plant antimicrobials: a mechanistic viewpoint. Antimicrob Resist Infect Control, 2019. **8**: p. 118.

63. Domadia, P.N., et al., Berberine targets assembly of Escherichia coli cell division protein FtsZ. Biochemistry, 2008. **47**(10): p. 3225-34.

64. Sun, N., et al., Rational design of berberine-based FtsZ inhibitors with broad-spectrum antibacterial activity. PLoS One, 2014. **9**(5): p. e97514.

65. Marinelli, L., A. Di Stefano, and I. Cacciatore, Carvacrol and its derivatives as antibacterial agents. Phytochemistry Reviews, 2018. **17**(4): p. 903-921.

66. Doyle, A.A., et al., Cinnamaldehydes: Synthesis, antibacterial evaluation, and the effect of molecular structure on antibacterial activity. Results in Chemistry, 2019. **1**: p. 100013.

67. Chalothorn, T., et al., Synthesis and antibacterial activity of emodin and its derivatives against methicillin-resistant Staphylococcus aureus. Tetrahedron Letters, 2019. **60**(35): p. 151004.

68. Taylor, P.W., Alternative natural sources for a new generation of antibacterial agents. Int J Antimicrob Agents, 2013. **42**(3): p. 195-201.

69. Walsh, C., Molecular mechanisms that confer antibacterial drug resistance. Nature, 2000. **406**(6797): p. 775-781.

70. Kohanski, M.A., et al., A common mechanism of cellular death induced by bactericidal antibiotics. Cell, 2007. **130**(5): p. 797-810.

71. Liu, Y. and J.A. Imlay, Cell death from antibiotics without the involvement of reactive oxygen species. Science, 2013. **339**(6124): p. 1210-3.

72. Keren, I., et al., Killing by bactericidal antibiotics does not depend on reactive oxygen species. Science, 2013. **339**(6124): p. 1213-6.

73. Van Acker, H., et al., The Role of Reactive Oxygen Species in Antibiotic-Induced Cell Death in Burkholderia cepacia Complex Bacteria. PLoS One, 2016. **11**(7): p. e0159837.

74. Ajiboye, T.O., et al., Contribution of reactive oxygen species to (+)-catechin-mediated bacterial lethality. Chem Biol Interact, 2016. **258**: p. 276-87.

75. Chen, Z., et al., Chloro-benzoquinones cause oxidative DNA damage through iron-mediated ROS production in Escherichia coli. Chemosphere, 2015. **135**: p. 379-86.

76. Xiong, L.G., et al., Tea polyphenol epigallocatechin gallate inhibits Escherichia coli by increasing endogenous oxidative stress. Food Chem, 2017. **217**: p. 196-204.

77. Tajima, N., et al., Determination of reactive oxygen generated from natural medicines and their antibacterial activity. J Pharm Anal, 2016. **6**(4): p. 214-218.

78. Nobre, L.S., et al., Binding of azole antibiotics to Staphylococcus aureus flavohemoglobin increases intracellular oxidative stress. J Bacteriol, 2010. **192**(6): p. 1527-33.

79. Matsumura, Y., et al., Mode of bactericidal action of silver zeolite and its comparison with that of silver nitrate. Appl Environ Microbiol, 2003. **69**(7): p. 4278-81.

80. Kumar, A., et al., Engineered ZnO and TiO(2) nanoparticles induce oxidative stress and DNA damage leading to reduced viability of Escherichia coli. Free Radic Biol Med, 2011. **51**(10): p. 1872-81.

81. Li, G.-q., et al., Sublethal vancomycin-induced ROS mediating antibiotic resistance in Staphylococcus aureus. Bioscience reports, 2015. **35**(6).

82. Subramanian, M., et al., Resveratrol induced inhibition of Escherichia coli proceeds via membrane oxidation and independent of diffusible reactive oxygen species generation. Redox Biol, 2014. **2**: p. 865-72.

83. Jodynis-Liebert, J. and M. Kujawska, Biphasic Dose-Response Induced by Phytochemicals: Experimental Evidence. J Clin Med, 2020. **9**(3).

84. Yang, Y., et al., Synergy effects of herb extracts: pharmacokinetics and pharmacodynamic basis. Fitoterapia, 2014. **92**: p. 133-47.

85. Pistelli, L., et al., Antimicrobial activity of crude extracts and pure compounds of Hypericum hircinum. Fitoterapia, 2000. **71 Suppl 1**: p. S138-40.

86. Rasoanaivo, P., et al., Whole plant extracts versus single compounds for the treatment of malaria: synergy and positive interactions. Malar J, 2011. **10 Suppl 1**(Suppl 1): p. S4.

87. Geddes, A.M., K.P. Klugman, and G.N. Rolinson, Introduction: historical perspective and development of amoxicillin/clavulanate. Int J Antimicrob Agents, 2007. **30 Suppl 2**: p. S109-12.

88. Stermitz, F.R., et al., Synergy in a medicinal plant: antimicrobial action of berberine potentiated by 5'-methoxyhydnocarpin, a multidrug pump inhibitor. Proc Natl Acad Sci U S A, 2000. **97**(4): p. 1433-7.

89. Chang, E.H., et al., Catechin-mediated restructuring of a bacterial toxin inhibits activity. Biochim Biophys Acta Gen Subj, 2019. **1863**(1): p. 191-198.

90. Peng, L., et al., Antibacterial activity and mechanism of berberine against Streptococcus agalactiae. Int J Clin Exp Pathol, 2015. **8**(5): p. 5217-23.

91. Noor Mohammadi, T., et al., Mechanism for antibacterial action of epigallocatechin gallate and theaflavin-3,3'-digallate on Clostridium perfringens. J Appl Microbiol, 2019. **126**(2): p. 633-640.

92. Rathee, J.S., et al., Antioxidant activity of piper betel leaf extract and its constituents. J Agric Food Chem, 2006. **54**(24): p. 9046-54.

93. Bhatt, S., K. Roy, and S.K. Nayak, Efficient one-pot synthesis of 2-arylbenzo [b] furans from 2-styrylphenols using CuBr2. Synthetic Communications®, 2010. **40**(18): p. 2736-2746.

94. Chen, H., et al., In vitro activity and post-antibiotic effects of linezolid in combination with fosfomycin against clinical isolates of Staphylococcus aureus. Infect Drug Resist, 2018. **11**: p. 2107-2115.

95. Pollard, J.E., et al., In vitro evaluation of the potential for resistance development to ceragenin CSA-13. J Antimicrob Chemother, 2012. **67**(11): p. 2665-72.

96. White, R.L., et al., Comparison of three different in vitro methods of detecting synergy: time-kill, checkerboard, and E test. Antimicrob Agents Chemother, 1996. **40**(8): p. 1914-8.

97. Mathur, H., et al., Bacteriocin-Antimicrobial Synergy: A Medical and Food Perspective. Front Microbiol, 2017. **8**: p. 1205.

98. Dawis, M.A., et al., In vitro activity of gatifloxacin alone and in combination with cefepime, meropenem, piperacillin and gentamicin against multidrug-resistant organisms. J Antimicrob Chemother, 2003. **51**(5): p. 1203-11.

99. Zhou, K., et al., Novel reference genes for quantifying transcriptional responses of Escherichia coli to protein overexpression by quantitative PCR. BMC molecular biology, 2011. **12**(1): p. 1-9.

100. Livak, K.J. and T.D. Schmittgen, Analysis of relative gene expression data using real-time quantitative PCR and the 2(-Delta Delta C(T)) Method. Methods, 2001. **25**(4): p. 402-8.

101. Subramanian, M., U. Shadakshari, and S. Chattopadhyay, A mechanistic study on the nuclease activities of some hydroxystilbenes. Bioorg Med Chem, 2004. **12**(5): p. 1231-7.

102. Solanky, D. and S.E. Haydel, Adaptation of the neutral bacterial comet assay to assess antimicrobial-mediated DNA double-strand breaks in Escherichia coli. J Microbiol Methods, 2012. **91**(2): p. 257-61.

103. Hassani, L., et al., A spectroscopic investigation of the interaction between c-MYC DNA and tetrapyridinoporphyrazinatozinc(II). J Biol Phys, 2014. **40**(3): p. 275-83.

104. Reyes, N., J.B. Aggen, and C.F. Kostrub, In vivo efficacy of the novel aminoglycoside ACHN-490 in murine infection models. Antimicrob Agents Chemother, 2011. **55**(4): p. 1728-33.

105. Kalyanaraman, B., C.C. Felix, and R.C. Sealy, Semiquinone anion radicals of catechol(amine)s, catechol estrogens, and their metal ion complexes. Environ Health Perspect, 1985. **64**: p. 185-98.

106. Forman, H.J., et al., Even free radicals should follow some rules: a guide to free radical research terminology and methodology. Free Radic Biol Med, 2015. **78**: p. 233-5.

107. Chen, J., S.C. Rogers, and M. Kavdia, Analysis of kinetics of dihydroethidium fluorescence with superoxide using xanthine oxidase and hypoxanthine assay. Ann Biomed Eng, 2013. **41**(2): p. 327-37.

108. Hori, M., et al., Identification of high excision capacity for 5-hydroxymethyluracil mispaired with guanine in DNA of Escherichia coli MutM, Nei and Nth DNA glycosylases. Nucleic Acids Res, 2003. **31**(4): p. 1191-6.

109. Mukherjee, A., C. Cao, and J. Lutkenhaus, Inhibition of FtsZ polymerization by SulA, an inhibitor of septation in Escherichia coli. Proc Natl Acad Sci U S A, 1998. **95**(6): p. 2885-90.

110. Dewachter, L., et al., A Single-Amino-Acid Substitution in Obg Activates a New Programmed Cell Death Pathway in Escherichia coli. mBio, 2015. **6**(6): p. e01935-15.

111. Vanhauteghem, D., et al., Exposure to the proton scavenger glycine under alkaline conditions induces Escherichia coli viability loss. PLoS One, 2013. **8**(3): p. e60328.

112. Spindler, E.C., et al., Deciphering the mode of action of the synthetic antimicrobial peptide Bac8c. Antimicrob Agents Chemother, 2011. **55**(4): p. 1706-16.

113. Cléach, J., et al., Use of Ratiometric Probes with a Spectrofluorometer for Bacterial Viability Measurement. J Microbiol Biotechnol, 2018. **28**(11): p. 1782-1790.

114. Epand, R.M., et al., Molecular mechanisms of membrane targeting antibiotics. Biochim Biophys Acta, 2016. **1858**(5): p. 980-7.

115. Clifton, L.A., et al., Effect of divalent cation removal on the structure of gram-negative bacterial outer membrane models. Langmuir, 2015. **31**(1): p. 404-12.

116. Keyamura, K. and T. Hishida, Topological DNA-binding of structural maintenance of chromosomes-like RecN promotes DNA double-strand break repair in Escherichia coli. Commun Biol, 2019. **2**: p. 413.

117. Matsumoto, Y., et al., Escherichia coli Nth and human hNTH1 DNA glycosylases are involved in removal of 8-oxoguanine from 8-oxoguanine/guanine mispairs in DNA. Nucleic Acids Res, 2001. **29**(9): p. 1975-81.

118. Tashjian, T.F., et al., Residues in the fingers domain of the translesion DNA polymerase DinB enable its unique participation in error-prone double-strand break repair. J Biol Chem, 2019. **294**(19): p. 7588-7600.

119. Warr, A.R., et al., Protease-deficient SOS constitutive cells have RecN-dependent cell division phenotypes. Mol Microbiol, 2019. **111**(2): p. 405-422.

120. Gundala, S.R., et al., Hydroxychavicol, a betel leaf component, inhibits prostate cancer through ROS-driven DNA damage and apoptosis. Toxicol Appl Pharmacol, 2014. **280**(1): p. 86-96.

121. Brynildsen, M.P., et al., Potentiating antibacterial activity by predictably enhancing endogenous microbial ROS production. Nat Biotechnol, 2013. **31**(2): p. 160-5.

122. Shen, Q., et al., Bactericidal activity of alpha-bromocinnamaldehyde against persisters in Escherichia coli. PLoS One, 2017. **12**(7): p. e0182122.

123. Goswami, M., et al., Involvement of Antibiotic Efflux Machinery in Glutathione-Mediated Decreased Ciprofloxacin Activity in Escherichia coli. Antimicrob Agents Chemother, 2016. **60**(7): p. 4369-74.

124. Chen, C.L., C.W. Chi, and T.Y. Liu, Enhanced hydroxychavicol-induced cytotoxic effects in glutathione-depleted HepG2 cells. Cancer Lett, 2000. **155**(1): p. 29-35.

125. Nakagawa, Y., et al., Biotransformation and cytotoxic effects of hydroxychavicol, an intermediate of safrole metabolism, in isolated rat hepatocytes. Chem Biol Interact, 2009. **180**(1): p. 89-97.

126. Fathima, A. and J.R. Rao, Selective toxicity of Catechin-a natural flavonoid towards bacteria. Appl Microbiol Biotechnol, 2016. **100**(14): p. 6395-6402.

127. Dixon, S.J. and B.R. Stockwell, The role of iron and reactive oxygen species in cell death. Nat Chem Biol, 2014. **10**(1): p. 9-17.

128. Morones-Ramirez, J.R., et al., Silver enhances antibiotic activity against gram-negative bacteria. Sci Transl Med, 2013. **5**(190): p. 190ra81.

129. Ali, I., et al., Hydroxychavicol: A phytochemical targeting cutaneous fungal infections. Sci Rep, 2016. **6**: p. 37867.

130. Yadav, S.K., et al., Inhibition of TNF-α, and NF-κB and JNK pathways accounts for the prophylactic action of the natural phenolic, allylpyrocatechol against

indomethacin gastropathy. Biochimica et Biophysica Acta (BBA)-General Subjects, 2013. **1830**(6): p. 3776-3786.

131. Sharma, S., et al., Evaluation of the antimicrobial, antioxidant, and anti-inflammatory activities of hydroxychavicol for its potential use as an oral care agent. Antimicrob Agents Chemother, 2009. **53**(1): p. 216-22.

132. NavaneethaKrishnan, S., J.L. Rosales, and K.Y. Lee, ROS-Mediated Cancer Cell Killing through Dietary Phytochemicals. Oxid Med Cell Longev, 2019. **2019**: p. 9051542.

133. Dwyer, D.J., et al., Antibiotic-induced bacterial cell death exhibits physiological and biochemical hallmarks of apoptosis. Mol Cell, 2012. **46**(5): p. 561-72.

134. Hong, Y., et al., Post-stress bacterial cell death mediated by reactive oxygen species. Proc Natl Acad Sci U S A, 2019. **116**(20): p. 10064-10071.

135. Dwyer, D.J., et al., Antibiotics induce redox-related physiological alterations as part of their lethality. Proc Natl Acad Sci U S A, 2014. **111**(20): p. E2100-9.

136. Wu, D., et al., D-Alanine:D-alanine ligase as a new target for the flavonoids quercetin and apigenin. Int J Antimicrob Agents, 2008. **32**(5): p. 421-6.

137. Tegos, G., et al., Multidrug pump inhibitors uncover remarkable activity of plant antimicrobials. Antimicrob Agents Chemother, 2002. **46**(10): p. 3133-41.

138. Tsuchiya, H., Membrane Interactions of Phytochemicals as Their Molecular Mechanism Applicable to the Discovery of Drug Leads from Plants. Molecules, 2015. **20**(10): p. 18923-66.

139. Ingólfsson, H.I., et al., Phytochemicals perturb membranes and promiscuously alter protein function. ACS Chem Biol, 2014. **9**(8): p. 1788-98.

140. Domalaon, R., et al., Antibiotic Hybrids: the Next Generation of Agents and Adjuvants against Gram-Negative Pathogens? Clin Microbiol Rev, 2018. **31**(2).

141. Farrag, H.A., et al., Natural outer membrane permeabilizers boost antibiotic action against irradiated resistant bacteria. J Biomed Sci, 2019. **26**(1): p. 69.

142. Singla, P., et al., Facially Amphiphilic Cholic Acid-Lysine Conjugates as Promising Antimicrobials. ACS Omega, 2020. **5**(8): p. 3952-3963.

143. Khan, I., et al., Antimicrobial Potential of Carvacrol against Uropathogenic Escherichia coli via Membrane Disruption, Depolarization, and Reactive Oxygen Species Generation. Front Microbiol, 2017. **8**: p. 2421.

144. Bhattacharya, S., et al., Healing property of the Piper betel phenol, allylpyrocatechol against indomethacin-induced stomach ulceration and mechanism of action. World J Gastroenterol, 2007. **13**(27): p. 3705-13.

145. Subramanian, M., S. Soundar, and S. Mangoli, DNA damage is a late event in resveratrol-mediated inhibition of Escherichia coli. Free Radic Res, 2016. **50**(7): p. 708-19.

146. Hwang, D. and Y.H. Lim, Resveratrol antibacterial activity against Escherichia coli is mediated by Z-ring formation inhibition via suppression of FtsZ expression. Sci Rep, 2015. **5**: p. 10029.

147. Lee, W. and D.G. Lee, Resveratrol induces membrane and DNA disruption via pro-oxidant activity against Salmonella typhimurium. Biochem Biophys Res Commun, 2017. **489**(2): p. 228-234.

148. Matsuoka, A., et al., The 4'-hydroxy group is responsible for the in vitro cytogenetic activity of resveratrol. Mutat Res, 2002. **521**(1-2): p. 29-35.

149. Potter, G.A., et al., The cancer preventative agent resveratrol is converted to the anticancer agent piceatannol by the cytochrome P450 enzyme CYP1B1. Br J Cancer, 2002. **86**(5): p. 774-8.

150. Snyder, S.A., A. Gollner, and M.I. Chiriac, Regioselective reactions for programmable resveratrol oligomer synthesis. Nature, 2011. **474**(7352): p. 461-6.

151. Betts, J.W. and D.W. Wareham, In vitro activity of curcumin in combination with epigallocatechin gallate (EGCG) versus multidrug-resistant Acinetobacter baumannii. BMC Microbiol, 2014. **14**: p. 172.

152. Fazly Bazzaz, B.S., et al., Effect of Catechins, Green tea Extract and Methylxanthines in Combination with Gentamicin Against Staphylococcus aureus and Pseudomonas aeruginosa: - Combination therapy against resistant bacteria. J Pharmacopuncture, 2016. **19**(4): p. 312-318.

153. Tyagi, P., et al., Bactericidal activity of curcumin I is associated with damaging of bacterial membrane. PLoS One, 2015. **10**(3): p. e0121313.

154. Rosado, H., et al., Impact of the β-Lactam Resistance Modifier (-)-Epicatechin Gallate on the Non-Random Distribution of Phospholipids across the Cytoplasmic Membrane of Staphylococcus aureus. Int J Mol Sci, 2015. **16**(8): p. 16710-27.

155. Madreiter-Sokolowski, C.T., A.A. Sokolowski, and W.F. Graier, Dosis Facit Sanitatem-Concentration-Dependent Effects of Resveratrol on Mitochondria. Nutrients, 2017. **9**(10): p. 1117

156. Dey, A., et al., Biphasic activity of resveratrol on indomethacin-induced gastric ulcers. Biochem Biophys Res Commun, 2009. **381**(1): p. 90-5.

157. Crowell, J.A., et al., Resveratrol-associated renal toxicity. Toxicol Sci, 2004. **82**(2): p. 614-9.

158. Salehi, B., et al., Resveratrol: A Double-Edged Sword in Health Benefits. Biomedicines, 2018. **6**(3).

159. Wang, P. and S. Sang, Metabolism and pharmacokinetics of resveratrol and pterostilbene. Biofactors, 2018. **44**(1): p. 16-25.

160. Riche, D.M., et al., Analysis of safety from a human clinical trial with pterostilbene. J Toxicol, 2013. **2013**: p. 463595.

161. Roupe, K.A., et al., Pharmacokinetics of selected stilbenes: rhapontigenin, piceatannol and pinosylvin in rats. J Pharm Pharmacol, 2006. **58**(11): p. 1443-50.

162. Park, E.J., et al., Antimetastatic activity of pinosylvin, a natural stilbenoid, is associated with the suppression of matrix metalloproteinases. J Nutr Biochem, 2012. **23**(8): p. 946-52.

163. Chen, W., et al., Determination of pinostilbene in rat plasma by LC-MS/MS: Application to a pharmacokinetic study. J Pharm Biomed Anal, 2016. **120**: p. 316-21.

164. Sun, Y., et al., Identification of pinostilbene as a major colonic metabolite of pterostilbene and its inhibitory effects on colon cancer cells. Mol Nutr Food Res, 2016. **60**(9): p. 1924-32.

165. Mao, P., et al., Pharmacokinetics, bioavailability, metabolism and excretion of δ-viniferin in rats. Acta Pharm Sin B, 2016. **6**(3): p. 243-52.

166. Sakharkar, M.K., et al., In vitro combinations of antibiotics and phytochemicals against Pseudomonas aeruginosa. J Microbiol Immunol Infect, 2009. **42**(5): p. 364-70.

167. Amin, M.U., et al., Antibiotic additive and synergistic action of rutin, morin and quercetin against methicillin resistant Staphylococcus aureus. BMC Complement Altern Med, 2015. **15**: p. 59.

168. Szekeres, T., et al., Resveratrol and resveratrol analogues--structure-activity relationship. Pharm Res, 2010. **27**(6): p. 1042-8.

169. Nawaz, W., et al., Therapeutic Versatility of Resveratrol Derivatives. Nutrients, 2017. **9**(11).

170. Ogas, T., T.P. Kondratyuk, and J.M. Pezzuto, Resveratrol analogs: promising chemopreventive agents. Ann N Y Acad Sci, 2013. **1290**: p. 21-9.

171. Berman, A.Y., et al., The therapeutic potential of resveratrol: a review of clinical trials. NPJ Precis Oncol, 2017. **1**.

172. Huang, X. and H.L. Zhu, Resveratrol and its analogues: promising antitumor agents. Anticancer Agents Med Chem, 2011. **11**(5): p. 479-90.

173. Peng, R.M., et al., Oral delivery system enhanced the bioavailability of stilbenes: Resveratrol and pterostilbene. Biofactors, 2018. **44**(1): p. 5-15.

174. Vitaglione, P., et al., Bioavailability of trans-resveratrol from red wine in humans. Mol Nutr Food Res, 2005. **49**(5): p. 495-504.

175. Boocock, D.J., et al., Quantitation of trans-resveratrol and detection of its metabolites in human plasma and urine by high performance liquid chromatography. J Chromatogr B Analyt Technol Biomed Life Sci, 2007. **848**(2): p. 182-7.

176. Morand, C., et al., Plasma metabolites of quercetin and their antioxidant properties. Am J Physiol, 1998. **275**(1): p. R212-9.

177. Yoshizumi, M., et al., Quercetin glucuronide prevents VSMC hypertrophy by angiotensin II via the inhibition of JNK and AP-1 signaling pathway. Biochem Biophys Res Commun, 2002. **293**(5): p. 1458-65.

178. Takizawa, Y., et al., The 4'-hydroxyl group of resveratrol is functionally important for direct activation of PPARα. PLoS One, 2015. **10**(3): p. e0120865.

179. Mahmood, H.Y., et al., Current Advances in Developing Inhibitors of Bacterial Multidrug Efflux Pumps. Curr Med Chem, 2016. **23**(10): p. 1062-81.

180. Yang, S.C., et al., Pterostilbene, a Methoxylated Resveratrol Derivative, Efficiently Eradicates Planktonic, Biofilm, and Intracellular MRSA by Topical Application. Front Microbiol, 2017. **8**: p. 1103.

181. Zheng, L.F., et al., DNA damage induced by resveratrol and its synthetic analogues in the presence of Cu (II) ions: mechanism and structure-activity relationship. Free Radic Biol Med, 2006. **41**(12): p. 1807-16.

182. Banudevi, S., S. Swaminathan, and K.U. Maheswari, Pleiotropic Role of Dietary Phytochemicals in Cancer: Emerging Perspectives for Combinational Therapy. Nutr Cancer, 2015. **67**(7): p. 1021-48.

183. Li, X.Z., et al., Hypohalous acid-mediated halogenation of resveratrol and its role in antioxidant and antimicrobial activities. Food Chem, 2012. **135**(3): p. 1239-44.

184. Chung, J.K., et al., Structure-toxicity relationship study of para-halogenated styrene analogues in CYP2E1 transgenic cells. Toxicol Lett, 2012. **210**(3): p. 353-9.

185. Egbuna, C., et al., Phytochemicals as Lead Compounds for New Drug Discovery. 2019: Elsevier.

186. Bernardini, S., et al., Natural products for human health: an historical overview of the drug discovery approaches. Nat Prod Res, 2018. **32**(16): p. 1926-1950.

187. Jang, M., et al., Cancer chemopreventive activity of resveratrol, a natural product derived from grapes. Science, 1997. **275**(5297): p. 218-20.

188. Zhang, X., et al., Resveratrol Protects against Helicobacter pylori-Associated Gastritis by Combating Oxidative Stress. Int J Mol Sci, 2015. **16**(11): p. 27757-69.

189. Abdul-Mutakabbir, J.C., et al., Teaching an Old Class New Tricks: A Novel Semi-Synthetic Aminoglycoside, Plazomicin. Infect Dis Ther, 2019. **8**(2): p. 155-170.

190. Radlinski, L.C., et al., Chemical Induction of Aminoglycoside Uptake Overcomes Antibiotic Tolerance and Resistance in Staphylococcus aureus. Cell Chem Biol, 2019. **26**(10): p. 1355-1364 e4.

191. Papas, P.N., C.A. Brusch, and G.C. Ceresia, Cranberry juice in the treatment of urinary tract infections. Southwest Med, 1966. **47**(1): p. 17-20.

192. Somu, C.A., et al., Efficacy of a herbal extract gel in the treatment of gingivitis: A clinical study. J Ayurveda Integr Med, 2012. **3**(2): p. 85-90.

193. Yee, Y.K., M.W. Koo, and M.L. Szeto, Chinese tea consumption and lower risk of Helicobacter infection. J Gastroenterol Hepatol, 2002. **17**(5): p. 552-5.

194. Xu, J., et al., The antibacterial mechanism of carvacrol and thymol against Escherichia coli. Letters in applied microbiology, 2008. **47**(3): p. 174-179.

195. Qiang, L., et al., Resveratrol improves efficacy of oral amoxicillin against childhood fast breathing pneumonia in a randomized placebo-controlled double blind clinical trial. Microb Pathog, 2018. **114**: p. 209-212.

196. Liu, Y., et al., Resveratrol Antagonizes Antimicrobial Lethality and Stimulates Recovery of Bacterial Mutants. PLoS One, 2016. **11**(4): p. e0153023.

197. Horino, T. and S. Hori, Metastatic infection during Staphylococcus aureus bacteremia. J Infect Chemother, 2020. **26**(2): p. 162-169.

198. Li, J., K.L. Echevarria, and K.A. Traugott, β-Lactam Therapy for Methicillin-Susceptible Staphylococcus aureus Bacteremia: A Comparative Review of Cefazolin versus Antistaphylococcal Penicillins. Pharmacotherapy, 2017. **37**(3): p. 346-360.

199. Rayner, C. and W.J. Munckhof, Antibiotics currently used in the treatment of infections caused by Staphylococcus aureus. Intern Med J, 2005. **35 Suppl 2**: p. S3-16.

200. Tacconelli, E., et al., Discovery, research, and development of new antibiotics: the WHO priority list of antibiotic-resistant bacteria and tuberculosis. Lancet Infect Dis, 2018. **18**(3): p. 318-327.

201. Wu, S.C., et al., Natural Products That Target Virulence Factors in Antibiotic-Resistant Staphylococcus aureus. J Agric Food Chem, 2019. **67**(48): p. 13195-13211.

202. Wang, G., et al., Hypericin enhances β-lactam antibiotics activity by inhibiting sarA expression in methicillin-resistant Staphylococcus aureus. Acta Pharm Sin B, 2019. **9**(6): p. 1174-1182.

203. Yu, H.H., et al., Antimicrobial activity of berberine alone and in combination with ampicillin or oxacillin against methicillin-resistant Staphylococcus aureus. J Med Food, 2005. **8**(4): p. 454-61.

204. Braga, L.C., et al., Pomegranate extract inhibits Staphylococcus aureus growth and subsequent enterotoxin production. J Ethnopharmacol, 2005. **96**(1-2): p. 335-9.

Thesis Abstract

Name of the Student: **Deepti Singh**

Name of the CI: **Bhabha Atomic Research Centre** Enrolment No.: **LIFE01201504014**

Thesis Title: **Investigation of molecular mechanisms of underlying antibacterial potential of Allylarene and Stilbene class of phytochemicals**

Discipline: **Life Sciences** Sub-Area of Discipline: **Microbiology**

Date of viva voce: **10/04/2021**

A scarcity of antibacterial agents/therapy against antibiotic resistant bacteria has become global concern. Phytochemicals remain an important repository of diverse molecules with several therapeutic benefits. Allylarenes and Stilbenes are two important classes of phytochemicals that have been investigated for their potential antibacterial activity in the current work. Hydroxychavicol (HC), a key component of *Piper betle* leaves was shown to induce of reactive oxygen species (ROS) in bacterial cells using biochemical and genetic approaches. Further, damage to iron sulphur proteins amplified the ROS, contributing to cyctoxicity. Employing direct quantification and DNA damage repair deficient mutants we showed HC treated cells undergo ROS mediated DNA damage. HC also affected several targets in the cell. A kinetic dissection of these events revealed HC treated cells to undergo oxidative stress, membrane damage and DNA damage in that order. The membrane damage by HC proceeds by stripping of Mg^{2+} from the outer membrane. This property formed the basis of co-operativity of HC with high molecular weight antibiotics in inhibiting *E. coli*. HC also inhibited a host of gram negative bacteria with varied antibiotic resistant profiles isolated from patients. This work also showed the non toxic nature of HC in animal experiments employing mice.

In the second part of the study we evaluated 11 different stilbenes and showed the effect of different substitutions on the antibacterial activity against the model organism *S. aureus*. We evaluated several parameters that contribute towards antibacterial activity and identified the property predominating in each molecule and collated a correlation to the change in structure. Based on this we identified Dimer stilbene (DS) as the best molecule. We evaluated the ability of DS to synergize with different classes of antibiotics. DS exhibited positive co-operativity with antibiotics that target protein synthesis. DS exhibited synergy with the aminoglycoside kanamycin and additive effect with tetracycline. Resistance generation to DS was null while to that of kanamycin was rapid. Kanamycin resistant *S. aureus* was equally susceptible to DS as compared to wildtype. DS eradicated *S. aureus* infection in mice as a standalone drug as well as in conjunction with kanamycin. Synergy with kanamycin was also observed in other stilbenes apart from DS. Our study reveals stilbenes could be a potent arsenal against combating *S. aureus* infections.

Thesis Highlight

Name of the Student: **Deepti Singh**

Name of the CI: **Bhabha Atomic Research Centre** Enrolment No.: **LIFE 01201504014**

Thesis Title: **Investigation of molecular mechanisms of underlying antibacterial potential of Allylarene and Stilbene class of phytochemicals**

Discipline: **Life Sciences** Sub-Area of Discipline: **Microbiology**

Date of viva voce: **10/04/2021**

Emergence of antibiotic resistant bacteria at an alarming rate is of great concern to human well being. In view of the alarming rate at which our existing treatments become unviable, it is imperative to find newer molecules and strategies to combat bacterial infections. With this objective, two classes of phytochemicals allylarenes and stilbenes were evaluated. Hydroxychavicol was identified from a number of allylarenes to be the best antibacterial molecule and its molecular basis, kinetics of target damage was elucidated. This information helped us to identify a strategy to sensitize gram negative bacteria to large molecular weight antibiotics.

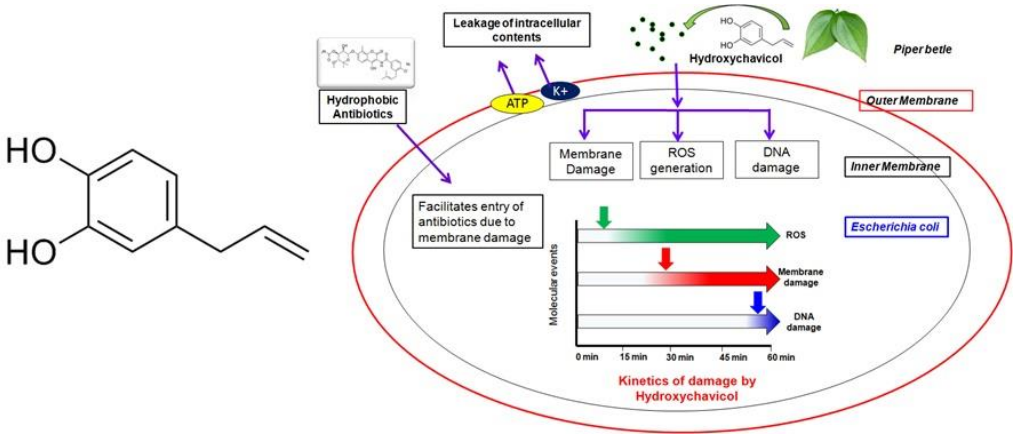

Figure 1. Graphical representation of HC antibacterial mechanism in E. coli.

Structure- function relationship study in stilbenes revealed, not only the antibacterial activity of stilbenes varied with different substitutions, the predominant mechanism of action also changes. The best stilbene, Dimer stilbene (DS) identified in the study exhibited positive co-operativity with kanamycin and eradicated *S. aureus* infection in a mouse model.

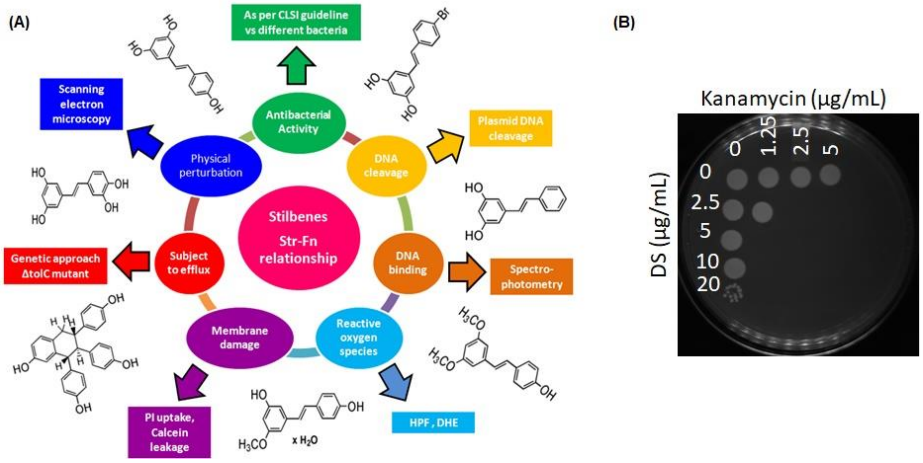

Figure 2. (A) Structure antibacterial activity relationship in stilbenes. (B) DS exhibits co-operativity with kanamycin.